Modeling and Control of Polymerization Processes

by

Rahul Bindlish

A dissertation submitted in partial fulfillment

of the requirements for the degree of

Doctor of Philosophy

(Chemical Engineering)

at the

UNIVERSITY OF WISCONSIN–MADISON

1999

To my parents

Acknowledgments

I feel fortunate to be able to experience graduate research under the able guidance of Professor James B. Rawlings. He always made me look at the bigger picture while ensuring that all the details tied together. I thoroughly enjoyed all the social outings, especially the annual picnics at his house. I have enjoyed being a member of the research group a lot. I would first like to express my gratitude to the senior members; Tony Mullins, Ken Muske, E. Scott Meadows, Rock Matthews, John C. Campbell, Peter Findeisen and Rolf Findeisen. Rock was always helpful and considerate. John made sure that everyone was included in every prank he came up with. Peter and Rolf became good friends in the short period of time they spent with the research group. I also thank my colleagues; Scott Middlebrooks and Chris Rao. Chris always presented an interesting viewpoint in any office discussion. A special thank you goes to Scott for helping me move to Madison. I should acknowledge the new members; Daniel Patience, Jenny Wang, Matt Tenny and Brian Odelson. Daniel was always there for office cricket. Matt and Brian were there for a game of darts. Jenny was always calm and cheerful. I also acknowledge John Eaton for maintaining the computing environment in our research group. I value the friendship and guidance of Dr. Robert E. Young, especially during my stay in industry. I would also like to thank the members of my committee, especially Professor Ray for his guidance and support. A special acknowledgment also goes to Professor Stewart for allowing me to use his parameter estimation code (GREG) for my research work. On the personal front, I would like to thank my family for their support and encouragement. In particular, I cherish the constant support of my wife Sirjana and all the smiles of my son Nishant.

Rahul Bindlish

University of Wisconsin–Madison
December 1999

Modeling and Control of Polymerization Processes

Rahul Bindlish

Under the supervision of Professor James B. Rawlings

At the University of Wisconsin–Madison

This dissertation presents modeling and control of prototypical industrial polymerization processes in the presence of disturbances and plant-model mismatch. The process model consists of the material and energy balances for the reactor, and simplified dynamic model for the downstream separator. The kinetic expressions are simplified by using the quasi-steady-state assumption for live polymer chains and the moments of chain length distribution for the live and dead polymer chains. The kinetic parameters in the process model are estimated from industrial data sets using the maximum likelihood method to give a validated fundamental model.

The process model is used to develop a model predictive controller (MPC) for the copolymerization process with the following typical characteristics

- Plant operations: plant start-up, product grade change, regulation around a set-point
- Regulated outputs: polymer production rate, copolymer composition and viscosity

- Manipulated variables: vinyl acetate feed rate, acetaldehyde feed rate, coolant temperature
- Measured disturbances: feed inhibitor, feed temperature

A target linearization model predictive controller gives superior performance compared to a linear model predictive controller during different plant operations.

The performance of the model predictive controllers is further evaluated using the theoretical benchmark of a minimum variance controller based on the process model. The modeling inadequacies that impose limitations on the performance of the feedback controllers are greater for the linear model in comparison to the non-linear model based on the correlation analysis of the process data. Correlation patterns also indicate that better feedback controller performance may be obtained by incorporating a dynamic disturbance model for feed inhibitor and feed temperature in the target linearization model predictive controller.

Contents

List of Tables

List of Figures

Chapter 1

Introduction

Polymers have been utilized by mankind for thousands of years. The modern plastics industry started with the vulcanization of natural rubber by Goodyear in 1839. Polymers are used as plastics, rubber, fibers, adhesives and coatings all over the world. The polymer industry has exhibited consistent and rapid growth in the last few decades. The plastics sales in the United States grew from 8.9×10^9 kg in 1970 to 31.3×10^9 kg in 1993 representing an increase of 252 percent [141]. The Gross Domestic product increased by 79 percent during the same time period. The per capita consumption of plastics for the United States was 111 kg/person in 1993. The plastics industry has been developing at a much faster rate in the last decade in the developing nations. The per capita consumption of polymers in the developing countries still has to increase manifold to match the consumption level in developed countries. Efficient production of polymers will result in higher competitive ability and profit margins for the chemical companies. A better quantitative understanding of the chemical and physical phenomena in the polymerization process will help to increase the economic efficiency for the manufacturer.

1.1 MMA-VA Polymers

The MMA-VA copolymers are studied in this dissertation. The copolymer is used as a precursor for the manufacture of poly-tertbutyrlaldehyde that is used as a sealant in car windshields. The copolymer is also used in paint coatings and art paper industry. The MMA-VA polymers are also widely used as follows.

1.1.1 Vinyl Acetate Polymers

Polyvinyl acetate (PVA) is the precursor for polyvinyl alcohol and polyvinylacetal resins. PVA varies with increasing molecular weight from viscous liquids to brittle polymeric materials. The polymer resins are neutral, tasteless, odorless, non-toxic products. These resins are soluble in organic solvents but insoluble in glycols and water. The strength properties increase with molecular weight; tensile strengths up to 50.3 MPa may be obtained. All grades of polymer become flexible when heated above room temperature. The polymer produced by normal free-radical polymerization is completely atactic and non-crystalline. The chemical properties of polyvinyl acetate are similar to that of an aliphatic ester. The physical and chemical properties can be modified significantly by copolymerization. The prices of polyvinyl acetate polymers depend on the form in which they are sold (resin or emulsion, homopolymer or copolymer). The prices of copolymer tend to be higher than that of homopolymer. The total production of polyvinyl acetates in United States in 1986 was 50×10^6 tonnes. Polyvinyl acetates are used as adhesives, paints, paper binders, textile finishes and chewing-gum bases.

1.1.2 Methyl Methacrylate Polymers

Polymethyl methacrylate (PMMA) is a tough, rubbery and moderately hard polymer. The mechanical properties of the polymer increase with higher molecular weights. However, beyond some critical molecular weight the increase in property values is slight and levels off asymptotically. PMMA is a hard rigid material at room temperature that can be easily bent and formed when heated above its glass transition temperature. PMMA has unique electrical properties. The surface resistivity of PMMA is higher than that of most polymeric materials. High resistance and non-tracking characteristics have resulted in its use in high voltage applications. Its excellent weather resistance has promoted its use for outdoor electrical applications. The total production capacity of methyl methacrylate in 1981 was estimated to be about 1140 tonnes. The United States accounts for about half of this capacity. Polymethyl methacrylate is used as paints, textile finishes, paper saturants and oil additives.

1.2 Dissertation overview

There are various polymerization processes that are used to make different products for consumer use. Chain growth polymerizations are an important class of these polymerization processes. The chain growth processes can be used to make copolymers and homopolymers. Copolymers give unique chemical and physical properties compared to homopolymers. Two industrial chain growth copolymerization processes are analyzed in this dissertation. The first process is an industrial chain growth polymerization process that is used to make various grades of a copolymer and a homopolymer. These grades are characterized by the composition and viscosity for the copolymer, and the average molecular weight for the homopolymer. A polymerization process model is developed in Chapter 4 and estimation of kinetic parameters in the model is investigated in Chapter 5 [16]. The parameter estimation problem for the copolymerization process is first analyzed using simulated data. This analysis is carried out to determine the kinetic parameters that are estimable using the information available in the measurements for a perfect model of the process. The estimable parameters are then also obtained for plant data to validate the process model. The maximum likelihood estimates for the homopolymerization process are also obtained using plant data. A disturbance model is then developed and augmented with the physical process model in Chapter 5. The data and parameters shown in this document for the industrial process have been scaled because of proprietary reasons. A second prototypical industrial copolymerization process is also studied so that the results of the feedback control study can be discussed and analyzed without any proprietary restrictions. The second process is the chain growth copolymerization of methyl methacrylate (MMA) and vinyl acetate (VA) with free radical kinetics. This copolymerization system is interesting because MMA is far more reactive than VA, as indicated by their respective reactivity ratios of 26 and 0.03. The product is characterized by the mole fraction of MMA in the copolymer and its intrinsic viscosity. The reaction mechanism and the kinetic parameters for this process are taken from the open literature [28] and discussed in Chapter 3. The process model is given realistic measured disturbances and plant-model mismatch based on our experience with the industrial copolymerization process. The feedback controller simulations in Chapter 6 give promising results for plant start-up, polymer grade changes and regulation in the presence of measured disturbances and plant-model mismatch. The performance of the feedback model predictive controller is then compared with the minimum variance controller that is used as a benchmark in Chapter 7. The modeling inadequacies that are responsible for limiting the performance of the two feedback controllers are identified by doing a correlation analysis.

1.3 Contribution of this Dissertation

This dissertation makes the following contributions to the field of polymerization control

- Parameter estimation from industrial data sets (Chapter 5)
- Representative polymer control problem having multi-rate sampling with delay and realistic disturbances (Chapter 6)
- Demonstration of typical industrial cases where fixed linear control laws fail (Chapter 6)

- Performance assessment and monitoring using the minimum variance control law based on a fundamental model as a benchmark (Chapter 7)

Chapter 2

Review of Previous Work

There are different polymerization processes having either step growth mechanism or chain growth mechanism [15, 134] that are used to make different commercial polymers. The modeling and control research for various polymer reactors has been reviewed in detail [100, 46, 83]. The literature on control of polymerization reactors can be divided into the four broad categories: modeling, parameter estimation, process control and performance monitoring. These four categories have been reviewed separately because there is a logical progression of these topics in the latter part of this document, although certain papers in polymerization control have covered more than one of these categories in detail.

2.1 Modeling

There is a growing need for a detailed quantitative understanding of the phenomena occurring in a polymer reactor. These mathematical descriptions or models can be used to design optimal feedback control strategies resulting in better profitability for the polymerization processes. The physical phenomena occurring in the polymerization reactor can be classified into the following three levels of modeling [136]:

- Microscale chemical kinetics
- Mesoscale physical/transport phenomena
- Macroscale reactor phenomena

The mathematical techniques for microscale kinetic modeling can be divided into two approaches, statistical methods and detailed species balance methods. The statistical methods are based on representing the polymerization process as a stochastic process [50, 99]. The statistical approach based on the Markov chain method fails when the reaction probabilities are not constant. The detailed species balance method based on solving kinetic differential equations has been recommended [132, 83]. The solution procedures for solving the resulting species balances have been reviewed in detail [134, 14]. The species balance approach has been applied to different types of polymerization processes. The polymer product characteristics are dependent on its chain length distribution. Ray details the different mathematical techniques for calculating polymer molecular weight distributions and their moments [132, 19]. The kinetics of copolymerization systems and their molecular weight distributions have been evaluated from the appropriate process models [131, 133]. The mathematical technique of generating functions to evaluate molecular weight distributions has been reviewed, applied and experimentally verified for a linear polycondensation process [32, 30, 31]. The quasi-steady-state assumption for the live polymer chains and the long-chain hypothesis for polymer product are common assumptions employed in modeling polymerization kinetics to reduce model complexity [154]. Fundamental physical models for different types of polymerization processes have been reported (Table 2.1).

Polymerization process	Review articles	Research articles
Polycondensation	[72]	[73, 103, 104]
Gas phase polymerization	[172]	[51, 38, 71, 68, 177]
Emulsion polymerization	[140, 41, 144]	[110, 118, 128, 129, 140, 116, 117]
Suspension polymerization	[176]	[77, 78, 178]

Table 2.1: Polymerization modeling literature

A physical model for anionic solution polymerization of butadiene has been developed for both batch and continuous processes [20, 48]. Most of the continuous polymerization reactors that are examined in the literature have been modeled as a CSTR. Zacca and Ray have given an elaborate model for the heterogeneous polymerization in loop reactors that does not make the CSTR assumption [177]. They illustrated the differences between the loop reactor with different recycle ratios and CSTR using simulations of their detailed model. Mesoscale transport phenomena needs to be considered for multi-phase polymerization processes. There has been significant work on interphase and intraphase transport phenomena in Ziegler-Natta olefin polymerization [52, 69, 70]. Experimental work on free radical polymerization to understand the mechanism of diffusion-controlled reactions has also been performed [179]. A droplet/particle population balance model has been developed to predict the evolution of drop-size distribution in agitated suspension polymerization reactors [22]. Steady-state multiplicity and complex dynamic behavior can be observed under certain operating conditions in continuous polymerization reactors [167, 89, 60, 146, 82, 161, 162, 122]. A good understanding of these complex dynamics is essential for the design and operation of such reactors. Empirical models can also be used to describe the physical phenomena taking place in polymerization reactors. There has been some work on empirical models using regression predictors to model and control polymer product quality [173, 101]. The use of empirical models has been recommended to avoid the computationally intensive on-line optimization involved in using theoretical models. A multi-way principal component analysis model based on historical data has been used to monitor new batches and detect faults in a batch polymerization process [113]. Most of the models that have been used to estimate and control polymerization processes are non-empirical and consist of detailed modeling equations describing physical phenomena.

2.2 Parameter Estimation

The models that have been developed need to be validated before they are used for monitoring, control and optimization of the polymerization processes. These models may have structural mismatch and/or parametric mismatch. Parametric mismatch can be corrected by estimating model parameters using available process data and information. Parameter estimates can be obtained by using least squares, maximum likelihood or Bayesian estimation [10]. Stewart has summarized the Bayesian and maximum likelihood approaches for parameter estimation from different types of multi-response data [157]. Biegler has presented a case study comparison on the efforts of different researchers who worked on the Dow parameter estimation problem that was distributed in 1981 [13]. This problem illustrates the estimation of parameters from industrial data after assuming a model structure for the process. Most of the research in the polymerization control literature has been done using simulation models so there is no need to estimate kinetic parameters after the model is developed and simulated [177, 5]. However, these researchers have introduced some sort of plant-model mismatch for the demonstration of their control strategies. There has been some work done using data sets from carefully monitored laboratory experiments that may not show typical behavior of a full-scale industrial process [33, 96, 21]. The unknown parameters have also been obtained by providing the appropriate experimental conditions to facilitate their estimation using linear regression [154]. Ogunnaike has reported estimating parameters in a fundamental model using plant start-up data for an industrial terpolymerization reactor [115]. On-line parameter estimation using weighted least squares has been compared to an extended Kalman filter using different simulation models for plant and process model [153]. The parameter estimates have also been reported from different experimental conditions for a polymerization process [6]. The parameter estimates obtained by researchers in polymerization processes have been mostly obtained by minimizing the weighted least-squares of measurement errors in outputs.

2.3 Control

The control of polymer reactors cannot be achieved in the same manner as other traditional chemical industries where the modeling problem is more straightforward [100]. The polymer processes are nonlinear and there is a lack of on-line measurements for the desired polymer properties. A brief discussion of these problems and some suggestions for overcoming them have been given by Ray [135]. The measurement techniques that are used in polymerization processes have been reviewed in detail [148, 41]. A detailed industrial perspective of the polymer control problem has been provided by Congalidis and Richards [29]. The application of an industrial model predictive control tool to polymerization processes has been reviewed [147].

The polymer control problem was initially tackled as an optimal control problem [92]. The idea was to evaluate first an optimal trajectory of inputs that would be closely followed during the course of the polymerization process. Optimal control and start-up of polymerization processes has been studied for a couple of decades [63, 174]. The minimum time problem for batch polymerization has been examined and solved as an optimal control problem using Pontryagin's maximum principle [124, 23, 163, 47, 150]. The optimal control problem has also been solved using a nonlinear programming problem formulation [12, 98, 75, 74]. Various simulation studies that solve the optimal control problem for polymerization processes have been carried out [53, 2, 169, 34, 94, 36, 55]. An attempt has been made to mimic real data and recompute optimal trajectories in case of failure [55]. Tensile strength of the polymer product has been directly related to the molecular weight distribution that is used to obtain the optimal control trajectory [35]. The optimal control profiles have been evaluated and then implemented experimentally [154, 145, 164, 36, 21]. The minimum-time optimal control policy obtained has been evaluated and experimentally implemented for the solution polymerization of methyl methacrylate [123]. The optimal grade transitions for a polymerization process have been evaluated using the control vector parameterization method [159]. These optimal control synthesis methods have yielded good results in the laboratory. However, problems arise in industrial reactors due to significant process disturbances and modeling errors.

A lot of optimal control problems have been solved to obtain the required reactor temperature profile that will result in attainment of process objectives. It has been assumed that the required reactor temperature control can be achieved easily. The temperature control problem may be the bottleneck in the control system design. In that case, the reactor temperature controller should be studied in more detail. The reactor temperature control problem has been studied in various simulation studies [64, 42, 59, 27]. Various experimental studies for reactor temperature control have also been carried out using different types of controllers [26, 33, 96, 125, 112, 102, 138]. A simple polymer reactor temperature cascade controller has been implemented for the experimental system used in methyl methacrylate polymerization [33]. The jacket set-point temperature was calculated from the energy balance and the time-varying heat transfer coefficient was estimated on-line using the extended Kalman filter. The industrial case study presented by Chylla and Haase [26] has detailed equations for reactor temperature control problem. Infeasible regions for reactor temperature based on steady-state multiplicity analysis for a jacketed styrene polymerization process with an energy balance for coolant are also provided [143].

The general objectives of ensuring polymer quality and quantity have been analyzed in various studies in different ways. The choice of different manipulated variables on the performance of a copolymerization reactor has been examined by using a nonlinear process model [165]. The multi-objective optimization problem for the optimal reactor operation has been solved by determining the non-inferior or Pareto optimal set of solutions. A similar multi-objective dynamic optimization has been done experimentally for a copolymerization process [25]. The control of cumulative polymer molecular weight has been explored by ensuring that the instantaneous polymer produced has the desired molecular weight [11]. A similar optimal open-loop control policy has been evaluated and then a feedback controller developed for the styrene-butadiene rubber process [88]. The optimal open-loop control policy was evaluated by ensuring that the instantaneous product quality does not change from its desired value. Steady-state optimization of polymer reactors has been carried out to get desired process results in simulation studies [85, 97, 44]. The steady-state optimization strategy has also been verified experimentally to produce the required polymers [44].

A large majority of articles in polymer control are concerned with dynamic controllers like the proportional-integral-derivative controller (PID), model predictive controller (MPC), adaptive controller, input-output linearization controller and gain scheduled controller. Various simulation studies have been reported for these dynamic controllers. Simulation studies consisting of appropriately chosen control loop pairings and tuned PID controllers have been carried out [139, 28, 152, 151, 3]. These PID controllers have also been implemented in laboratory scale experiments [24, 45]. A model predictive control scheme is compared with a PID controller in a simulation study for methylmethacrylate polymerization [65]. Model predictive controllers based on Volterra models have been evaluated in simulations [106, 105]. The model predictive controller based on Volterra models is claimed to do better than that based on a linear model since the Volterra model captures some nonlinearities [106]. Dynamic Matrix Controller (DMC) is a popular from of model predictive controller that is widely used in the industry [109]. A DMC scheme has been evaluated and compared to a PID controller to control temperature and conversion for styrene polymerization [59]. A QDMC scheme for the bulk polymerization of styrene has also been reported [56]. A DMC scheme has also been developed to control reactor temperature and number average molecular weight for a semibatch polymerization process [121]. A DMC scheme is compared with a self-tuning regulator for methylmethacrylate polymerization in a simulation study [84]. Adaptive control has been used for controlling polymer reactors [166, 168]. The adaptive controller has also been augmented by a PID controller to obtain desired polymer in the laboratory [168].

Non-linear control of polymer processes based on input-output linearization has been attempted by various researchers [4, 154, 155, 5, 170, 171]. The feedback linearization approach does not incorporate constraints properly in the controller formulation thereby imposing performance limitations for realistic situations. A feedforward-feedback controller based on complete input-output linearization has been developed after establishing the conditions for solvability of the control problem [5]. A similar globally linearizing controller was implemented experimentally for a batch polymerization reactor and shown to perform better than a conventional PID controller [154]. An open-loop optimal policy based on global input/output linearization methods was evaluated for polyethylene reactors [108]. The globally linearizing controller was also implemented for the control of a polymerization reactor with a singular characteristic matrix by using a dynamic linearizing state feedback instead of a static one [156]. A feedback linearizing controller has also been implemented using the linear model predictive control structure to evaluate the control moves for the transformed inputs [90].

Non-linear control based on gain scheduling has also been reported [86, 43]. Klatt and Engell have performed gain scheduling around the nominal trajectory generated by the feedforward controller instead of the traditional method of scheduling for a number of operating points. Gain scheduling has also been performed in a two-dimensional space by explicitly accounting for the time variation of the scheduling variable [43]. Standard scheduling methods based on a set of linear models using Bayesian estimation for model selection to achieve nonlinear controller design for polymerization processes have been used [8, 91]. A set of linear models will require extensive bookkeeping and will fail to achieve required process objectives when there is a significant disturbance or the required grade is significantly different. A set of linear models will always give sub-optimal results in addition to the fact that there are no clear guidelines to choose a sufficient set of linear models. An infinite set of linear models spanning the entire operating spectrum is similar to having a non-linear model predictive controller framework. The set of linear models has the advantage that the models can be empirical and do not require any knowledge of reaction kinetics or other process information. The linear model based approach will be efficient in the absence of significant disturbances or product grade changes.

Most polymer control studies have not considered long sampling time with associated delays for key product quality measures. Ellis *et al.* have taken into account the realistic situation of periodic and time-delayed measurements of average molecular weight in the polymer control problem [45]. Multi-rate sampling in polymerization control, using an Extended Kalman Filter and PID controllers, has been considered for polystyrene [81]. The non-linear model has also been directly used in a multi-rate state estimator for solution polymerization of styrene [160].

There have been some simulation studies on polymer control from industrial practitioners [115, 109]. A two-tier cascade control scheme has been used by industrial researchers to deal with the unavailability of on-line key product quality variable measurements [115, 114]. In the two-tier system, the setpoints for the on-line outputs are based on the targets for the laboratory outputs. Hence, the infrequent laboratory measurements are not used in the feedback control loop. The model predictive controller developed by Ogunnaike is based on a linear model and its performance is evaluated using the nonlinear model as the plant [115].

The polymer control problem has also been solved by using empirical control schemes drawn from process insight and experience [119, 37, 1]. Penlidis *et al.* split the feed to the CSTR trains [119] to achieve process design and control objectives. Ahn *et al.* used catalyst mixtures to obtain the required molecular weight distribution in propylene polymerization [1]. A mid-course correction control policy also has been suggested for polymer processes because there is a lack of product quality measurements during the course of the batch production [173]. This mid-course policy has been implemented using models for the polymerization of styrene-butadiene rubber. Thus, the polymerization control problem has been solved using different feedback control techniques.

2.4 Monitoring

The performance of feedback controllers has to be evaluated and monitored to justify implementation of advanced control schemes. The control loop performance can be assessed by comparing it with the minimum variance control law that is used as a benchmark [7, 62, 40]. The original minimum variance controller used a process model [7] whereas the current research work [62, 40, 79] has emphasized that the minimum-variance calculation can be performed without a model. A detailed review of process monitoring, with a brief tutorial and future directions for research, has been provided [126]. An industrial perspective on process monitoring and diagnosis with data has been reported [87]. The performance of multivariable feedback controllers has also been discussed for specialized cases [61, 66, 67]. The general multivariable performance monitoring problem with interacting control loops and variable delays cannot be solved using the existing techniques reported in the literature [126]. After assessing the performance of the feedback controller against the theoretical benchmark of minimum variance control, the modeling inadequacies may be identified by doing correlation checks [17]. These correlation checks identify the modeling inadequacies that may be present in the process model.

2.5 Comments

The models that have been reported in the literature for polymerization processes are detailed first-principles physical models. The parameter estimation problem for these processes has not been examined in much detail because most work has been done with simulation models in which all the parameter values are assumed. The feedback control problem was initially tackled as the development of an open-loop control policy for the process. There has been work on feedback control strategies using PID controllers, globally linearizing controllers, gain scheduling and model predictive control schemes. Most of the work does not address the following typical characteristics of polymerization control

- Multi-rate sampling of product quality measures with associated delays
- Realistic disturbances and plant-model mismatch for the process
- Performance assessment and monitoring of the feedback control scheme

Many researchers have addressed the fact that polymerization processes are non-linear; therefore a control law based on a non-linear model may yield better results. However, the motivation for a non-linear control law for polymerization processes has not been shown clearly by demonstrating a case where the control law based on a fixed linear model fails. These issues are addressed in this dissertation on polymerization control.

Chapter 3

Process Description and Model for MMA-VA process

The MMA-VA copolymerization process consists of a well-mixed reactor followed by a product separator, both shown in Figure 3.1. The process is used to make various grades of copolymer. These grades are characterized by the mole fraction of monomer A (MMA) in the copolymer product and the intrinsic viscosity of the copolymer product. The copolymer viscosity and composition are varied for each grade depending upon the market requirements. The feed to the reactor consists of the monomers (MMA and VA), initiator (AIBN), transfer agent (acetaldehyde) and inhibitor (m-dinitrobenzene) dissolved in a solvent (benzene). The transfer agent is used to provide better control of the polymer molecular weight. A coolant is employed for the removal of heat released due to polymerization. The polymer product is separated from the unreacted hydrocarbons in a downstream separator. A physical model based on first principles is proposed to enable us to capture the information in the process output measurements and develop appropriate feedback control strategies. The process model is a quantitative representation of the various reactions taking place in the reactor along with other physical phenomena governing the process of polymerization. The flow rate and composition of the feed, and product streams are measured along with the reactor temperature. The polymer production rate is obtained by an on-line measurement of the refractive index that yields conversion thereby giving the production rate. An off-line laboratory measurement is also made for the polymer viscosity and composition. The polymer viscosity is measured using a capillary viscometer and the polymer product composition is measured using NMR spectroscopy. The polymer product quality measurements of viscosity and composition are characterized by large delays and sampling intervals.

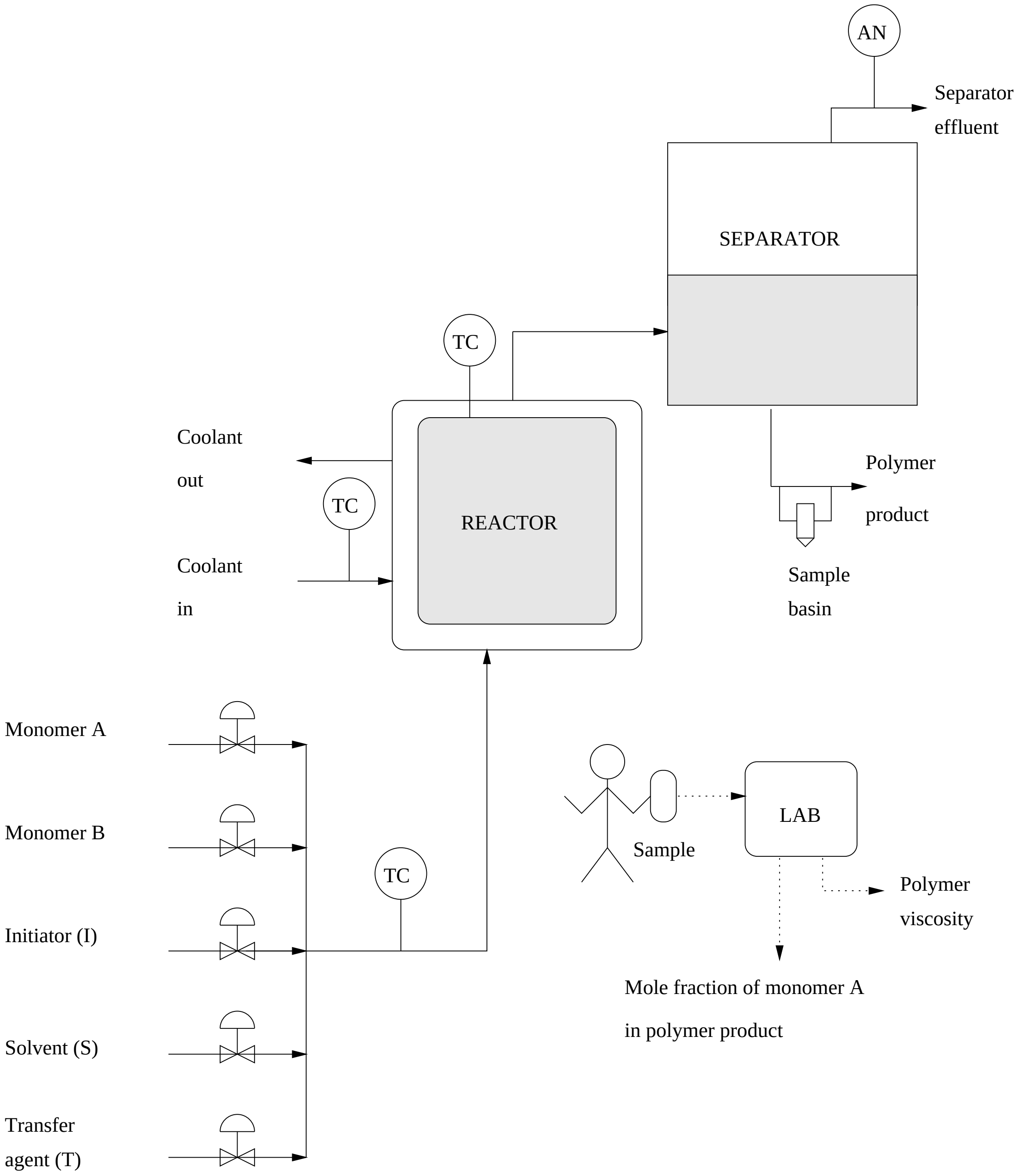

Figure 3.1: MMA-VA polymerization process

3.1 Polymerization Kinetics

The kinetics of copolymerization have been discussed extensively by Ray [133, 132]. The copolymerization of methyl methacrylate (A) and vinyl acetate (B) is carried out using free-radical kinetics in the presence of initiator (I), solvent (S), chain transfer agent (T) and inhibitor (Z). $A_{n,m}\bullet$ and $B_{n,m}\bullet$ symbolize live polymer chains containing n units of monomer A and m units of monomer B that terminate in A and B, respectively. $P_{n,m}$ represents a dead polymer chain containing n units of monomer A and m units of monomer B. The reaction mechanism may be divided into the following reactions [28].

Initiation. The initiator can decompose to form free radicals ($I\bullet$) that add to a molecule of monomer to form free-radical active centers. The solvent (S) and transfer agent (T) can also form free radicals that can result in free radical active centers.

$$I \overset{k_i}{\to} 2I\bullet \tag{3.1}$$

$$I\bullet + A \overset{k_{ii}}{\to} A_{1,0}\bullet \tag{3.2}$$

$$I\bullet + B \overset{k_{ii}}{\to} B_{0,1}\bullet \tag{3.3}$$

$$S\bullet + A \overset{k_{is}}{\to} A_{1,0}\bullet \tag{3.4}$$

$$S\bullet + B \overset{k_{is}}{\to} B_{0,1}\bullet \tag{3.5}$$

$$T\bullet + A \overset{k_{it}}{\to} A_{1,0}\bullet \tag{3.6}$$

$$T\bullet + B \overset{k_{it}}{\to} B_{0,1}\bullet \tag{3.7}$$

Propagation. A chain growth reaction mechanism is proposed for the live polymer chains ($A_{n,m}\bullet$ and $B_{n,m}\bullet$).

$$A_{n,m}\bullet + A \overset{k_{paa}}{\to} A_{n+1,m}\bullet \tag{3.8}$$

$$A_{n,m}\bullet + B \overset{k_{pab}}{\to} B_{n,m+1}\bullet \tag{3.9}$$

$$B_{n,m}\bullet + A \overset{k_{pba}}{\to} A_{n+1,m}\bullet \tag{3.10}$$

$$B_{n,m}\bullet + B \overset{k_{pbb}}{\to} B_{n,m+1}\bullet \tag{3.11}$$

Transfer. There are transfer reactions associated with the monomers (A and B), solvent (S) and transfer agent (T). The monomer, solvent or transfer agent reacts with the live polymer chain ($A_{n,m}\bullet$ or $B_{n,m}\bullet$) to form a dead polymer chain ($P_{n,m}$) and a free radical.

$$A_{n,m}\bullet + A \xrightarrow{k_{xaa}} P_{n,m} + A_{1,0}\bullet \tag{3.12}$$
$$A_{n,m}\bullet + B \xrightarrow{k_{xab}} P_{n,m} + B_{0,1}\bullet \tag{3.13}$$
$$B_{n,m}\bullet + A \xrightarrow{k_{xba}} P_{n,m} + A_{1,0}\bullet \tag{3.14}$$
$$B_{n,m}\bullet + B \xrightarrow{k_{xbb}} P_{n,m} + B_{0,1}\bullet \tag{3.15}$$
$$A_{n,m}\bullet + S \xrightarrow{k_{xas}} P_{n,m} + S\bullet \tag{3.16}$$
$$B_{n,m}\bullet + S \xrightarrow{k_{xbs}} P_{n,m} + S\bullet \tag{3.17}$$
$$A_{n,m}\bullet + T \xrightarrow{k_{xat}} P_{n,m} + T\bullet \tag{3.18}$$
$$B_{n,m}\bullet + T \xrightarrow{k_{xbt}} P_{n,m} + T\bullet \tag{3.19}$$

Termination by coupling. The termination of polymerization occurs due to combination of two growing chains to form a single dead polymer molecule

$$A_{n,m}\bullet + A_{r,q}\bullet \xrightarrow{k_{caa}} P_{n+r,m+q} \tag{3.20}$$
$$A_{n,m}\bullet + B_{r,q}\bullet \xrightarrow{k_{cab}} P_{n+r,m+q} \tag{3.21}$$
$$B_{n,m}\bullet + B_{r,q}\bullet \xrightarrow{k_{cbb}} P_{n+r,m+q} \tag{3.22}$$

Termination by disproportionation. The termination of polymerization also occurs due to disproportionation of two growing chains to form two dead polymer molecules

$$A_{n,m}\bullet + A_{r,q}\bullet \xrightarrow{k_{daa}} P_{n,m} + P_{r,q} \tag{3.23}$$
$$A_{n,m}\bullet + B_{r,q}\bullet \xrightarrow{k_{dab}} P_{n,m} + P_{r,q} \tag{3.24}$$
$$B_{n,m}\bullet + B_{r,q}\bullet \xrightarrow{k_{dbb}} P_{n,m} + P_{r,q} \tag{3.25}$$

Inhibition. The live polymer chains ($A_{n,m}\bullet$ and $B_{n,m}\bullet$) can also terminate into dead polymer chains ($P_{n,m}$) due to the presence of an inhibitor (Z)

$$A_{n,m}\bullet + Z \xrightarrow{k_{za}} P_{n,m} \tag{3.26}$$
$$B_{n,m}\bullet + Z \xrightarrow{k_{zb}} P_{n,m} \tag{3.27}$$

The above reactions are assumed to be irreversible and first order with respect to each reactant. The kinetic rate constants for the above reactions are assumed to have a dependence on temperature given by the Arrhenius equation. These rate constants are assumed to be independent of reactor composition or chain length. These rate constants are not corrected for the gel effect that becomes important at high monomer conversions. This reaction mechanism is proposed to quantify the information available in the process measurements due to polymerization reactions.

Molar Production Rates. The molar production rates of reactor species can be written as

$$R_a = -\sum_{j=i,s,t} k_{ij} c_a c_{j\bullet} - \sum_{j=a,b} k_{pja} c_a c_{j\bullet} - \sum_{j=a,b} k_{xja} c_a c_{j\bullet} \tag{3.28}$$

$$R_b = -\sum_{j=i,s,t} k_{ij} c_b c_{j\bullet} - \sum_{j=a,b} k_{pjb} c_b c_{j\bullet} - \sum_{j=a,b} k_{xjb} c_b c_{j\bullet} \tag{3.29}$$

$$R_i = -k_i c_i \tag{3.30}$$

$$R_s = -\sum_{j=a,b} k_{xjs} c_s c_{j\bullet} \tag{3.31}$$

$$R_t = -\sum_{j=a,b} k_{xjt} c_t c_{j\bullet} \tag{3.32}$$

$$R_z = -\sum_{j=a,b} k_{zj} c_z c_{j\bullet} \tag{3.33}$$

3.2 Process Model

The differential material balances including the rate expressions and the energy balance coupled with the equations for the physical phenomena constitute the dynamic process model. The following assumptions are made for developing the process model

- Perfectly mixed tank (Appendix A)
- Linear mixing rule for reactor density (Appendix B)

The mole balances for the reactor concentrations (c_k) can be obtained using feed concentrations ($c_{k,f}$) and molar production rates (R_k)

$$\frac{dc_k}{dt} = \frac{c_{k,f} - c_k}{\theta_r} + R_k, \qquad k = a, b, i, s, t, z \tag{3.34}$$

with the reactor residence time (θ_r) evaluated as

$$\theta_r = \frac{V_r}{Q_f} \tag{3.35}$$

The species molar concentrations in the feed ($c_{k,f}$) can be determined from molar feed rates ($F_{k,f}$) and volumetric feed rate (Q_f).

$$c_{k,f} = \frac{F_{k,f}}{Q_f}, \qquad k = a, b, i, s, t, z \tag{3.36}$$

The molar feed rates ($F_{k,f}$) can be determined from the mass feed rates ($G_{k,f}$)

$$F_{k,f} = \frac{G_{k,f}}{M_k}, \qquad k = a, b, i, s, t, z \tag{3.37}$$

The instantaneous polymerization rate (G_{pi}) can be evaluated using molar production rates (R_a and R_b) along with molecular weights (M_a and M_b).

$$G_{pi} = -R_a M_a - R_b M_b \tag{3.38}$$

The functions of states and kinetic parameters that appear in the process model are

$$\beta = \frac{(k_{pab} + k_{xab})c_b}{(k_{pba} + k_{xba})c_a} \tag{3.39}$$

$$l_1 = k_{caa} + 2\beta k_{cab} + k_{cbb}\beta^2 + k_{daa} + 2\beta k_{dab} + k_{dbb}\beta^2 \tag{3.40}$$

$$l_2 = (k_{za} + k_{zb}\beta)c_z \tag{3.41}$$

$$l_3 = -2k_i c_i \tag{3.42}$$

$$\alpha_1 = \frac{k_{paa}c_a}{\sum_{j=a,b}(k_{paj}c_j + k_{caj}c_{j\bullet} + k_{daj}c_{j\bullet}) + \sum_{j=a,b,s,t}(k_{xaj}c_j) + k_{za}c_z} \tag{3.43}$$

$$\alpha_2 = \frac{k_{pbb}c_b}{\sum_{j=a,b}(k_{pbj}c_j + k_{cbj}c_{j\bullet} + k_{dbj}c_{j\bullet}) + \sum_{j=a,b,s,t}(k_{xbj}c_j) + k_{zb}c_z} \tag{3.44}$$

$$c_1 = \frac{2k_i c_i + \sum_{j=a,b}\sum_{k=s,t} k_{xjk}c_{j\bullet}c_k}{k_{paa}(c_a + c_b)} + \frac{\sum_{j=a,b} k_{xja}c_{j\bullet}}{k_{paa}} \tag{3.45}$$

$$c_2 = \frac{2k_i c_i + \sum_{j=a,b}\sum_{k=s,t} k_{xjk}c_{j\bullet}c_k}{k_{pbb}(c_a + c_b)} + \frac{\sum_{j=a,b} k_{xjb}c_{j\bullet}}{k_{pbb}} \tag{3.46}$$

The model is simplified using quasi-steady-state approximations for the live polymer. The equations for the active and dead polymer chains are simplified by taking the zeroth, first and second moments.

3.2.1 Quasi-Steady-State Approximations

The differential equations for the live polymer chains are transformed into algebraic equations using the quasi-steady-state approximations for the live polymers because of their faster kinetic equilibration relative to other species [28]. These approximations also reduce the stiffness arising from multiple time-scales in the system of differential equations representing the process model. The rate of conversion of live polymer chains ended by monomer A to live polymer chains ended by monomer B is taken equal to the rate of conversion of live polymer chains ended by monomer B to live polymer chains ended by monomer A thereby resulting in

$$k_{pab}c_{a\bullet}c_b + k_{xab}c_{a\bullet}c_b = k_{pba}c_{b\bullet}c_a + k_{xba}c_{b\bullet}c_a \tag{3.47}$$

Equation 3.47 gives the following relationship for the molar concentrations of live polymer chains

$$c_{b\bullet} = \beta c_{a\bullet} \tag{3.48}$$

The rate of generation of free radicals is the same as their rate of consumption for the quasi-steady-state assumption resulting in

$$\begin{aligned} 2k_i c_i \quad &= \quad k_{caa}c_{a\bullet}^2 + 2k_{cab}c_{a\bullet}c_{b\bullet} + k_{cbb}c_{b\bullet}^2 \\ &\quad +k_{daa}c_{a\bullet}^2 + 2k_{dab}c_{a\bullet}c_{b\bullet} + k_{dbb}c_{b\bullet}^2 + k_{za}c_{a\bullet}c_z + k_{zb}c_{b\bullet}c_z \end{aligned} \tag{3.49}$$

Equation 3.49 gives the following relationship for the molar concentration of live polymer chains ended by monomer A ($c_{a\bullet}$)

$$c_{a\bullet} = \frac{-l_2 + \sqrt{l_2^2 - 4l_1l_3}}{2l_1} \tag{3.50}$$

A relationship can be found between the concentration of live polymer chains of length (n, m) ended by A ($A_{n,m\bullet}$) and the concentration of live polymer chains of length $(n-1, m)$ ($A_{n-1,m\bullet}$ and $B_{n-1,m\bullet}$) by making the quasi-steady-state assumption for the live polymer chains ended by A ($A_{n,m\bullet}$)

$$\begin{aligned} &A_{n-1,m\bullet}(k_{paa}c_a) + B_{n-1,m\bullet}(k_{pba}c_a) = \\ &A_{n,m\bullet}\Big(\sum_{j=a,b}(k_{paj}c_j + k_{caj}c_{j\bullet} + k_{daj}c_{j\bullet}) + \sum_{j=a,b,s,t}(k_{xaj}c_j) + k_{za}c_z\Big) \end{aligned} \tag{3.51}$$

Equation 3.51 can be simplified to get the following expression for the live polymer chains ended by A ($A_{n,m\bullet}$)

$$A_{n-1,m\bullet}\alpha_1 + B_{n-1,m\bullet}\frac{\alpha_1\gamma}{r_1} = A_{n,m\bullet} \tag{3.52}$$

A similar relationship can be found between the concentration of live polymer chains of length (n, m) ended by B ($B_{n,m\bullet}$) and the concentration of live polymer chains of length $(n, m-1)$ ($A_{n,m-1\bullet}$ and $B_{n,m-1\bullet}$) by making the quasi-steady-state assumption for the live polymer chains ended by B ($B_{n,m\bullet}$)

$$\begin{aligned} &B_{n,m-1\bullet}(k_{pbb}c_b) + A_{n,m-1\bullet}(k_{pab}c_b) = \\ &B_{n,m\bullet}\Big(\sum_{j=a,b}(k_{pbj}c_j + k_{cbj}c_{j\bullet} + k_{dbj}c_{j\bullet}) + \sum_{j=a,b,s,t}(k_{xbj}c_j) + k_{zb}c_z\Big) \end{aligned} \tag{3.53}$$

Equation 3.53 can be simplified to get the following expression for the live polymer chains ended by B ($B_{n,m\bullet}$)

$$B_{n,m-1\bullet}\alpha_2 + A_{n,m-1\bullet}\frac{\alpha_2}{\gamma r_2} = B_{n,m\bullet} \tag{3.54}$$

The quasi-steady-state assumptions for the live polymer chains of single chain length ended by A ($A_{1,0\bullet}$) and the live polymer chains of single chain length ended by B ($B_{0,1\bullet}$) result in the following equations

$$A_{1,0\bullet} = c_1\alpha_1 \tag{3.55}$$
$$B_{0,1\bullet} = c_2\alpha_2 \tag{3.56}$$

The above equations for the live polymer chains enable us to explicitly evaluate their molar concentrations at different times without introducing significant errors because the relative rate of change for the live polymers is orders of magnitude higher than the other reactor species based on typical values.

3.2.2 Dead Copolymer Composition

The molar concentrations of the two monomers in the dead copolymer (λ_a and λ_b) can be evaluated by using the following molar balances

$$\frac{d\lambda_a}{dt} = \frac{\lambda_{a,f} - \lambda_a}{\theta_r} - R_a \tag{3.57}$$
$$\frac{d\lambda_b}{dt} = \frac{\lambda_{b,f} - \lambda_b}{\theta_r} - R_b \tag{3.58}$$

The mole fraction of monomer A (Y_{ap}) in the dead polymer can be evaluated as

$$Y_{ap} = \frac{\lambda_a}{\lambda_a + \lambda_b} \tag{3.59}$$

3.2.3 Energy balance

The reactor energy balance can be written for the continuous stirred tank reactor to obtain reactor temperature (T_r) after making the appropriate assumptions (Appendix C).

$$\frac{dT_r}{dt} = \frac{(-\Delta H_{paa}k_{paa}c_a c_{a\bullet} - \Delta H_{pba}k_{pba}c_a c_{b\bullet} - \Delta H_{pab}k_{pab}c_b c_{a\bullet} - \Delta H_{pbb}k_{pbb}c_b c_{b\bullet})}{\rho_r C_{pr}} + \frac{T_f - T_r}{\theta_r} - \frac{U_r S_r (T_r - T_j)}{V_r C_{pr}\rho_r} \tag{3.60}$$

The energy balance only takes into account the propagation reactions for the live polymer chains ($A_{n,m\bullet}$ and $B_{n,m\bullet}$) because their reaction rates are far greater than the other reactions for the polymerization process (Figure **??**).

3.2.4 Moments for the Active and Dead Polymers

The intrinsic viscosity of the polymer, which is measured for the copolymer, can be obtained from the average molecular weight using the Mark-Houwink equation

$$[\eta] = KM_v^a \tag{3.61}$$

where K and a are characteristic constants. The viscosity average molecular weight (M_v) is replaced by the weight average molecular weight (M_w) in equation 3.61. The corresponding constants (K and a) are taken from literature [18]. The weight average molecular weight for the polymer is obtained using leading moments for the molecular weight distribution. Hence, there is no need in this work to evaluate explicitly the entire chain length distribution of the polymer. The moments for the molecular weight distribution can be calculated by employing generating functions and other mathematical tools [132]. In this case, the leading moments for the polymer are obtained by explicitly evaluating the series summations involved. The zeroth, first and second moments of the molecular weight distribution for the dead polymer can be defined as

$$\psi_k^p = \sum_{n=0}^{\infty} \sum_{m=0}^{\infty} (nM_a + mM_b)^k P_{n,m}, \qquad k = 0, 1, 2 \tag{3.62}$$

Leading moments of the differential molecular weight distribution are also used to describe the state of the live polymer chains. The zeroth, first and second moments of the molecular weight distribution for the live polymer can be defined as

$$\psi_k^{a\bullet} = \sum_{n=0}^{\infty} \sum_{m=0}^{\infty} (nM_a + mM_b)^k A_{n,m\bullet}, \qquad k = 0, 1, 2 \tag{3.63}$$

$$\psi_k^{b\bullet} = \sum_{n=0}^{\infty} \sum_{m=0}^{\infty} (nM_a + mM_b)^k B_{n,m\bullet}, \qquad k = 0, 1, 2 \tag{3.64}$$

The number average molecular weight (M_n) and the weight average molecular weight (M_w) can be computed using the following relationships

$$M_n = \frac{\psi_1^p}{\psi_0^p} \tag{3.65}$$

$$M_w = \frac{\psi_2^p}{\psi_1^p} \tag{3.66}$$

The resulting equations for the zeroth, first and second moments for the live polymers are

$$\begin{aligned}
\psi_0^{a\bullet} &= c_{a\bullet} && (3.67)\\
\psi_0^{b\bullet} &= c_{b\bullet} && (3.68)\\
\psi_1^{a\bullet} &= \frac{M_a c_1 \alpha_1}{(1-\alpha_1)^2} + \frac{\alpha_1 \gamma}{r_1}\left(\frac{\psi_1^{b\bullet}}{1-\alpha_1} + \frac{M_a \psi_0^{b\bullet}}{(1-\alpha_1)^2}\right) && (3.69)\\
\psi_1^{b\bullet} &= \frac{M_b c_2 \alpha_2}{(1-\alpha_2)^2} + \frac{\alpha_2}{\gamma r_2}\left(\frac{\psi_1^{a\bullet}}{1-\alpha_2} + \frac{M_b \psi_0^{a\bullet}}{(1-\alpha_2)^2}\right) && (3.70)\\
\psi_2^{a\bullet} &= M_a^2 c_1 \alpha_1 \frac{(1+\alpha_1)}{(1-\alpha_1)^3} + \frac{\alpha_1 \gamma}{r_1}\left(\frac{\psi_2^{b\bullet}}{1-\alpha_1} + \frac{M_a^2 \psi_0^{b\bullet}(1+\alpha_1)}{(1-\alpha_1)^3} + \frac{2M_a \psi_1^{b\bullet}}{(1-\alpha_1)^2}\right) && (3.71)\\
\psi_2^{b\bullet} &= M_b^2 c_2 \alpha_2 \frac{(1+\alpha_2)}{(1-\alpha_2)^3} + \frac{\alpha_2}{\gamma r_2}\left(\frac{\psi_2^{a\bullet}}{1-\alpha_2} + \frac{M_b^2 \psi_0^{a\bullet}(1+\alpha_2)}{(1-\alpha_2)^3} + \frac{2M_b \psi_1^{a\bullet}}{(1-\alpha_2)^2}\right) && (3.72)
\end{aligned}$$

Equations 3.69, 3.70, 3.71, and 3.72 for the moments of live polymer are equivalent to those obtained in literature [25]. The zeroth, first and second moments for the dead polymer change due to polymerization reactions as

$$\begin{aligned}
\frac{d\psi_0^p}{dt} &= \frac{\psi_{0f}^p - \psi_0^p}{\theta_r} + \sum_{j=a,b}\sum_{k=a,b}\left(\frac{1}{2}k_{cjk}c_{j\bullet}c_{k\bullet} + k_{djk}c_{j\bullet}c_{k\bullet} + k_{xjk}c_{j\bullet}c_k\right)\\
&\quad + \sum_{j=a,b}\left((k_{xjt}c_t + k_{zj}c_z + k_{xjs}c_s)c_{j\bullet}\right) && (3.73)\\
\frac{d\psi_1^p}{dt} &= \frac{\psi_{1f}^p - \psi_1^p}{\theta_r} + \sum_{j=a,b}\sum_{k=a,b}\left((k_{cjk} + k_{djk})\psi_0^{j\bullet}\psi_1^{k\bullet} + k_{xjk}\psi_1^{j\bullet}c_k\right)\\
&\quad + \sum_{j=a,b}\left((k_{xjt}c_t + k_{zj}c_z + k_{xjs}c_s)\psi_1^{j\bullet}\right) && (3.74)\\
\frac{d\psi_2^p}{dt} &= \frac{\psi_{2f}^p - \psi_2^p}{\theta_r} + \sum_{j=a,b}\sum_{k=a,b}\left(k_{cjk}(\psi_0^{j\bullet}\psi_2^{k\bullet} + \psi_1^{j\bullet}\psi_1^{k\bullet}) + k_{djk}\psi_0^{j\bullet}\psi_2^{k\bullet} + k_{xjk}\psi_2^{j\bullet}c_k\right)\\
&\quad + \sum_{j=a,b}\left((k_{xjt}c_t + k_{zj}c_z + k_{xjs}c_s)\psi_2^{j\bullet}\right) && (3.75)
\end{aligned}$$

Equations 3.73, 3.74,and 3.75 for the moments of dead polymer are equivalent to those obtained in literature [28, 25].

3.2.5 Separator balances

The separator is modeled as a first-order lag on the species concentrations ($c_{k,s}$) with constant level

$$\frac{dc_{k,s}}{dt} = \frac{c_{k,sf} - c_{k,s}}{\theta_s}, \qquad k = a, b, i, s, t, z \tag{3.76}$$

where the separator residence time (θ_s) can be evaluated as

$$\theta_s = \frac{V_s}{Q_f} \tag{3.77}$$

3.2.6 Model parameters

The kinetic rate constants are of the Arrhenius type

$$k = Ae^{(-E/RT)} \tag{3.78}$$

The values of the pre-exponential factors (A) and the activation energies (E) are obtained from literature [28] and shown in Table 3.1. The following assumptions are also made

Pre-exponential factor			Activation energy		
A_i	4.5×10^{14}	s^{-1}	E_i	1.25×10^5	kJ/kmol
A_{caa}	4.209×10^{11}	m^3/kmol·s	E_{caa}	2.69×10^4	kJ/kmol
A_{cbb}	1.61×10^9	m^3/kmol·s	E_{cbb}	4.00×10^3	kJ/kmol
A_{daa}	0.0	m^3/kmol·s	E_{daa}	0.0	kJ/kmol
A_{dbb}	0.0	m^3/kmol·s	E_{dbb}	0.0	kJ/kmol
A_{paa}	3.207×10^6	m^3/kmol·s	E_{paa}	2.42×10^4	kJ/kmol
A_{pab}	1.233×10^5	m^3/kmol·s	E_{pab}	2.42×10^4	kJ/kmol
A_{pba}	2.103×10^8	m^3/kmol·s	E_{pba}	1.8×10^4	kJ/kmol
A_{pbb}	6.308×10^6	m^3/kmol·s	E_{pbb}	2.42×10^4	kJ/kmol
A_{xaa}	32.08	m^3/kmol·s	E_{xaa}	2.42×10^4	kJ/kmol
A_{xab}	1.234	m^3/kmol·s	E_{xab}	2.42×10^4	kJ/kmol
A_{xas}	86.6	m^3/kmol·s	E_{xas}	2.42×10^4	kJ/kmol
A_{xat}	2085.0	m^3/kmol·s	E_{xat}	2.42×10^4	kJ/kmol
A_{xba}	5.257×10^4	m^3/kmol·s	E_{xba}	1.8×10^4	kJ/kmol
A_{xbb}	1577.0	m^3/kmol·s	E_{xbb}	1.8×10^4	kJ/kmol
A_{xbs}	1514.0	m^3/kmol·s	E_{xbs}	1.8×10^4	kJ/kmol
A_{xbt}	4.163×10^5	m^3/kmol·s	E_{xbt}	2.42×10^4	kJ/kmol
A_{za}	2.2	m^3/kmol·s	E_{za}	0.0	kJ/kmol
A_{zb}	1.13×10^5	m^3/kmol·s	E_{zb}	0.0	kJ/kmol

Table 3.1: Kinetic parameters for MMA-VA copolymerization

for the kinetic parameters

$$k_{cba} = k_{cab} = \sqrt{k_{caa}k_{cbb}} \tag{3.79}$$

$$k_{dba} = k_{dab} = \sqrt{k_{daa}k_{dbb}} \tag{3.80}$$

The physical parameters [28] for the polymerization process are shown in Table 3.2. The thermodynamic parameters for the process are taken from literature (Table 3.3).

Physical parameter	Value
Reactor volume (V_r)	1.0 m^3
Reactor heat transfer area (S_r)	4.6 m^2
Separator volume (V_s)	4.0 m^3

Table 3.2: Physical parameters for MMA-VA copolymerization

Thermodynamic parameter	Value		Reference
Overall heat transfer coefficient (U_r)	6.0×10^{-2}	kJ/m^2·s·K	[28]
Heat of reaction 3.8 ($-\Delta H_{paa}$)	54.0×10^3	kJ/kmol	[28]
Heat of reaction 3.10 ($-\Delta H_{pba}$)	54.0×10^3	kJ/kmol	[28]
Heat of reaction 3.9 ($-\Delta H_{pab}$)	86.0×10^3	kJ/kmol	[28]
Heat of reaction 3.11 ($-\Delta H_{pbb}$)	86.0×10^3	kJ/kmol	[28]
Specific heat of MMA (C_{p_a})	1.9	kJ/kg·K	[107]
Specific heat of VA (C_{p_b})	1.7556	kJ/kg·K	[54]
Specific heat of benzene (C_{p_s})	1.672	kJ/kg·K	[120]
Specific heat of polymer (C_{p_p})	1.44	kJ/kg·K	[18]
Density of MMA (ρ_a)	940.0	kg/m^3	[18]
Density of VA (ρ_b)	931.7	kg/m^3	[18]
Density of benzene (ρ_s)	878.65	kg/m^3	[18]

Table 3.3: Thermodynamic parameters for MMA-VA copolymerization

3.2.7 Process Model Simulations

The process model is simulated for a reactor start-up by keeping all inputs constant except the MMA feed rate (Figure 3.2) The reactor is initially filled with a solvent without either of the two monomers or copolymer. All the inputs to the process are maintained constant except the MMA feed rate for start-up. The MMA concentration in the separator overhead increases with an increase in the MMA feed rate (Figure 3.3). The VA concentration in the separator overhead rises initially from zero but then decreases with an increase in MMA feed rate (Figure 3.4) because more live polymer chains are present to react with VA when the MMA feed rate is higher. The benzene concentration in the separator effluent decreases initially and then decreases further with an increase in the MMA feed rate (Figure 3.5) due to increased amounts of live polymer chains in the reactor resulting from higher amount of MMA in the feed. The increased amount of MMA in reactor also results in higher reactor temperature (Figure 3.6) and copolymer production rate (Figure 3.7). The mole fraction of MMA in the copolymer (Figure 3.8) and copolymer viscosity (Figure 3.9) increase with an increase in the MMA feed rate.

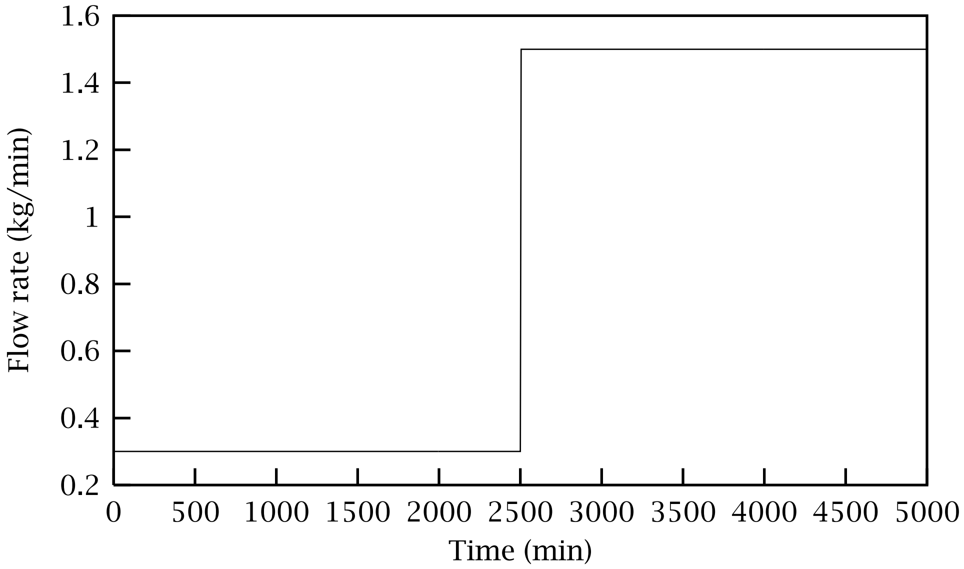

Figure 3.2: MMA feed rate to reactor

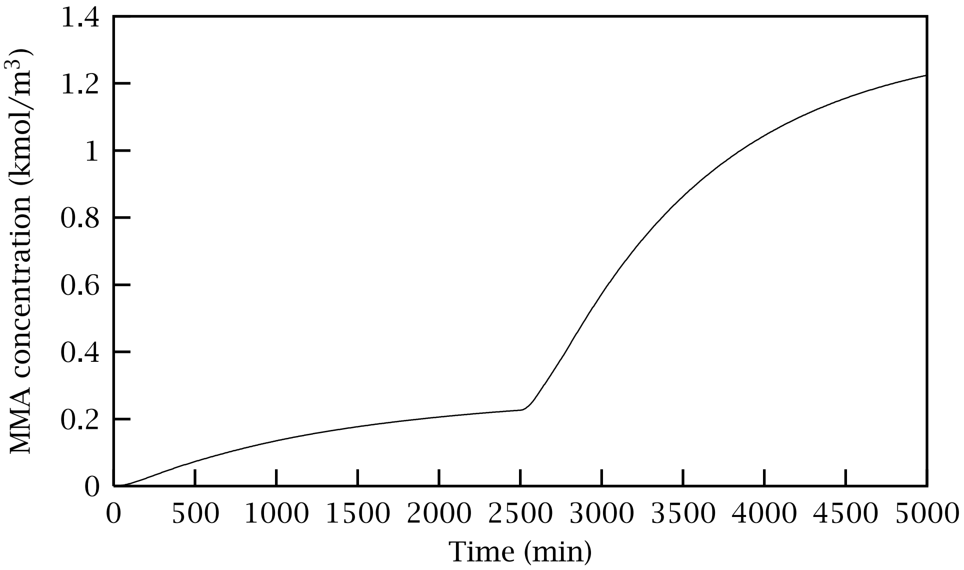

Figure 3.3: Separator effluent MMA

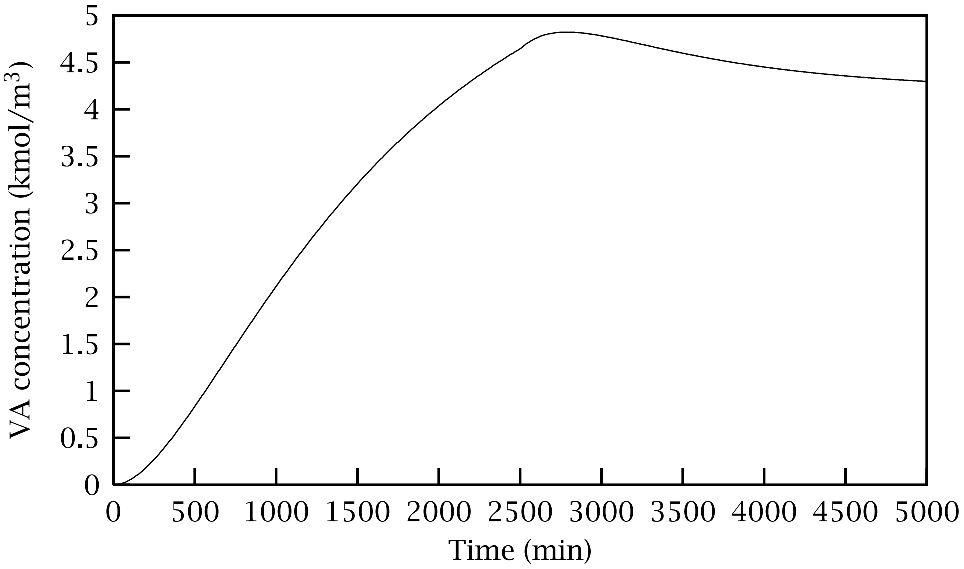

Figure 3.4: Separator effluent VA

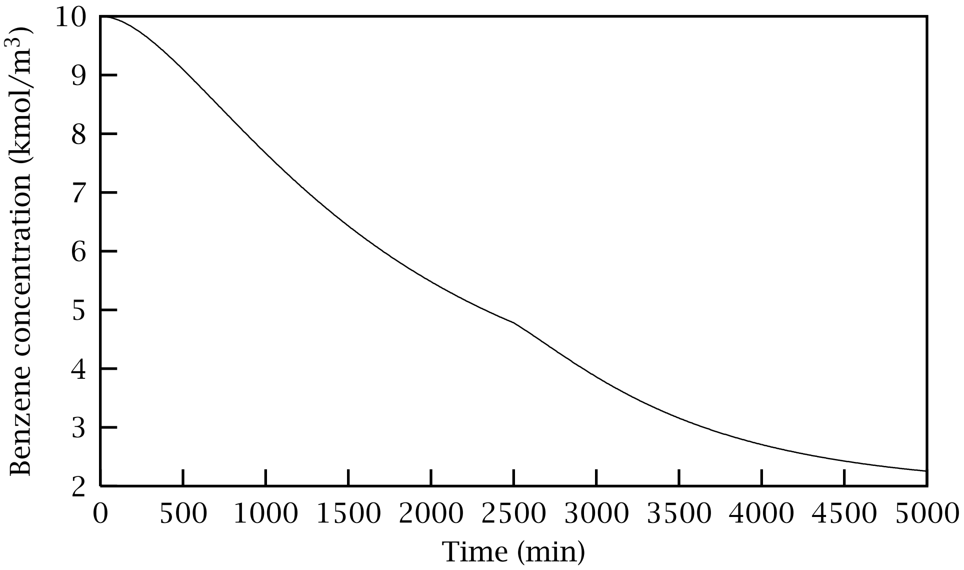

Figure 3.5: Separator effluent benzene

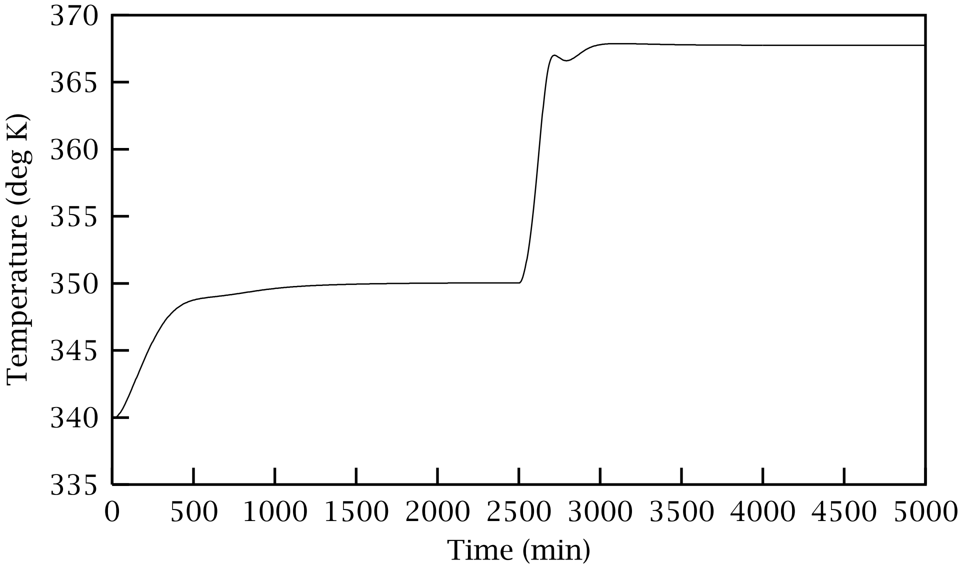

Figure 3.6: Reactor temperature

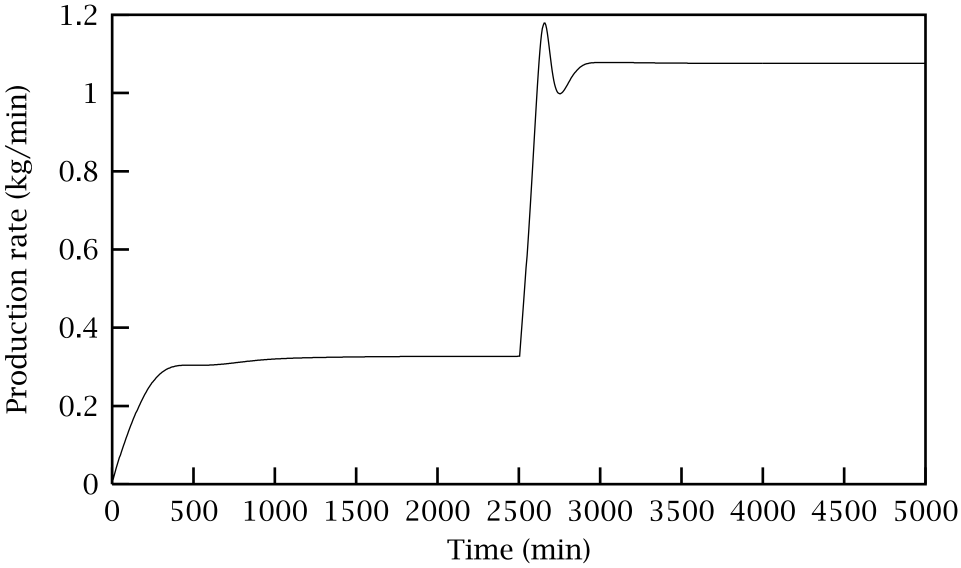

Figure 3.7: Polymer production rate

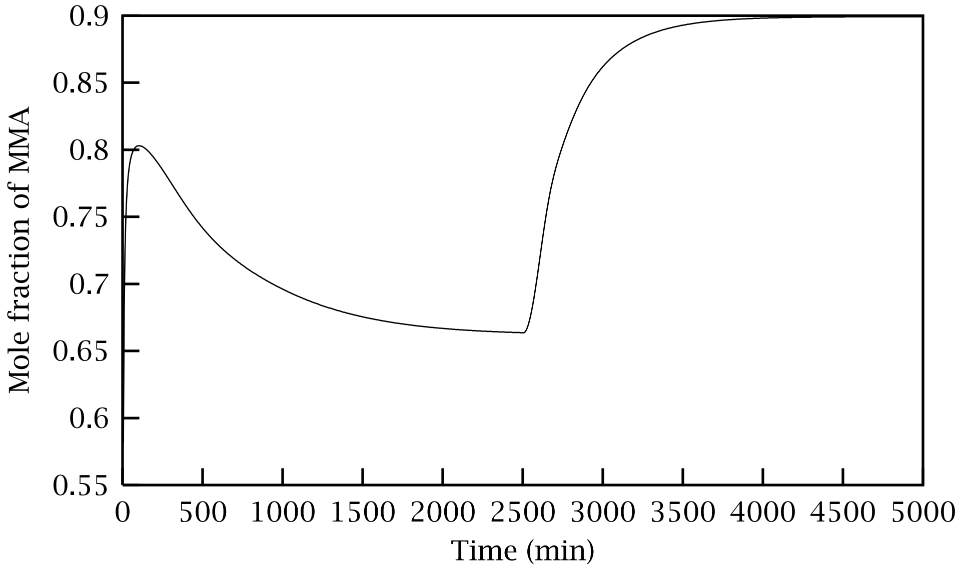

Figure 3.8: Copolymer product composition

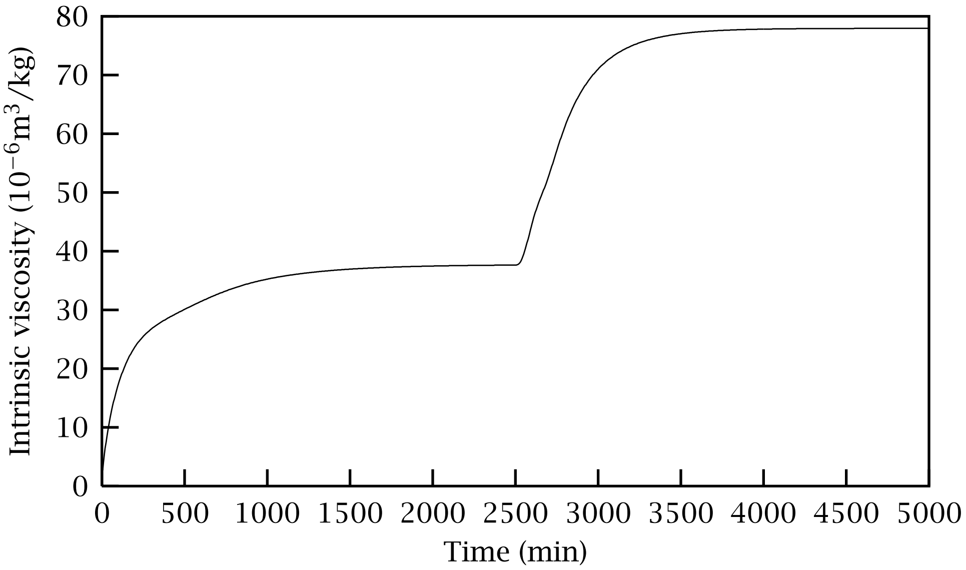

Figure 3.9: Intrinsic viscosity of copolymer

Chapter 4

Process Description and Model for the Industrial process

The industrial polymerization process consists of a well-mixed reactor followed by a product separator, both shown in Figure 4.1. The process is used to make various grades of copolymer and homopolymer. The copolymer grades are characterized by the ratio of comonomer to monomer in the copolymer product. The polymer viscosity is also varied for each copolymer grade depending upon the market requirements. The homopolymer grades are characterized by the average molecular weight of the product. The hydrocarbon feed consists of monomer, comonomer and inhibitor dissolved in a solvent. A cocatalyst is also dissolved in the solvent and fed to the reactor as catalyst feed. The transfer agent is used only to make the homopolymer while the comonomer is used only for the copolymer. A coolant is employed for the removal of heat released due to polymerization. The polymer product is separated from the unreacted hydrocarbons in a downstream separator. A basic physical model based on first principles is proposed to enable us to capture the information in the process output measurements and further use it to develop appropriate feedback control strategies. The process model [16] is a quantitative representation of the various reactions taking place in the reactor along with other physical phenomena governing the process of polymerization. The flow rate and composition of the feed and product streams is measured along with the reactor temperature. An off-line laboratory measurement is also made for the polymer viscosity of copolymer and average molecular weight of homopolymer.

4.1 Polymerization Kinetics

The kinetics of copolymerization have been discussed extensively by Ray [133, 132]. The copolymerization of monomer (M) and comonomer (C) is carried out at low temperature using an inorganic catalyst (A). The catalyst is accompanied by a cocatalyst

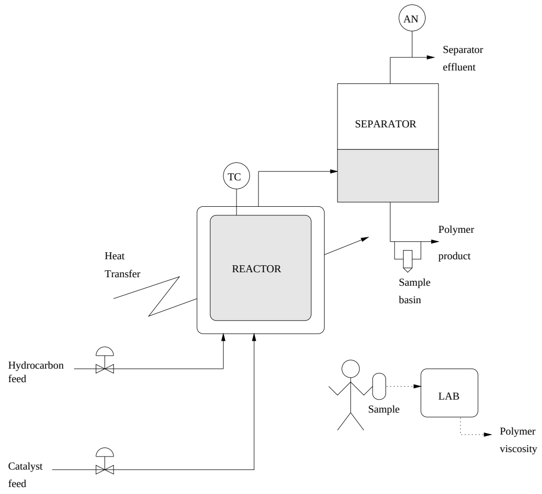

Figure 4.1: Industrial polymerization process

(RH) that renders it more reactive. A transfer agent (T) is fed into the reactor to make homopolymer in the absence of comonomer (C). The reactor also consists of certain inhibitor (B) that contributes to the termination of active polymer chains. The reaction mechanism, which is an ideal copolymerization based on the reactivity ratios [80], may be divided into five reactions as discussed below.

Catalyst Activation. A cocatalyst (RH) interacts with the catalyst (A) to produce an activated catalyst ($A^\star$) that is a proton donor. The catalyst activation reaction is

$$A + RH \xrightarrow{k_i} A^\star \tag{4.1}$$

Initiation. The dead monomer (M) or comonomer (C) reacts with the activated catalyst ($A^\star$) to form an active polymer of single chain length (P_1^+) as follows

$$A^\star + M \xrightarrow{k_{1_M}} P_1^+ \tag{4.2}$$

$$A^\star + C \xrightarrow{k_{1_C}} P_1^+ \tag{4.3}$$

Propagation. A chain growth reaction mechanism is proposed for the active polymer chains (P_j^+). The monomer (M) or comonomer (C) may react with the active polymer chain (P_j^+) to form another active polymer chain (P_{j+1}^+)

$$P_j^+ + M \xrightarrow{k_{p_M}} P_{j+1}^+ \tag{4.4}$$

$$P_j^+ + C \xrightarrow{k_{p_C}} P_{j+1}^+ \tag{4.5}$$

The model uses the long-chain hypothesis for the active polymer chains by not taking into account any differences between active polymer chains (P_j^+) ended by monomer or comonomer.

Transfer. There are transfer reactions associated with the monomer (M), comonomer (C) and transfer agent (T). The monomer (M) or comonomer (C) reacts with the active polymer (P_j^+) to form a dead polymer (P_j) and an active polymer of single chain length (P_1^+) during the polymerization process. A similar reaction occurs with the transfer agent (T).

$$P_j^+ + M \overset{k_{tr_M}}{\rightarrow} P_j + P_1^+ \tag{4.6}$$

$$P_j^+ + C \overset{k_{tr_C}}{\rightarrow} P_j + P_1^+ \tag{4.7}$$

$$P_j^+ + T \overset{k_{tr_T}}{\rightarrow} P_j + P_1^+ \tag{4.8}$$

Termination. The termination of polymerization occurs via the reaction of an active polymer (P_j^+) with the monomer (M), comonomer (C) or inhibitor (B) as follows

$$P_j^+ + M \overset{k_{T_M}}{\rightarrow} P_{j+1} \tag{4.9}$$

$$P_j^+ + C \overset{k_{T_C}}{\rightarrow} P_{j+1} \tag{4.10}$$

$$P_j^+ + B \overset{k_{T_B}}{\rightarrow} P_{j+1} \tag{4.11}$$

The reactions due to the comonomer do not take place for the homopolymerization process. The above reactions are assumed to be irreversible and first order with respect to each reactant. The kinetic rate constants for the above reactions are assumed to have a dependence on temperature given by the Arrhenius equation. These rate constants are assumed to be independent of reactor composition or chain length (j) of the active polymer (P_j^+). This simple reaction mechanism is proposed to quantify the information available in the process measurements due to polymerization reactions. A few of the above reactions are assumed to be negligible compared to the rest of them based on previous laboratory and simulation studies. The rate constants corresponding to those reactions are set to zero. These reactions are not clearly identified in this report so that the exact proprietary kinetic scheme for the polymerization process is not disclosed.

Rate Expressions. The molar production rates of reactor species can be written as

$$\begin{aligned}
r_{RH} &= -k_i[RH] && (4.12)\\
r_{A^\star} &= k_i[RH] - k_{1_M}[A^\star][M] - k_{1_C}[A^\star][C] && (4.13)\\
r_M &= -k_{1_M}[A^\star][M] - (k_{p_M} + k_{tr_M} + k_{T_M})[M][P^+], \qquad [P^+] = \sum_{j=1}^{\infty}[P_j^+] && (4.14)\\
r_C &= -k_{1_C}[A^\star][C] - (k_{p_C} + k_{tr_C} + k_{T_C})[C][P^+] && (4.15)\\
r_T &= -k_{tr_T}[T][P^+] && (4.16)\\
r_B &= -k_{T_B}[B][P^+] && (4.17)\\
r_{P_1^+} &= k_{1_M}[A^\star][M] + k_{1_C}[A^\star][C] + k_{tr_M}[M][P^+] + k_{tr_C}[C][P^+] + \\
&\quad k_{tr_T}[T][P^+] - (k_{p_M} + k_{tr_M} + k_{T_M})[M][P_1^+] - \\
&\quad (k_{p_C} + k_{tr_C} + k_{T_C})[C][P_1^+] - k_{tr_T}[T][P_1^+] - k_{T_B}[B][P_1^+] && (4.18)\\
r_{P_j^+} &= (k_{p_M}[M] + k_{p_C}[C])([P_{j-1}^+] - [P_j^+]) - (k_{tr_M} + k_{T_M})[M][P_j^+] - \\
&\quad (k_{tr_C} + k_{T_C})[C][P_j^+] - (k_{tr_T}[T] + k_{T_B}[B])[P_j^+], \qquad j = 2, 3.....\infty && (4.19)\\
r_{P^+} &= k_{1_M}[A^\star][M] + k_{1_C}[A^\star][C] - k_{T_M}[M][P^+] - k_{T_C}[C][P^+] - \\
&\quad k_{T_B}[B][P^+] && (4.20)\\
r_{P_1} &= k_{tr_M}[M][P_1^+] + k_{tr_C}[C][P_1^+] + k_{tr_T}[T][P_1^+] && (4.21)\\
r_{P_j} &= k_{tr_M}[M][P_j^+] + k_{tr_C}[C][P_j^+] + k_{tr_T}[T][P_j^+] + \\
&\quad k_{T_M}[M][P_{j-1}^+] + k_{T_C}[C][P_{j-1}^+] + k_{T_B}[B][P_{j-1}^+], \qquad j = 2, 3.....\infty && (4.22)\\
r_P &= k_{tr_M}[M][P^+] + k_{tr_C}[C][P^+] + k_{tr_T}[T][P^+] + \\
&\quad k_{T_M}[M][P^+] + k_{T_C}[C][P^+] + k_{T_B}[B][P^+], \qquad [P] = \sum_{j=1}^{\infty}[P_j] && (4.23)
\end{aligned}$$

4.2 Process Model

The differential material balances including the rate expressions coupled with the equations for the physical phenomena constitute the dynamic process model. The density of the reactor contents (ρ) is calculated using the ideal mixing rule for volume.

$$\rho = (\frac{x_S}{\rho_S} + \frac{x_M}{\rho_M} + \frac{1 - x_S - x_M}{\rho_L})^{-1} \tag{4.24}$$

The mass fraction of solids in the reactor (x_S) is evaluated as

$$x_S = \frac{\lambda_1^+ M_M}{c_1 \rho} + x_P \tag{4.25}$$

The average molecular weight for a single polymer unit (M_{P_1}) is calculated based on the rates of reaction for the monomer and comonomer

$$M_{P_1} = \frac{M_M r_M + M_C r_C}{r_M + r_C} \tag{4.26}$$

The probability of propagation of active polymer chains (α) can be written as

$$\alpha = \frac{k_{p_M}\frac{x_M}{M_M} + k_{p_C}\frac{x_C}{M_C}}{(k_{p_M} + k_{tr_M} + k_{T_M})\frac{x_M}{M_M} + (k_{p_C} + k_{tr_C} + k_{T_C})\frac{x_C}{M_C} + k_{tr_T}\frac{x_T}{M_T} + k_{T_B}\frac{x_B}{M_B}} \tag{4.27}$$

The functions of states that appear in the process model are

$$\beta = [(k_{tr_M} + \frac{k_{T_M}}{\alpha})\frac{x_M}{M_M} + (k_{tr_C} + \frac{k_{T_C}}{\alpha})\frac{x_C}{M_C} + \frac{k_{tr_T}x_T}{M_T} + \frac{k_{T_B}x_B}{\alpha M_B}]c_1\rho \tag{4.28}$$

$$\beta' = [\frac{k_{T_M}x_M}{M_M} + \frac{k_{T_C}x_C}{M_C} + \frac{k_{T_B}x_B}{M_B}]\frac{c_1\rho}{\alpha} \tag{4.29}$$

$$a = \frac{VM_{P_1}}{c_1} \tag{4.30}$$

The model is simplified using quasi-steady-state approximations for the active polymer. The equations for the active and dead polymer chains are simplified by taking the zeroth and first moment.

4.2.1 Quasi-Steady-State Approximations

The differential equations for the active polymer chains are transformed into algebraic equations using the quasi-steady-state approximations for the active polymers because of their faster kinetic equilibration relative to other species. These approximations also reduce the stiffness due to different time-scales in the system of differential equations representing the process model. The rate of generation of the active polymer chains is the same as their rate of consumption for the quasi-steady-state assumption ($r_{P^+} = 0$) resulting in

$$[P^+] = \frac{k_{1_M}[A^\star][M] + k_{1_C}[A^\star][C]}{k_{T_M}[M] + k_{T_C}[C] + k_{T_B}[B]} \tag{4.31}$$

Converting the species molar concentrations to mass fractions gives

$$[P^+] = \frac{(k_{1_M}\frac{x_M}{M_M} + k_{1_C}\frac{x_C}{M_C})\frac{x_{A^\star}}{M_{A^\star}}c_1\rho}{k_{T_M}\frac{x_M}{M_M} + k_{T_C}\frac{x_C}{M_C} + k_{T_B}\frac{x_B}{M_B}} \tag{4.32}$$

A similar assumption for the active polymer chains of single chain length ($r_{P_1^+} = 0$) yields

$$\begin{aligned} [P^+]([M](k_{tr_M} + k_{T_M}) + [C](k_{tr_C} + k_{T_C}) + k_{T_B}[B] + k_{tr_T}[T]) &= \\ [P_1^+]([M](k_{p_M} + k_{tr_M} + k_{T_M}) + [C](k_{p_C} + k_{tr_C} + k_{T_C}) + k_{tr_T}[T] + k_{T_B}[B]) & \end{aligned} \tag{4.33}$$

The above equation can be simplified by using the expression for the probability of propagation of active polymer chains given in equation 4.27.

$$[P_1^+] = [P^+](1 - \alpha) \tag{4.34}$$

A relationship can be found between the concentration of active polymer chains of length j ($[P_j^+]$) and the concentration of active polymer chains of length $(j-1)$ ($[P_{j-1}^+]$) by making the quasi-steady-state assumption for the active polymer chains with length j ($r_{P_j^+} = 0$)

$$\begin{aligned} [P_j^+]([M](k_{p_M} + k_{tr_M} + k_{T_M}) + [C](k_{p_C} + k_{tr_C} + k_{T_C}) + k_{tr_T}[T] + k_{T_B}[B]) &= \\ [P_{j-1}^+](k_{p_M}[M] + k_{p_C}[C]) & \end{aligned} \tag{4.35}$$

$$[P_j^+] = \alpha[P_{j-1}^+] \tag{4.36}$$

The above equations for the active polymer chains enable us to explicitly evaluate their molar concentrations ($[P_j^+]$) at different times without introducing significant errors because the relative rate of change for the active polymers is orders of magnitude higher than the other reactor species.

4.2.2 Moments for the Active and Dead Polymers

The polymer viscosity is measured for the copolymer and the average molecular weight is measured for the homopolymer. The polymer viscosity can be obtained from the average molecular weight using an empirical formula. The weight average molecular weight for the polymer is obtained using leading moments for the molecular weight distribution. Hence, there is no need in this research to evaluate explicitly the entire chain length distribution of the polymer. The moments for the molecular weight distribution can be calculated by employing generating functions and other mathematical tools [132]. In this case, the leading moments for the polymer are obtained by explicitly evaluating the series summations involved. The zeroth and first moments for the mass fraction of the dead polymer can be defined as

$$\lambda_k = \sum_{j=1}^{\infty} j^k x_{P_j}, \qquad k = 0, 1 \tag{4.37}$$

$$x_P = \lambda_0 \tag{4.38}$$

Leading moments of the differential molecular weight distribution are also used to describe the state of the active polymer chains. The zeroth and the first moments of the number chain length distribution for the active polymer chains can be defined as

$$\lambda_k^+ = \sum_{j=1}^{\infty} j^k [P_j^+], \qquad k = 0, 1 \tag{4.39}$$

The resulting equations for the zeroth and the first moment of the chain length distribution for the active polymers are

$$\lambda_0^+ = [P^+] \tag{4.40}$$

$$\lambda_1^+ = \sum_{j=1}^{\infty} j[P_j^+] \tag{4.41}$$

Using equations 4.34 and 4.36 to evaluate the sum to get the first moment (λ_1^+)

$$\lambda_1^+ = [P^+](1-\alpha)(1 + 2\alpha + 3\alpha^2 + 4\alpha^3 + \cdots) \tag{4.42}$$

$$\lambda_1^+ = \frac{[P^+]}{1-\alpha} \tag{4.43}$$

The zeroth moment for the mass fraction of the dead polymer changes due to polymerization reactions as

$$\lambda_0 = \sum_{j=1}^{\infty} x_{P_j} \tag{4.44}$$

$$\frac{d\lambda_0}{dt} = \frac{a}{\rho V}(r_{P_1} + \sum_{j=2}^{\infty} j r_{P_j}) \tag{4.45}$$

$$= \frac{a}{\rho V}((\beta - \beta')[P^+](1-\alpha) + \beta[P^+](1-\alpha)(2\alpha + 3\alpha^2 + 4\alpha^3 + \cdots)) \tag{4.46}$$

$$= \frac{a}{\rho V}(\beta[P^+](1-\alpha)(1 + 2\alpha + 3\alpha^2 + 4\alpha^3 + \cdots) - \beta'[P^+](1-\alpha)) \tag{4.47}$$

$$= \frac{a}{\rho V}(\frac{\beta[P^+]}{1-\alpha} - \beta'[P^+](1-\alpha)) \tag{4.48}$$

Similarly, the first moment for the mass fraction of the dead polymer changes due to polymerization reactions as

$$\lambda_1 = \sum_{j=1}^{\infty} j x_{P_j} \tag{4.49}$$

$$\frac{d\lambda_1}{dt} = \frac{a}{\rho V}(r_{P_1} + \sum_{j=2}^{\infty} j^2 r_{P_j}) \tag{4.50}$$

$$= \frac{a}{\rho V}((\beta - \beta')[P^+](1-\alpha) + \sum_{j=2}^{\infty} j^2 \beta[P_j^+]) \tag{4.51}$$

$$= \frac{a[P^+](1-\alpha)}{\rho V}(\beta(1 + 4\alpha + 9\alpha^2 + 16\alpha^3 + \cdots) - \beta') \tag{4.52}$$

$$= \frac{a[P^+](1-\alpha)}{\rho V}(\frac{\beta(1+\alpha)}{(1-\alpha)^3} - \beta') \tag{4.53}$$

These moments for the chain length distribution give the weight average chain length for the polymer product.

4.2.3 Differential Equations for the Process

The differential component balances for the various species in the reactor are obtained by using the CSTR assumption. The assumption that the species are well mixed in the reactor is justified because of the low Peclet number obtained from dimensional analysis [175].

$$\begin{aligned}
\frac{dx_M}{dt} &= \frac{1}{\rho V}[-x_M(w_1+w_2)+x_{M_1}w_1] - k_{1_M}\frac{c_1 x_{A^\star}\rho}{M_{A^\star}}x_M \\
&\quad -(k_{p_M}+k_{tr_M}+k_{T_M})[P^+]x_M \qquad (4.54)\\
\frac{dx_C}{dt} &= \frac{1}{\rho V}[-x_C(w_1+w_2)+x_{C_1}w_1] - k_{1_C}\frac{c_1 x_{A^\star}\rho}{M_{A^\star}}x_C \\
&\quad -(k_{p_C}+k_{tr_C}+k_{T_C})[P^+]x_C \qquad (4.55)\\
\frac{d\lambda_0}{dt} &= \frac{1}{\rho V}[-x_P(w_1+w_2)+\frac{a\beta[P^+]}{1-\alpha} - a\beta'[P^+](1-\alpha)] \qquad (4.56)\\
\frac{d\lambda_1}{dt} &= \frac{1}{\rho V}[-\lambda_1(w_1+w_2)+a[P^+](1-\alpha)(\frac{\beta(1+\alpha)}{(1-\alpha)^3}-\beta')] \qquad (4.57)\\
\frac{dx_B}{dt} &= \frac{1}{\rho V}[-x_B(w_1+w_2)+x_{B_1}w_1] - k_{T_B}[P^+]x_B \qquad (4.58)\\
\frac{dx_T}{dt} &= \frac{1}{\rho V}[-x_T(w_1+w_2)+w_T] - k_{tr_T}[P^+]x_T \qquad (4.59)\\
\frac{dx_{RH}}{dt} &= \frac{1}{\rho V}[-x_{RH}(w_1+w_2)+x_{RH_2}w_2] - k_i x_{RH} \qquad (4.60)\\
\frac{dx_{A^\star}}{dt} &= \frac{1}{\rho V}[-x_{A^\star}(w_1+w_2)] + \frac{k_i x_{RH}[M_{A^\star}]}{M_{RH}} - c_1\rho x_{A^\star}(\frac{k_{1_M}x_M}{M_M}+\frac{k_{1_C}x_C}{M_C}) \qquad (4.61)
\end{aligned}$$

An energy balance cannot be closed effectively to obtain a differential equation for the reactor temperature because of lack of reliable measurements for the reactor coolant. Hence, the reactor temperature is used as a measured input in the process model. The above differential equations along with the algebraic equations constitute the dynamic model of the reactor. The reactor is followed by a separation unit that has dynamics due to mixing. The residence time (τ) of the unreacted hydrocarbon in the separator is expressed as a first order lag. The mass fraction of monomer in the effluent gas (x_{M_e}) and mass fraction of comonomer in the effluent gas (x_{C_e}) are being evaluated as

$$\frac{dx_{M_e}}{dt} = \frac{1}{\tau}[-x_{M_e}+\frac{x_M}{1-x_S}] \qquad (4.62)$$

$$\frac{dx_{C_e}}{dt} = \frac{1}{\tau}[-x_{C_e}+\frac{x_C}{1-x_S}] \qquad (4.63)$$

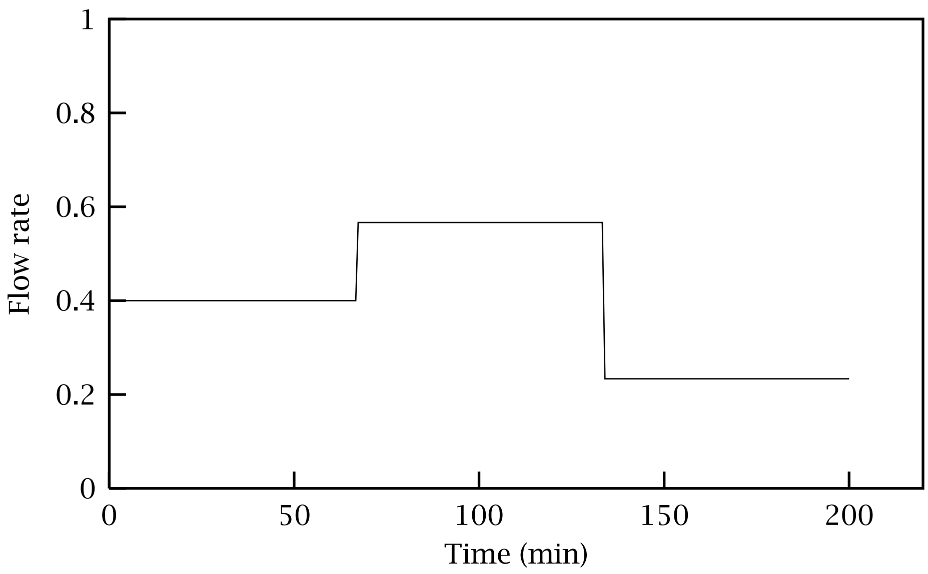

Figure 4.2: Catalyst feed rate for copolymer (scaled model simulation)

4.2.4 Process Model Simulations

The process model is simulated by keeping all inputs constant except the catalyst feed rate (Figure 4.2) to determine the extent of model non-linearity. The monomer mass percent in the separator effluent (M^{se}) and the comonomer mass percent in the separator effluent (C^{se}) decrease with an increase in the catalyst feed rate (w_2) due to increased amounts of activated catalyst ($A^\star$) in the reactor. The increased amounts of activated catalyst also results in higher relative amounts of active polymers with shorter chain lengths resulting in lower polymer viscosity (μ). The responses of monomer mass percent in the separator overhead (Figure 4.3), comonomer mass percent in the separator overhead (Figure 4.4) and polymer viscosity (Figure 4.5) to the catalyst feed rate show that the process outputs are non-linear.

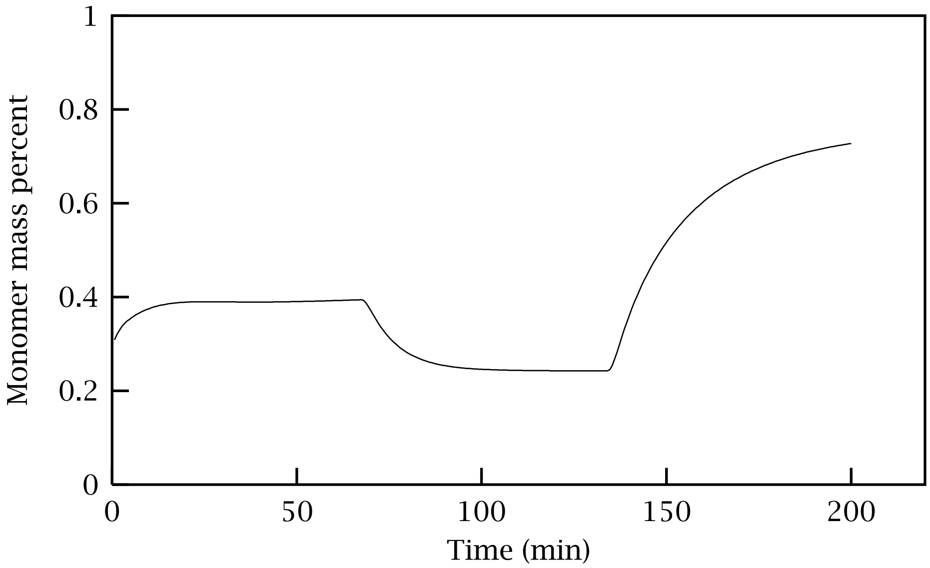

Figure 4.3: Monomer mass percent in separator effluent (scaled model simulation)

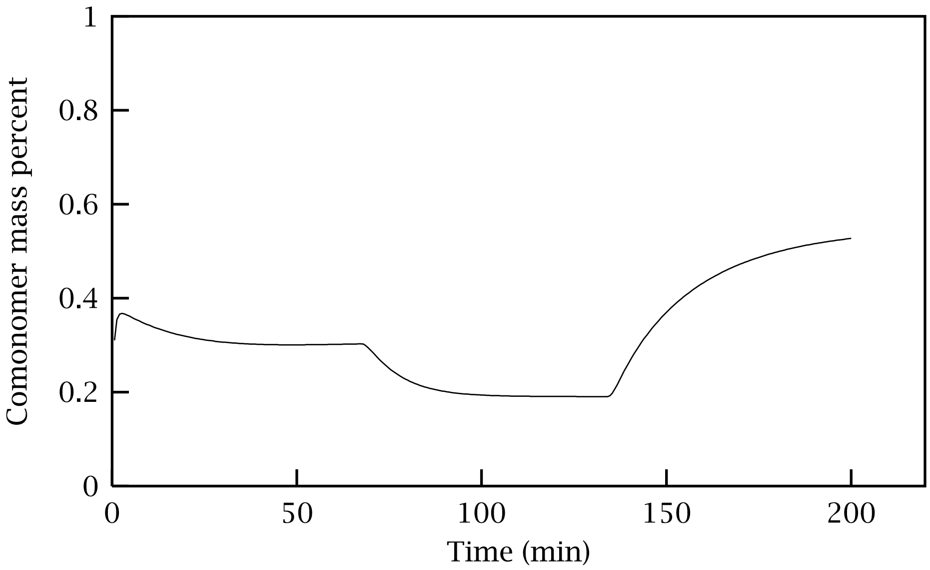

Figure 4.4: Comonomer mass percent in separator effluent (scaled model simulation)

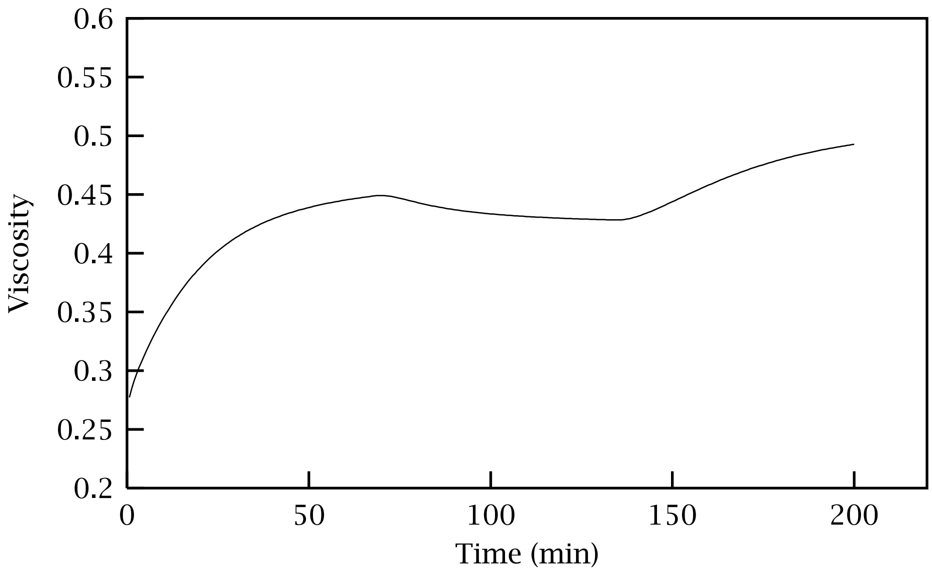

Figure 4.5: Polymer viscosity (scaled model simulation)

Chapter 5

Parameter Estimation

Parameter estimation is carried out for the industrial polymerization process to validate the process model. Several physical and kinetic parameters appear in the process model developed in the previous section. The physical parameters like the reactor volume and species densities are fixed based on our knowledge of the industrial process. Each kinetic parameter has a pre-exponential factor and an activation energy associated with it.

$$k = k_o e^{(-E/RT)} \tag{5.1}$$

The activation energies (E) have been fixed based on previous simulation and experimental studies. The pre-exponential factors (k_o) of the kinetic parameters are estimated from historical plant data.

5.1 Likelihood Function Formulation

The maximum likelihood estimate [10] is applied to evaluate the parameters (θ) in the process model. The likelihood function, which is the joint probability distribution function of the observations, is maximized with respect to the unknown parameters. The problem is formulated in terms of maximizing the logarithm of the likelihood function ($\ln L$) since it is a simpler expression than the likelihood function (L) itself. This formulation results in the same value of parameters (θ) because the logarithm is a monotonic increasing function of its argument. There are various experiments ($i = 1 \cdots n$) with sensor outputs ($a = 1 \cdots m$) containing process information that are utilized for parameter estimation. The errors ($e_{ia}(\theta)$) in the sensor outputs are assumed to be independent and normally distributed with a variance v_a. The logarithm of the likelihood function (L) can be expressed as:

$$\ln L = -(nm/2)\ln(2\pi) - (n/2)\sum_{a=1}^{m}\ln(v_a) - 1/2\sum_{a=1}^{m} v_a^{-1}\left(\sum_{i=1}^{n} e_{ia}^2(\theta)\right) \tag{5.2}$$

The error variance (v_a) is evaluated by maximizing $\ln L$ with respect to each v_a.

$$v_a(\theta) = (1/n) \sum_{i=1}^{n} e_{ia}^2(\theta) \tag{5.3}$$

The logarithm of L can be reduced to

$$\ln L = (mn/2)(\ln(n/2\pi) - 1) - (n/2) \sum_{a=1}^{m} \ln(\sum_{i=1}^{n} e_{ia}^2(\theta)) \tag{5.4}$$

Maximizing $\ln L$ is equivalent to minimizing

$$\phi(\theta) = (n/2) \sum_{a=1}^{m} \ln(\sum_{i=1}^{n} e_{ia}^2(\theta)) \tag{5.5}$$

The above objective function (ϕ) is minimized to obtain a maximum likelihood estimate for the kinetic parameters. The confidence intervals are obtained by linearizing the model equations at the values of the estimated parameters. It can be shown [10] for maximum likelihood estimates with normal distributions that the covariance matrix of the sampling distribution of the parameter estimate (V_θ) can be obtained from the Hessian of the logarithm of the likelihood function ($\ln L$) at the optimal parameter estimates ($\theta^\star$)

$$V_\theta \approx H^{\star^{-1}} = -(\frac{\partial^2 lnL}{\partial\theta\partial\theta})^{-1}_{\theta=\theta^\star} \tag{5.6}$$

If the sampling distribution of parameter estimates ($\theta^\star$) is normal and unbiased then

$$(\theta - \theta^\star)^T V_\theta^{-1} (\theta - \theta^\star) \le \chi^2(l) \tag{5.7}$$

where l is the number of parameters (θ). The 95% confidence regions for the parameters (equation 5.7) are obtained after computing the covariance of the estimates (V_θ).

5.2 Simulated Data

The parameter estimation problem is first examined using simulated data corrupted with noise. This study is carried out to obtain the well-determined kinetic parameters for the case without plant-model mismatch. The pre-exponential factors of the kinetic parameters k_{p_M}, k_{tr_C} and k_{T_C} are estimated. These parameters are chosen because the singular value decomposition of the Hessian indicates that these three parameters may be estimable. The inputs for the simulation of the reactor are hydrocarbon feed (w_1), catalyst feed (w_2), transfer agent feed (w_T), monomer mass fraction in w_1 (x_{M_1}), comonomer mass fraction in w_1 (x_{C_1}), inhibitor mass fraction in w_1 (x_{B_1}), mass fraction

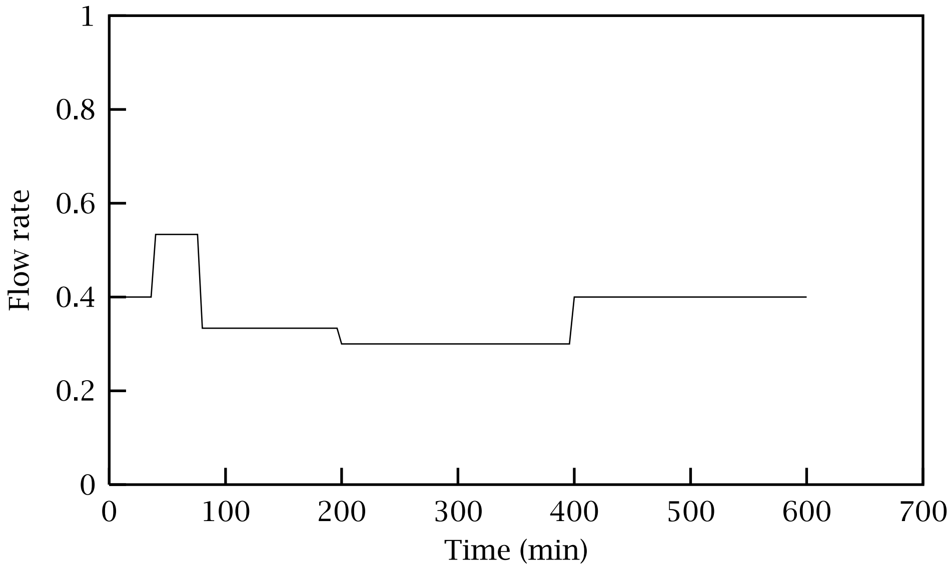

Figure 5.1: Catalyst feed rate for copolymer (scaled simulated input)

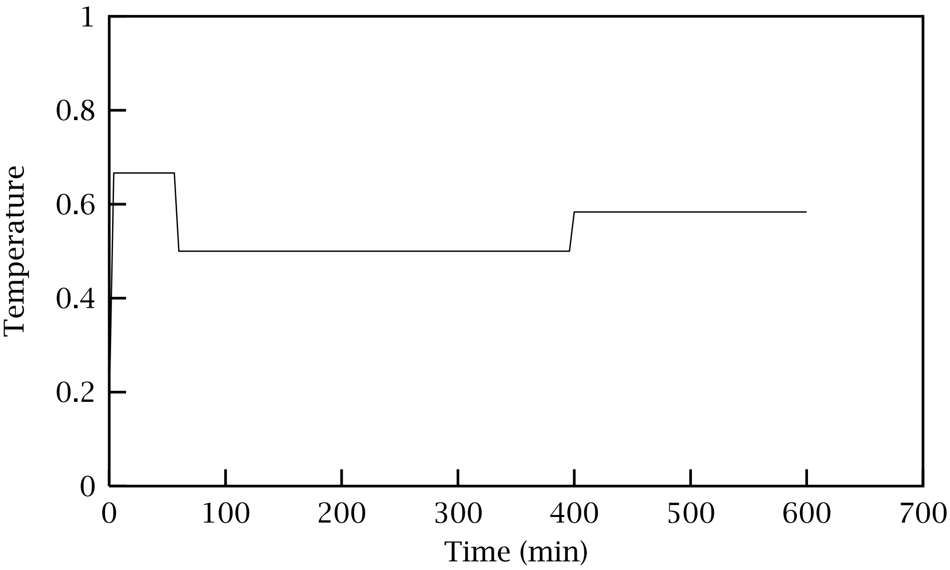

Figure 5.2: Reactor temperature for copolymer (scaled simulated input)

of cocatalyst in w_2 (x_{RH_2}) and temperature of reactor (T). The catalyst feed (Figure 5.1) and reactor temperature (Figure 5.2) are varied during the polymerization process. The monomer mass percent in the separator effluent (M^{se}), the comonomer mass percent in the separator effluent (C^{se}) and the polymer viscosity (μ) are the available measurements used in parameter estimation. These simulated measurements obtained using nominal parameter values are corrupted with noise (Figures 5.3, 5.4 and 5.5) and then used to estimate the kinetic parameters.

5.2.1 Estimation Problem Analysis

The least-squares estimation problem is first analyzed for the linearized model to obtain the well-determined kinetic parameters. The linear least-squares problem with process measurements (y) can be written as

$$y = J\theta \tag{5.8}$$

$$f(\theta) = (y - J\theta)^T (y - J\theta) \tag{5.9}$$

The Hessian of the least-squares objective function (5.9) can be written as

$$H = J^T J \tag{5.10}$$

The singular value decomposition gives

$$J^T = u\Sigma v^T \tag{5.11}$$

$$J = v\Sigma u^T \tag{5.12}$$

$$H = u\Sigma^2 u^T \tag{5.13}$$

$$\|J\| = \|\Sigma\| \tag{5.14}$$

$$\|H\| = \|\Sigma^2\| \tag{5.15}$$

Using the perturbation bound [93] for the case where there are more measurements (y) compared to parameters (θ) results in the following expressions

$$\frac{\|d\theta\|}{\|\theta\|} \leq \operatorname{cond}(J) \frac{\|y\|}{\|J\|\|\theta\|} \frac{\|dy\|}{\|y\|} \tag{5.16}$$

$$\|d\theta\| \leq \frac{\operatorname{cond}(J)}{\|J\|} \|dy\| \tag{5.17}$$

The error bound for the parameters (θ) can be obtained using the norms given in equations 5.14 and 5.15

$$\|d\theta\| \leq \sqrt{\frac{\sigma_{\max}(H)}{(\sigma_{\min}(H))^2}} \|dy\| \tag{5.18}$$

This error bound (equation 5.18) gives the well-determined set of parameters based on the process information available in the sensor outputs.

This estimable set of parameters is chosen to avoid saddle points and ill-conditioned solutions. The Hessian of the objective function shown in equation 5.5 is evaluated using second-order finite differences. There are two sources of error in the evaluation of numerical derivatives, truncation error (caused due to neglected terms of Taylor series) and round-off error (caused by inaccuracies in computed function values). The truncation error is an increasing function of step-size (h), while the round-off error is a decreasing function of h. The step-size for the finite differences is chosen using a procedure [58] to balance these two sources of error. The Hessian (H) at the optimal parameter values for the simulated data with added random noise is

$$
\begin{array}{cc}
 & \begin{array}{cccccc} k_{p_{M_o}} & k_{tr_{C_o}} & k_{T_{C_o}} & k_{p_{C_o}} & k_{i_o} & k_{1_{M_o}} \end{array} \\
H = & \begin{bmatrix}
3.49\times10^{5} & -1.29\times10^{4} & -5.93\times10^{5} & 2.56\times10^{5} & 1.59\times10^{4} & 8.14\times10^{2} \\
-1.29\times10^{4} & 5.26\times10^{4} & -6.29\times10^{3} & -3.34\times10^{4} & 4.13\times10^{2} & 2.26\times10^{1} \\
-5.93\times10^{5} & -6.29\times10^{3} & 1.34\times10^{6} & -7.44\times10^{5} & -3.61\times10^{4} & -1.86\times10^{3} \\
2.56\times10^{5} & -3.34\times10^{4} & -7.44\times10^{5} & 5.21\times10^{5} & 1.98\times10^{4} & 1.03\times10^{3} \\
1.59\times10^{4} & 4.13\times10^{2} & -3.61\times10^{4} & 1.98\times10^{4} & 1.02\times10^{3} & 5.35\times10^{1} \\
8.14\times10^{2} & 2.26\times10^{1} & -1.86\times10^{3} & 1.03\times10^{3} & 5.35\times10^{1} & 3.02
\end{bmatrix}
\end{array}
$$

The singular value decomposition of H gives

$$H = u\Sigma^2 u^T \tag{5.19}$$

where

$$
\Sigma^2 = \begin{bmatrix}
2.03\times10^{6} & 0 & 0 & 0 & 0 & 0 \\
0 & 1.71\times10^{5} & 0 & 0 & 0 & 0 \\
0 & 0 & 6.76\times10^{4} & 0 & 0 & 0 \\
0 & 0 & 0 & 4.68\times10^{1} & 0 & 0 \\
0 & 0 & 0 & 0 & 1.50 & 0 \\
0 & 0 & 0 & 0 & 0 & 1.79\times10^{-1}
\end{bmatrix}
$$

$$
u = \begin{bmatrix}
-0.36 & 0.68 & -0.39 & -0.01 & -0.50 & 0.00 \\
0.01 & 0.13 & 0.86 & -0.01 & -0.50 & 0.00 \\
0.81 & -0.10 & -0.28 & 0.02 & -0.50 & -0.00 \\
-0.46 & -0.71 & -0.18 & -0.01 & -0.50 & 0.00 \\
-0.02 & 0.00 & 0.01 & 1.00 & -0.00 & -0.07 \\
-0.00 & 0.00 & 0.00 & 0.07 & -0.00 & 1.00
\end{bmatrix}
$$

The columns of u indicate that only three of the first four parameters can be estimated based on the error bound (equation 5.18). Substituting the appropriate values in equation 5.18 gives

$$\|\Delta\theta\| \leq 0.021\|\Delta y\| \tag{5.20}$$

	$k_{p_{M_o}}$	$k_{tr_{C_o}}$	$k_{T_{C_o}}$	Number of iterations
Initial Guess	30.000	27.700	25.500	
Estimate	30.000	27.709	25.499	4
95% Confidence Interval	±0.007	±0.009	±0.003	
Initial Guess	34.000	27.700	25.500	
Estimate	30.000	27.709	25.499	6
95% Confidence Interval	±0.007	±0.009	±0.003	
Initial Guess	30.000	31.000	25.500	
Estimate	30.000	27.709	25.499	7
95% Confidence Interval	±0.007	±0.009	±0.003	
Initial Guess	30.000	27.700	21.000	
Estimate	30.000	27.709	25.499	6
95% Confidence Interval	±0.007	±0.009	±0.003	
Initial Guess	33.000	31.000	22.000	
Estimate	30.000	27.709	25.499	6
95% Confidence Interval	±0.007	±0.009	±0.003	

Table 5.1: Scaled parameter estimates resulting from simulated copolymer data

5.2.2 Estimation Results

The maximum likelihood estimates for the three well-determined parameters are obtained by starting at different initial guess values using GREG [158] to test and confirm the conclusion from the Hessian analysis that the parameter estimation problem is well defined for those three parameters. The parameter estimates and the confidence intervals obtained from GREG (Table 5.1) are identical irrespective of the initial guess values. The sensor measurements corresponding to the estimates in the last row of Table 5.1 are compared with the simulated data. The predicted responses from the parameter estimates fit the simulated data extremely well (Figures 5.3, 5.4 and 5.5). An attempt to estimate more than three kinetic parameters results in different modal estimate values depending on initial guess points giving identical fits to noisy data. Hence, the analysis indicates that only three parameters (Table 5.1) are estimable using simulated data with no plant-model mismatch. More parameters can be estimated if the reactor composition is also measured. It is currently not feasible to measure the reactor composition because of the nature of the polymer.

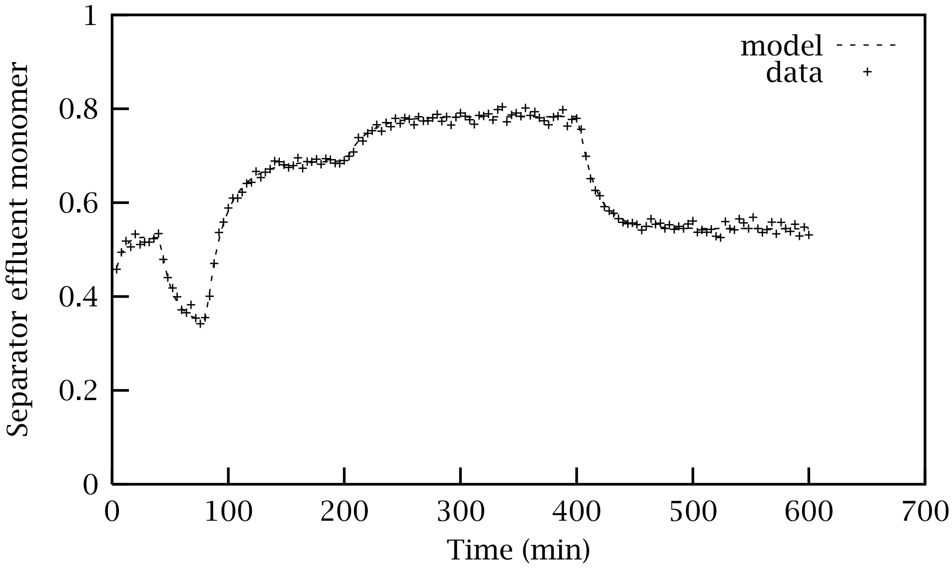

Figure 5.3: Monomer mass percent in separator effluent (scaled simulated copolymer data)

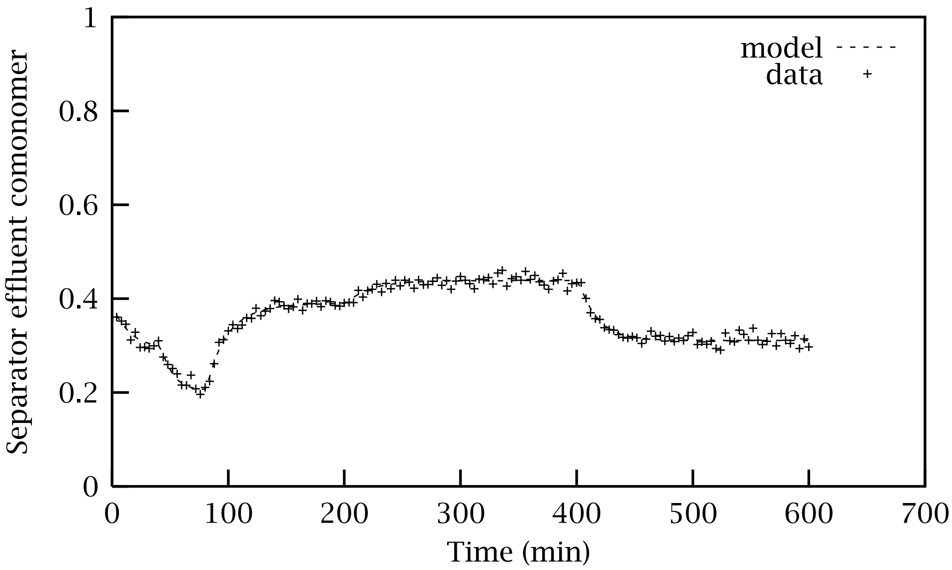

Figure 5.4: Comonomer mass percent in separator effluent (scaled simulated copolymer data)

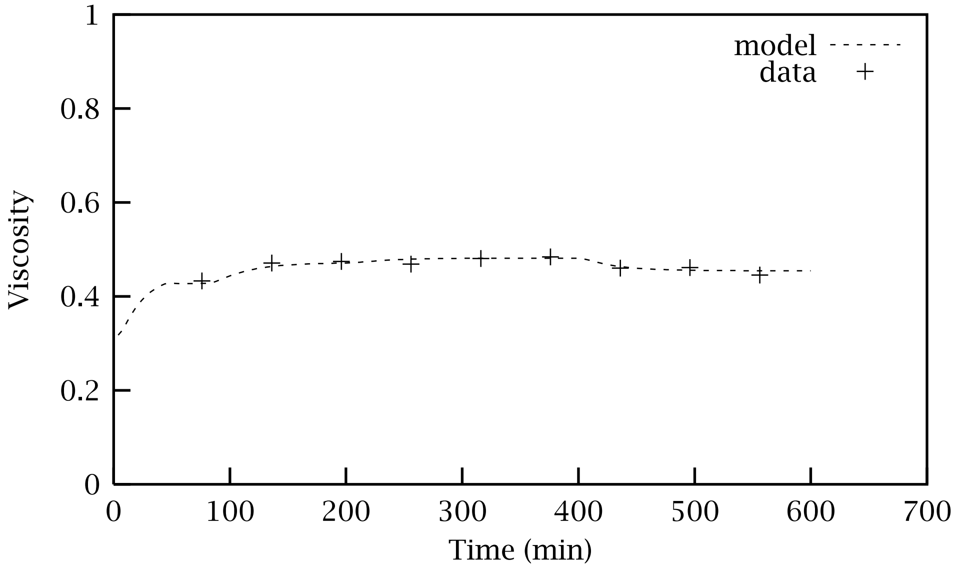

Figure 5.5: Polymer viscosity (scaled simulated copolymer data)

	$k_{p_{M_o}}$	$k_{p_{C_o}}$
Data Set 1	30.412 ± 0.027	32.740 ± 0.013
Data Set 2	30.296 ± 0.029	32.880 ± 0.018
Data Set 3	30.282 ± 0.017	32.676 ± 0.009
Data Set 1 + 2 + 3	30.348 ± 0.016	32.720 ± 0.008

Table 5.2: Scaled parameter estimates resulting from copolymer plant data

5.3 Estimation for Copolymer

The parameter estimation results for copolymer plant data are typical of the thirteen industrial datasets. The pre-exponential factors of the kinetic parameters k_{p_M} (propagation due to monomer) and k_{p_C} (propagation due to comonomer) are obtained using historical plant data. These two parameters are chosen based on the analysis of the Hessian for parameter estimation. The analysis indicates that the plant data are informative enough to estimate only two of the six unknown kinetic parameters. The kinetic parameter estimates using historical plant data are given in Table 5.2. The parameter estimates and the confidence intervals obtained from different datasets are similar. The 95% confidence intervals for the above parameters are tight (order of magnitude $= 10^{-3} \sim 10^{-2}$). The predicted measurements corresponding to the estimates in the last row of Table 5.2 fit the validation data set reasonably well. The predicted responses of the monomer mass percent in the separator effluent (Figure 5.6), the comonomer mass

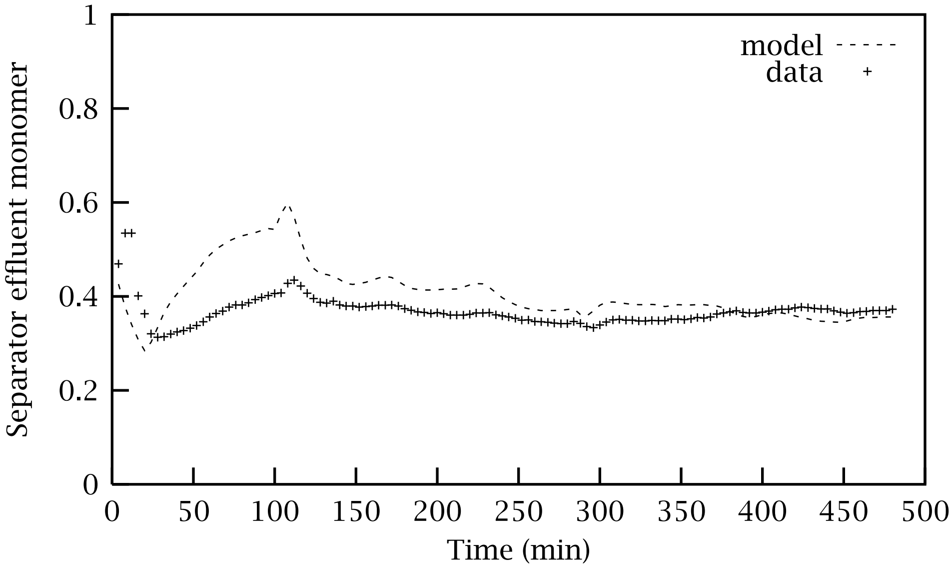

Figure 5.6: Monomer mass percent in separator effluent (scaled validation copolymer plant data)

percent in the separator effluent (Figure 5.7) and the polymer viscosity (Figure 5.8) are compared with the plant data for the validation data set.

5.4 Estimation for Homopolymer

The reactors are also used to make different grades of homopolymer without a comonomer in the process. A transfer agent is also fed into the reactor to make homopolymer. The polymer molecular weight (M_P) and the monomer mass percent in separator effluent (M^{se}) are the available measurements. The maximum likelihood estimates for the kinetic parameters ($k_{p_{M_o}}$ and $k_{tr_{T_o}}$) are obtained using historical plant data. These two parameters are estimable based on the Hessian analysis. The analysis indicates that only two of the four unknown kinetic parameters are estimable. The kinetic parameter estimates are obtained using plant data for different grades of homopolymer from the process (Table 5.3). Similar parameter estimates are obtained from different data sets. The predicted measurements corresponding to the modal estimates in the last row of Table 5.3 are compared with the homopolymer validation data set from the reactor. The predicted responses of the monomer mass percent in the separator effluent (Figure 5.9) and the polymer molecular weight (Figure 5.10) match the homopolymer plant data closely.

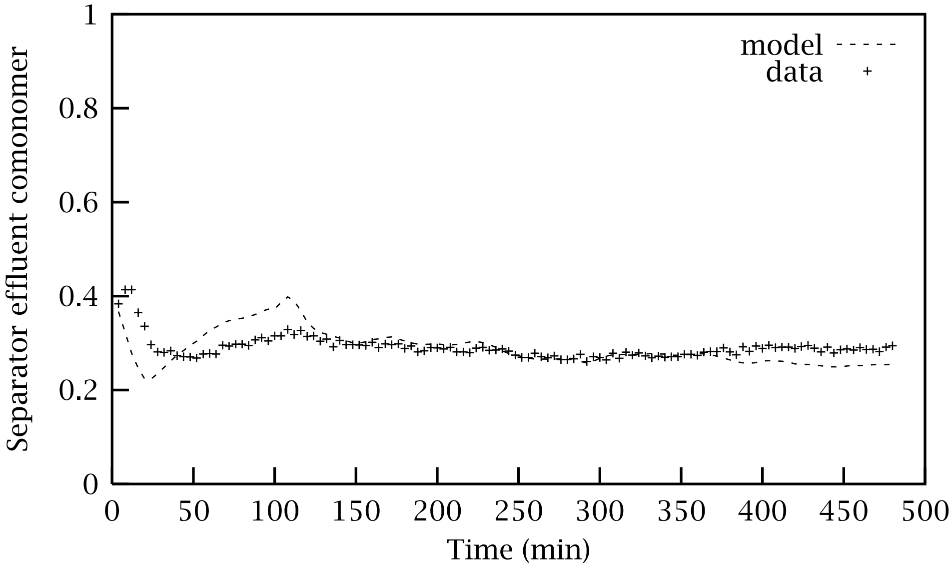

Figure 5.7: Comonomer mass percent in separator effluent (scaled validation copolymer plant data)

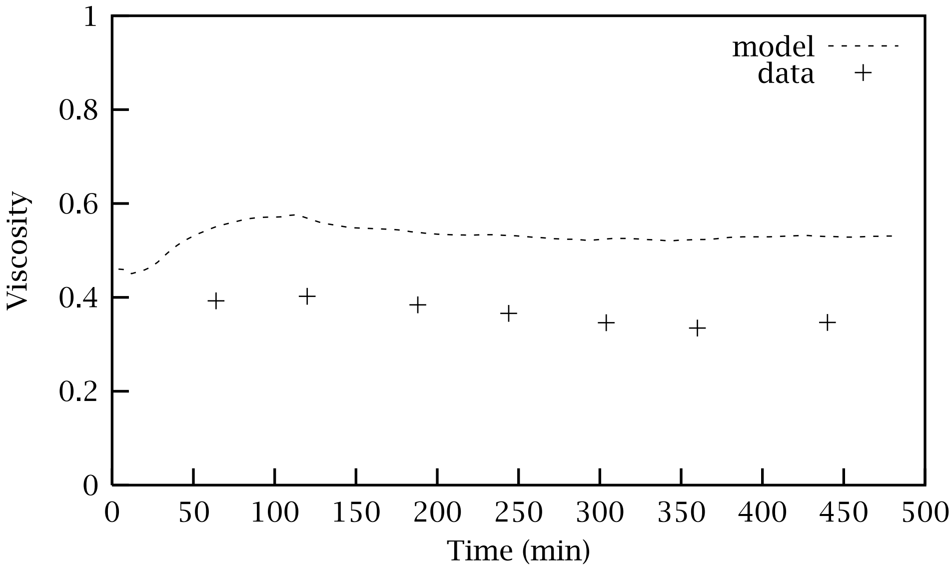

Figure 5.8: Polymer viscosity (scaled validation copolymer plant data)

	$k_{p_{M_o}}$	$k_{tr_{T_o}}$
Data Set 1	33.738 ± 0.262	27.074 ± 0.479
Data Set 2	33.126 ± 0.126	25.217 ± 0.188
Data Set 1 + 2	33.550 ± 0.149	26.111 ± 0.337

Table 5.3: Scaled parameter estimates resulting from homopolymer plant data

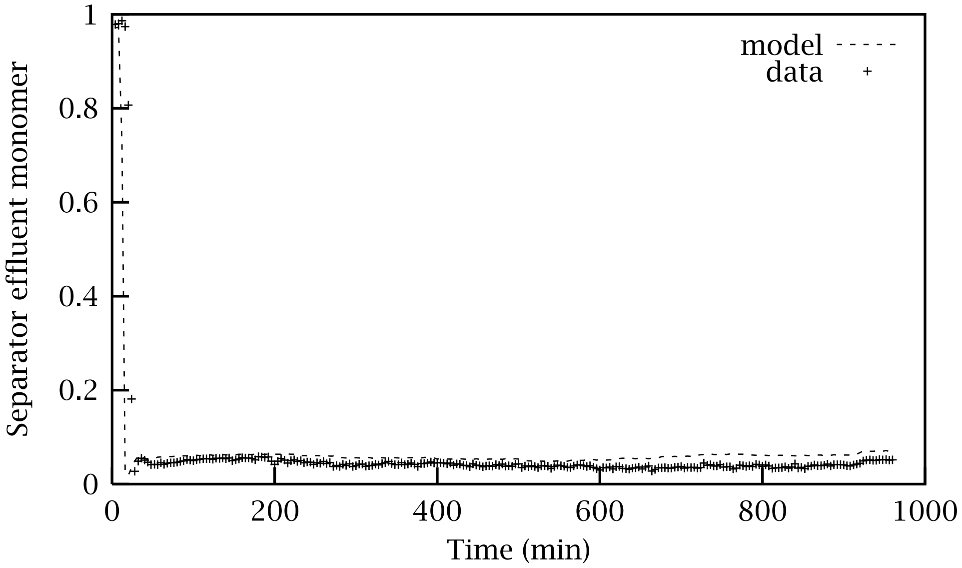

Figure 5.9: Monomer mass percent in separator effluent (scaled validation homopolymer plant data)

5.5 Disturbance Model

The disturbance model formulation is shown for the industrial polymerization process. The fundamental model shows some mismatch with the plant data (Figures 5.6, 5.7 and 5.8). This mismatch or bias can arise from disturbances in process inputs, states and outputs. An output disturbance model [130] is employed to compensate for the mismatch with plant data by assuming that the bias is primarily due to a disturbance in process measurements.

5.5.1 Output Disturbance Model Formulation

The process model can be written as

$$\frac{dx}{dt} = f(x,u,d,t) \tag{5.21}$$
$$y = h(x,u,d,t) \tag{5.22}$$

where

$$x = [x_M, x_C, \lambda_0, \lambda_1, x_B, x_T, x_{RH}, x_{A^\star}, x_{M_e}, x_{C_e}]^T \tag{5.23}$$
$$u = w_2 \tag{5.24}$$
$$d = [w_1, w_d, x_{M_1}, x_{C_1}, x_{B_1}, x_{RH_2}, T]^T \tag{5.25}$$
$$y = [M^{se}, C^{se}, \mu]^T \tag{5.26}$$

Linearizing, discretizing and incorporating an output disturbance (p_k) gives the following stochastic model in terms of deviation variables

$$x_{k+1} = Ax_k + Bu_k + B^m d_k + Gw_k \tag{5.27}$$
$$p_{k+1} = p_k + \xi_k \tag{5.28}$$
$$y_k = Cx_k + p_k + v_k \tag{5.29}$$

The Kalman filter gain [76] for the above augmented system is $L = [L_x, L_p]$ based on the covariances of state noise (w_k), noise in sensor measurement (v_k) and noise in output disturbance (ξ_k). The resulting extended Kalman filter for the nonlinear system can be written as

$$\begin{aligned}\hat{x}_{k+1} &= \hat{x}_{k,k-1} + \int_{t_k}^{t_{k+1}} f(\hat{x}_{k,k-1}, u_k, d_k, t)dt \\ &\quad + L_x(y_k - h(x_k, u_k, d_k, t) - \hat{p}_{k,k-1})\end{aligned} \tag{5.30}$$
$$\hat{p}_{k+1,k} = \hat{p}_{k,k-1} + L_p(y_k - h(x_k, u_k, d_k, t) - \hat{p}_{k,k-1}) \tag{5.31}$$

This output disturbance model formulation is employed with $L = [0, I]$ to account for the bias between model predictions and plant data. In general, there are disturbances in the process inputs and states so this observer is not optimal.

5.5.2 Disturbance Model for Copolymer

The disturbance model predictions corresponding to the estimates in the last row of Table 5.2 are compared with the data for the validation data set. The monomer mass percent in the separator effluent (Figure 5.11), the comonomer mass percent in the separator effluent (Figure 5.12) and the polymer viscosity (Figure 5.13) are compared with the plant data. The estimate of the output disturbance in the polymer viscosity measurement is not updated at each sample time because the viscosity is measured infrequently. The output disturbance for the monomer mass percent in the separator effluent (Figure 5.11) and the comonomer mass percent in the separator effluent (Figure 5.12) is higher initially and then approaches zero later. The high initial output disturbance can be attributed to questionable estimates of reactor initial conditions. The output disturbance in the polymer viscosity (Figure 5.13) is nearly a constant bias in the viscosity measurement. The predictions using the output disturbance model match the plant data closely. Hence, the output disturbance model should provide a suitable framework to develop feedback control strategies. The model is used to make open-loop predictions for developing and implementing feedback control schemes for the process. The effectiveness of the model for different open-loop prediction horizons is shown in Figures 5.14 and 5.15. These results show that the model gives reasonably good open-loop predictions even for long prediction horizons. Hence, the model is appropriate for use with feedback control strategies.

5.5.3 Disturbance Model for Homopolymer

The output disturbance model formulation is also employed for the homopolymer case to account for the bias between model predictions and plant data. The parameter estimates in the last row of Table 5.3 are used to obtain disturbance model predictions for the homopolymer validation data set, that are compared to plant data (Figures 5.16 and 5.17). The polymer molecular weight is a laboratory measurement (Figure 5.17) with longer sampling intervals. The output disturbances for the monomer mass percent in the separator effluent (Figure 5.16) and the polymer molecular weight (Figure 5.17) are relatively small over time. Therefore, the output disturbance model should provide good model predictive capabilities to develop feedback control strategies for the homopolymerization process also.

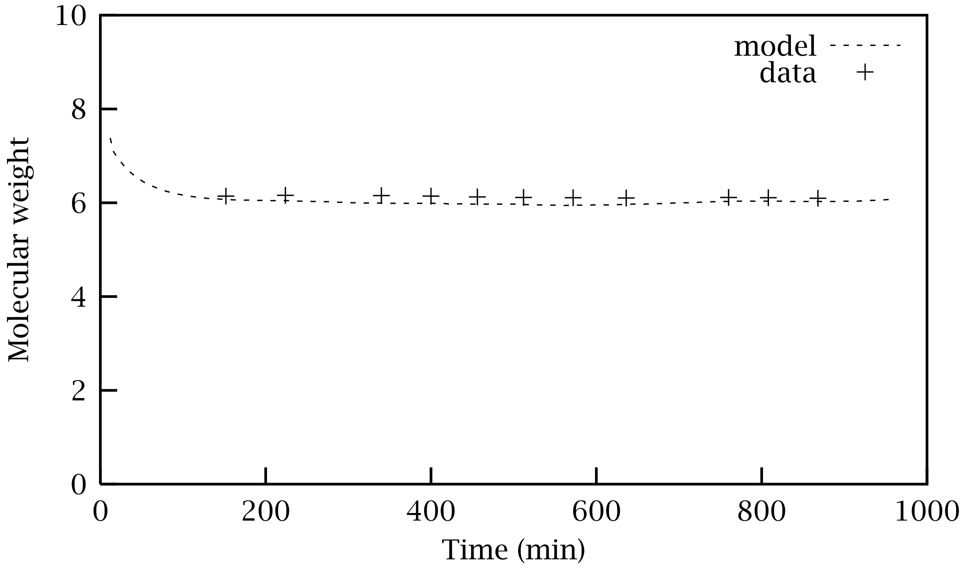

Figure 5.10: Polymer molecular weight (scaled validation homopolymer plant data)

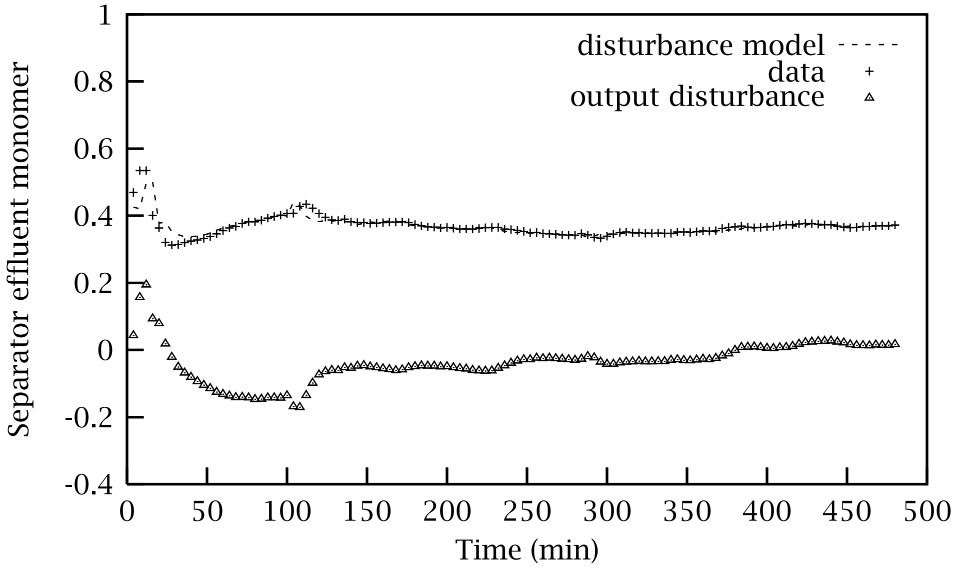

Figure 5.11: Monomer mass percent in separator effluent (output disturbance model for copolymer)

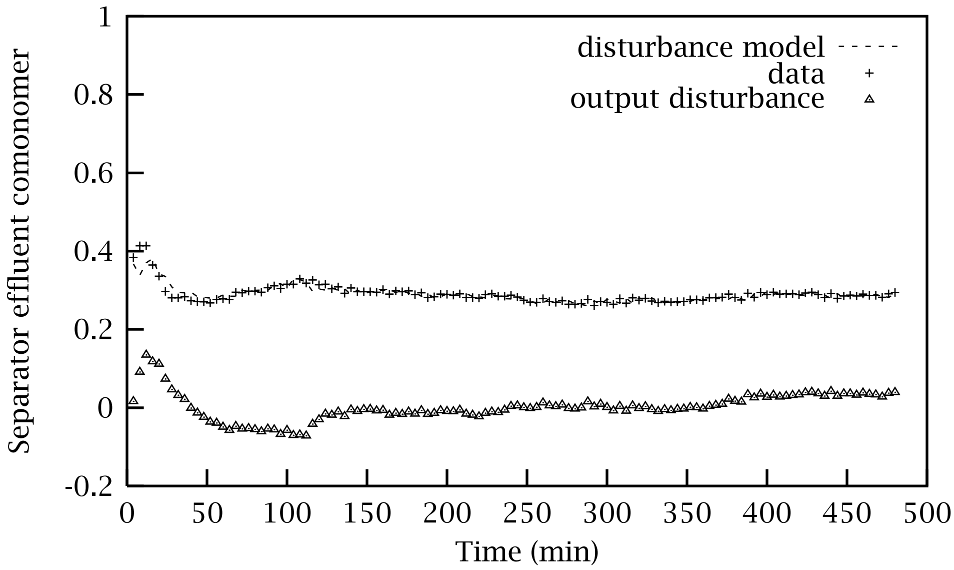

Figure 5.12: Comonomer mass percent in separator effluent (output disturbance model for copolymer)

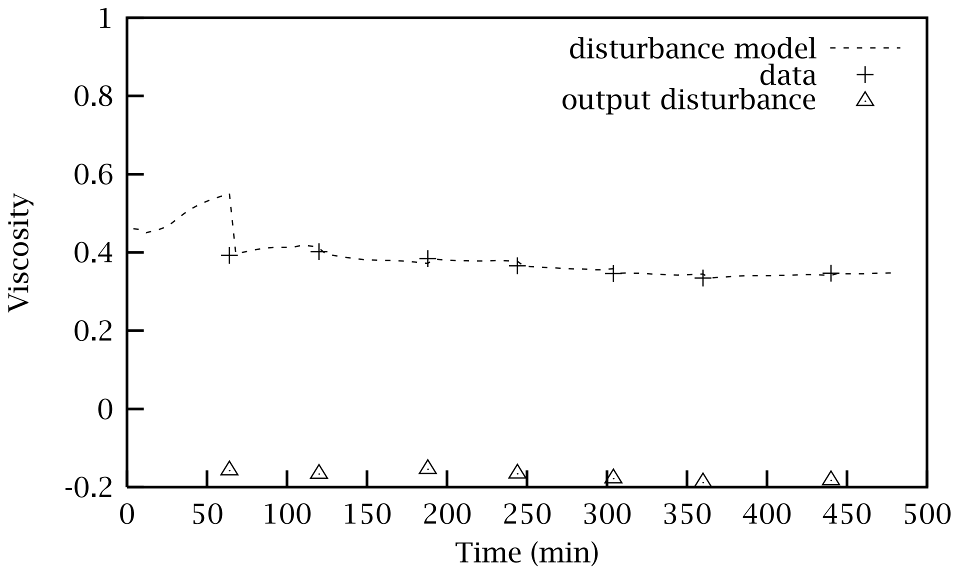

Figure 5.13: Polymer viscosity (output disturbance model for copolymer)

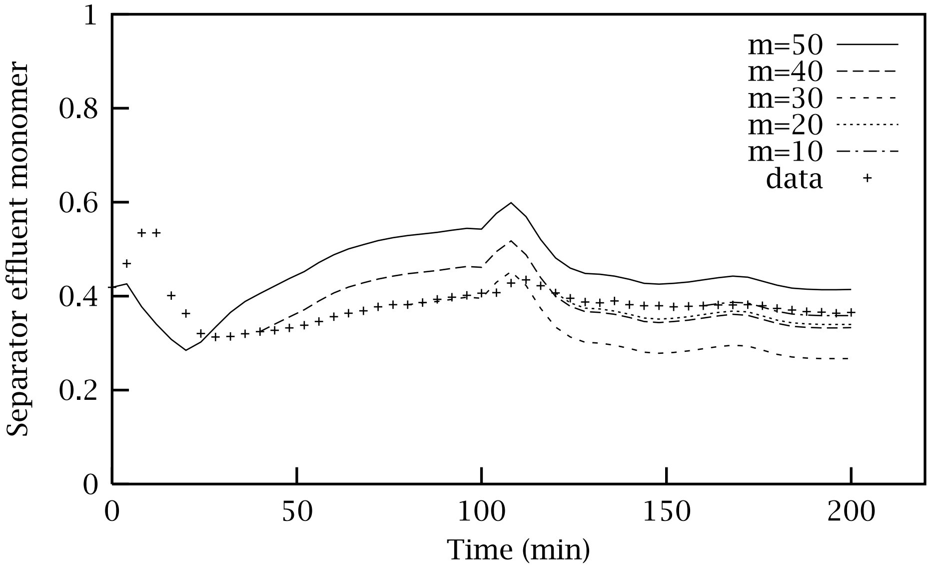

Figure 5.14: Monomer mass percent in separator effluent (output disturbance model with prediction horizon = m)

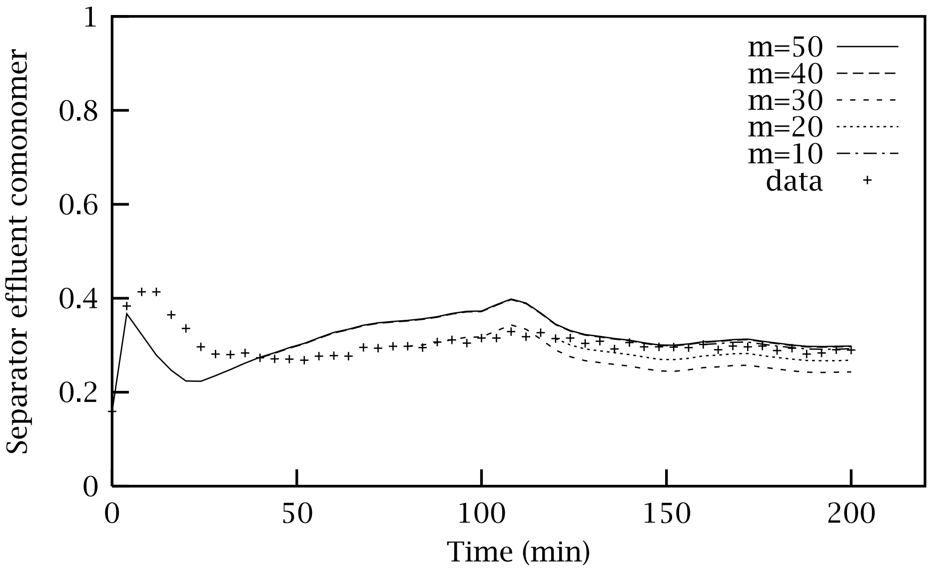

Figure 5.15: Comonomer mass percent in separator effluent (output disturbance model with prediction horizon = m)

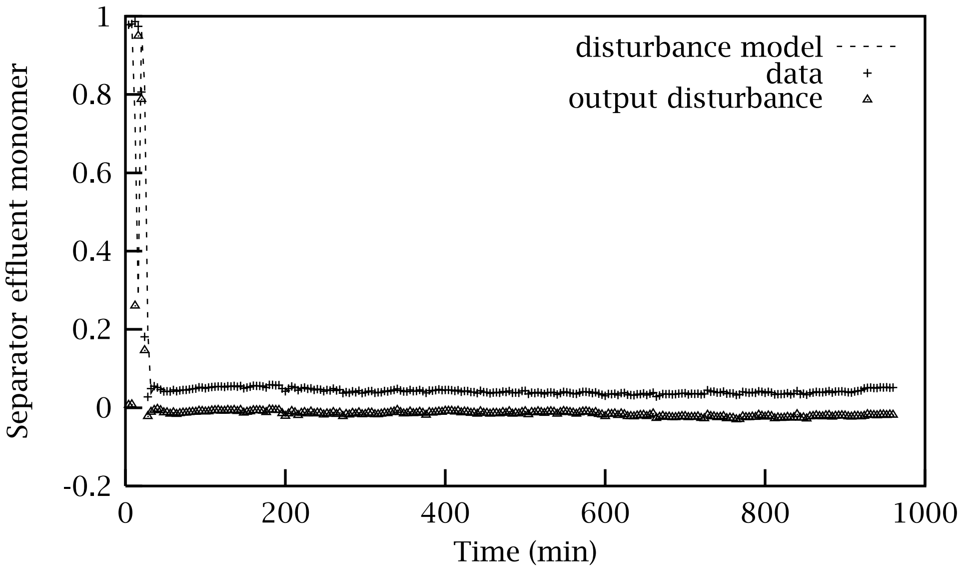

Figure 5.16: Monomer mass percent in separator effluent (output disturbance model for homopolymer)

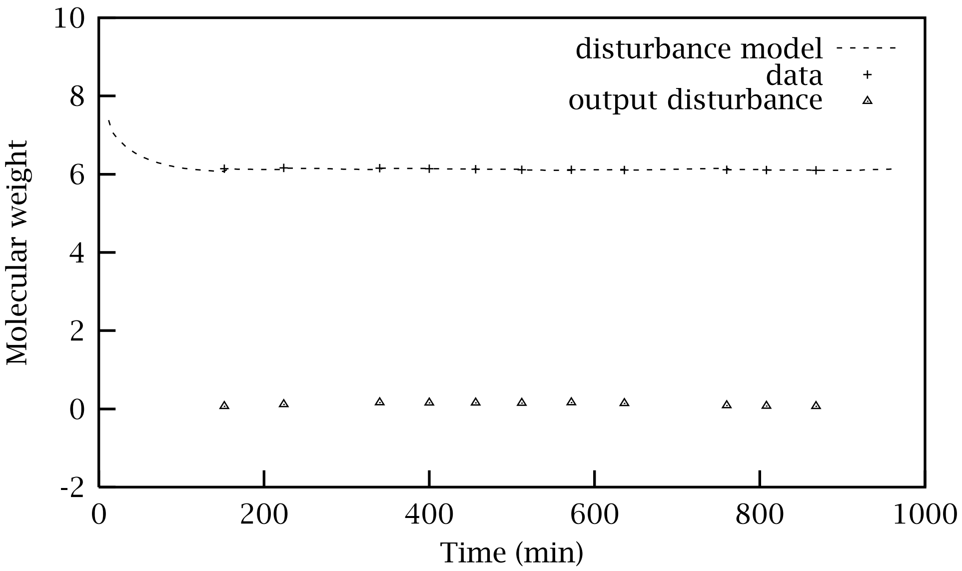

Figure 5.17: Polymer molecular weight (output disturbance model for homopolymer)

Chapter 6

Feedback Control

The MMA-VA copolymer product is characterized by its composition and viscosity. The general copolymerization control problem (Figure 3.1) for this process has multiple inputs (feed rates and coolant temperature) and multiple outputs (reactor temperature, separator effluent composition, production rate, copolymer composition and copolymer viscosity). The ratio of the two monomers in the feed can be used to alter the composition of the copolymer product. The feed rate of MMA is maintained constant (0.3 kg/min) whereas the feed rate of VA is manipulated to achieve the required copolymer properties. The amount of initiator that initiates the chain polymerization process by forming free radicals is also maintained constant (0.003 kg/min). The amount of solvent (0.6 kg/min) that is fed to the polymerization reactor is dictated by the solubilities of the feed constituents and also by heat transfer requirements for the process. The general copolymerization control problem will then be characterized by

- Inputs: Vinyl acetate (VA) feed rate, Acetaldehyde feed rate, coolant temperature
- Outputs: separator effluent composition, reactor temperature, polymer production rate, copolymer viscosity, copolymer composition

The separator effluent compositions, reactor temperature and polymer production rate are on-line measurements that are available at every sampling time. The copolymer composition and viscosity are laboratory measurements with delay. The polymer production requirements are dictated by the market demand and capacity of the polymer finishing line. The polymer composition and viscosity are also product quality measures that are set according to market needs. The feed rate of m-DNB that acts as an inhibitor along with the feed temperature are the measured disturbances entering the process. This feedback control problem for the polymerization process is challenging because of the following factors:

- Lack of on-line measurements for key product quality measures

- Significant plant-model mismatch and disturbances
- Frequent polymer grade changes, including plant start-up

A model predictive controller is developed next to achieve the necessary feedback during plant start-up and product grade change for the polymerization process. The nonlinear model that was identified in Chapter 3 is used to develop the target linearization model predictive controller (TLMPC). The process model can be written as

$$\frac{dx}{dt} = f(x,u,d,t) \tag{6.1}$$

$$y = h(x) \tag{6.2}$$

where

$$x = [c_a, c_b, c_i, c_s, c_t, c_z, \lambda_a, \lambda_b, T_r, \psi_0^p, \psi_1^p, \psi_2^p, c_{a,s}, c_{b,s}, c_{s,s}]^T \tag{6.3}$$

$$u = [G_{b,f}, G_{t,f}, T_j]^T \tag{6.4}$$

$$d = [G_{a,f}, G_{i,f}, G_{s,f}, G_{z,f}, T_f]^T \tag{6.5}$$

$$y = [c_{a,s}, c_{b,s}, c_{s,s}, T_r, G_{pi}, Y_{ap}, [\eta]]^T \tag{6.6}$$

In the feedback controller simulations, the plant is represented by the above non-linear model simulation along with an additive output disturbance ($b(t)$) that is based on our experiences with the industrial copolymerization process. The variation of output disturbance ($b(t)$) with time is used to give the following plant representation for simulations.

$$\frac{dx}{dt} = f(x,u,d) \tag{6.7}$$

$$y = h(x) \quad + b(t) \tag{6.8}$$

A linear process model is obtained by evaluating the Jacobian at the steady state from the non-linear process model using Maple [137]. The discretized linear model in terms of deviation variables can be written as

$$x_{k+1} = Ax_k + Bu_k + B^m d_k \tag{6.9}$$

$$y_k = Cx_k \tag{6.10}$$

The feedback controller results are obtained by using a fixed linear model and also by re-linearizing at every sample time to carry out plant start-up, polymer grade changes and regulation around a setpoint. The fixed linearized model is a $15th$ order linear model with left-half plane poles (b).

$$b = [-0.00261, -0.00261, -0.00261, -0.00261, -0.00065, -0.00065, -0.00065, -0.00637, -0.00638, -0.00610, -0.00334, -0.00284, -0.00262, -0.00261, -0.00261]$$

The linear model states are neither observable nor controllable. These states are detectable and stabilizable since the eigenvalues of the A matrix are less than unity.

6.1 MPC Formulation

The existing model predictive control formulation based on an infinite horizon linear quadratic regulator [111, 149] is used with some modifications to obtain a target linearization model predictive controller (TLMPC) for the polymerization process. The non-linear model is re-linearized at a steady-state obtained from the target calculation to obtain a new linear model at every sample time. The effectiveness of the feedback controller to track step changes in set-points arising from grade transitions that may also include plant start-up in the presence of measured disturbances entering the process is evaluated. The TLMPC target tracking problem can be divided into four parts as follows

6.1.1 Target Computation

The steady-state targets for the states (x_{ss}) and inputs (u_{ss}) can be evaluated using a non-linear program with a positive definite weighting matrix (Q_s) to minimize the deviations of the outputs from their targets ($\bar{y}$) and another positive definite matrix (R_s) to minimize the deviation of the input vector from its desired value ($\bar{u}$). The non-linear target tracking optimization problem can then be written as follows

$$\min_{x_{ss},u_{ss}} \Phi = (y_{ss} + P - \bar{y})^T Q_s (y_{ss} + P - \bar{y})) + (u_{ss} - \bar{u})^T R_s (u_{ss} - \bar{u})) \qquad (6.11)$$

subject to the constraints

$$f(x_{ss}, u_{ss}, d) = 0 \qquad (6.12)$$

$$y_{ss} = h(x_{ss}) \qquad (6.13)$$

along with the lower and upper limits for the inputs (u_{ss}). The effect of constant disturbances on outputs (P) has been accounted for in the above formulation. The linear model is re-evaluated at the steady-state target (x_{ss}, u_{ss}) for the current measured disturbance (d).

6.1.2 Measured Disturbances

A feed-forward control of the measured disturbances is based on the linearized model obtained at the steady-state target (x_{ss}, u_{ss}, d)

$$x_{k+1}^m = x_k^m + B^m d_k \qquad (6.14)$$

$$y_k^m = C^m x_k^m \qquad (6.15)$$

where

$$x^m = [c_a, c_b, c_i, c_s, c_t, c_z, \lambda_a, \lambda_b, T_r, \psi_0^p, \psi_1^p, \psi_2^p, c_{a,s}, c_{b,s}, c_{s,s}]^T \tag{6.16}$$

$$d = [G_{a,f}, G_{i,f}, G_{s,f}, G_{z,f}, T_f]^T \tag{6.17}$$

$$y^m = [c_{a,s}, c_{b,s}, c_{s,s}, T_r, G_{pi}, Y_{ap}, [\eta]]^T \tag{6.18}$$

The above feed-forward linear model for the measured disturbances is obtained at every sample time.

6.1.3 Regulator

The receding horizon regulator can be expressed as the following open-loop quadratic objective function

$$\min_{u^N} \Phi_k = \sum_{j=0}^{\infty} (y_{k+j}^T Q y_{k+j} + u_{k+j}^T R u_{k+j} + \Delta u_{k+j}^T S \Delta u_{k+j}) \tag{6.19}$$

where Q is the weighting matrix on the outputs, R is the weighting matrix on the inputs and S is the weighting matrix on the rate of change of inputs. The upper and lower limits for the inputs representing physical limitations for the process are also present. The solution of the above optimization problem is intractable because there are infinite decision variables. The optimization problem is formulated with finite decision variables to make the problem tractable. The inequality constraints are active for this finite number of sample times along the prediction horizon. In that case, the state and input trajectories approach the setpoint exponentially and one can use the unconstrained feedback law $u = kx$ for all future times [57] resulting in the following expression for equation 6.19

$$\begin{aligned} \min_{u^k \cdots u^{k+N}} \Phi_k \quad = \quad & x_{k+N}^T \bar{Q} x_{k+N} + \Delta u_{k+N}^T S \Delta u_{k+N} + \\ & \sum_{j=0}^{N-1} (x_{k+j}^T C^T Q C x_{k+j} + u_{k+j}^T R u_{k+j} + \Delta u_{k+j}^T S \Delta u_{k+j}) \end{aligned} \tag{6.20}$$

The vector of future open-loop control moves ($u^k \cdots u^{k+N}$) is computed from equation 6.20 and the first input value is then injected into the plant. This process is repeated at each subsequent time interval with feedback using the plant measurements to update the state vector. The terminal state penalty matrix ($\bar{Q}$) for a stable system can be determined from the discrete time algebraic Riccati equation.

6.1.4 Filter

The output disturbance model outlined by equations 5.27, 5.28 and 5.29 in Chapter 5 is used to incorporate feedback to obtain state estimates. The estimates of the states ($\hat{x}$) and the output disturbances ($\hat{p}$) can then be obtained using the extended Kalman filter for the non-linear model

$$\begin{aligned}\hat{x}_{k+1} &= \hat{x}_{k,k-1} + \int_{t_k}^{t_{k+1}} f(\hat{x}_{k,k-1}, u_k, d_k, t)dt \\ &\quad + L_x(y_k - h(x_k, u_k, d_k, t) - \hat{p}_{k,k-1}) \end{aligned} \tag{6.21}$$

$$\hat{p}_{k+1,k} = \hat{p}_{k,k-1} + L_p(y_k - h(x_k, u_k, d_k, t) - \hat{p}_{k,k-1}) \tag{6.22}$$

The above outlined filter ($L = [L_x, L_p]$) is then used to provide feedback. The copolymer composition and viscosity are not measured at every sample time and have an associated delay. The time-varying linear system can be reformulated as a time invariant raised system [49] to obtain the filter gain. The equivalent filter gain can then be expressed as

$$L = 0 \quad \text{measurement missing} \tag{6.23}$$

$$L = [L_x, L_p] \quad \text{measurement present} \tag{6.24}$$

Hence, there is no updating of state estimates coming from the missing plant measurements. The laboratory measurements from the plant are adjusted for the delay (k_d) and then used to update the estimate of the associated output disturbance ($\hat{p}$).

$$\hat{p}_{k-k_d+1,k-k_d} = y_{k-k_d} - h(\hat{x}_{k-k_d,k-k_d-1}) \tag{6.25}$$

The above target linearization model predictive controller (TLMPC) is compared with the linear model predictive controller (LMPC) [57, 149, 127] for feedback control of polymerization processes during plant start-up, polymer grade change and regulation around a setpoint.

6.2 MPC Results

The MMA-VA copolymerization process is extremely non-linear and could benefit from TLMPC feedback to achieve process objectives. Three different scenarios for polymerization control have been examined:

- Plant start-up
- Polymer grade change
- Regulation at a fixed setpoint

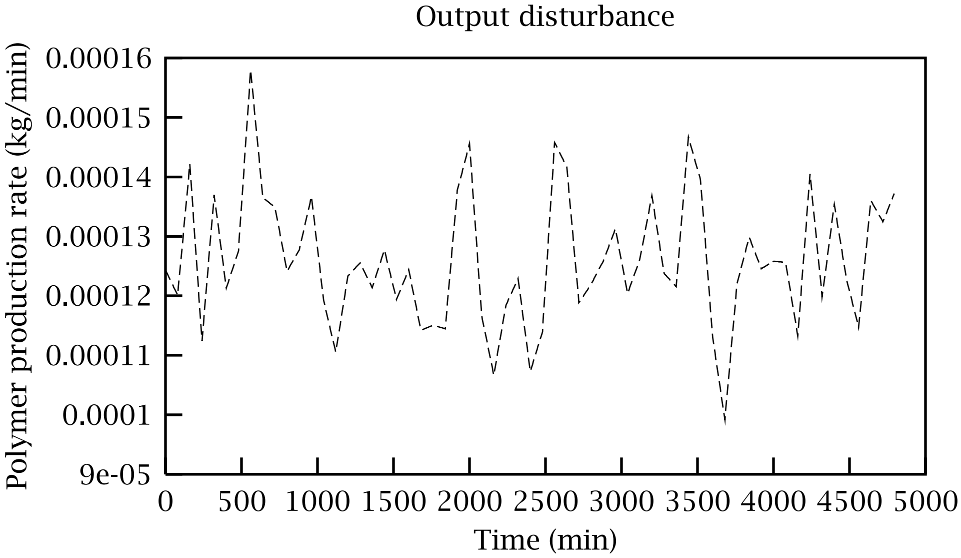

Figure 6.1: Output disturbance in polymer production rate

In these feedback control simulations, the plant is represented by the non-linear model simulation along with an additive output disturbance ($b(t)$) that is based on our experience with data from the industrial polymerization process. The variation of output disturbance ($b(t)$) with time is used to give the following plant representation for simulations.

$$\begin{aligned} \frac{dx}{dt} &= f(x(t), u(t), d(t), t) \\ y &= h(x) \quad + b(t) \end{aligned}$$

The measured disturbances (d) also vary with time and are based on our experience with industrial datasets. These realistic disturbances (d) and plant-model mismatch (b) are used to mimic a typical polymerization process in the following simulations. The time varying output disturbances for regulated measurements (Figures 6.1, 6.2 and 6.3) and measured disturbances (Figures 6.4 and 6.5) that are used in the feedback control simulations are shown.

The feedback control simulations also take into account that copolymer composition and viscosity have a larger sampling time with associated delay. The feedback controllers are tuned appropriately to give the desired control action. The quadratic penalty on the deviation of the outputs (Q) from their desired values ($\bar{y}$) is set to its nominal value

$$Q = \frac{1}{\bar{y}^2} \tag{6.26}$$

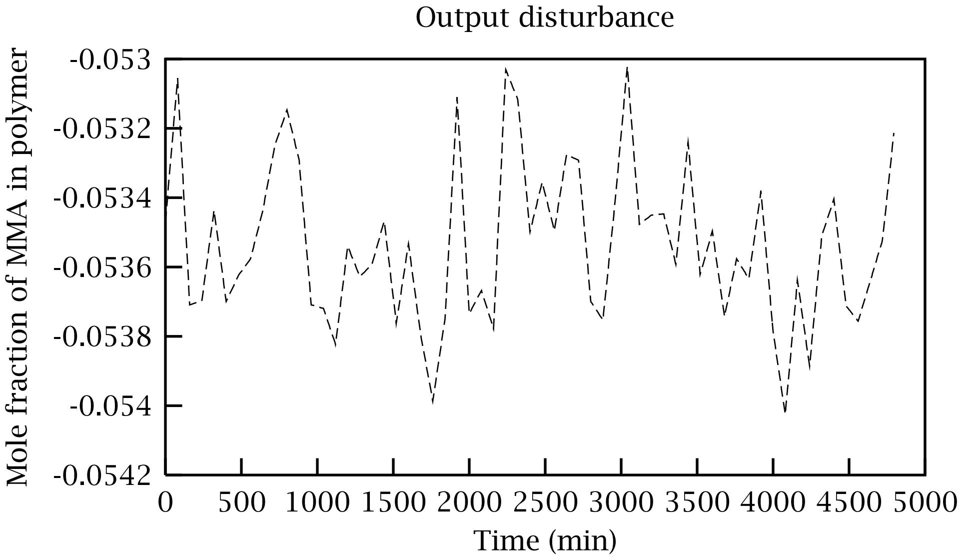

Figure 6.2: Output disturbance in copolymer composition

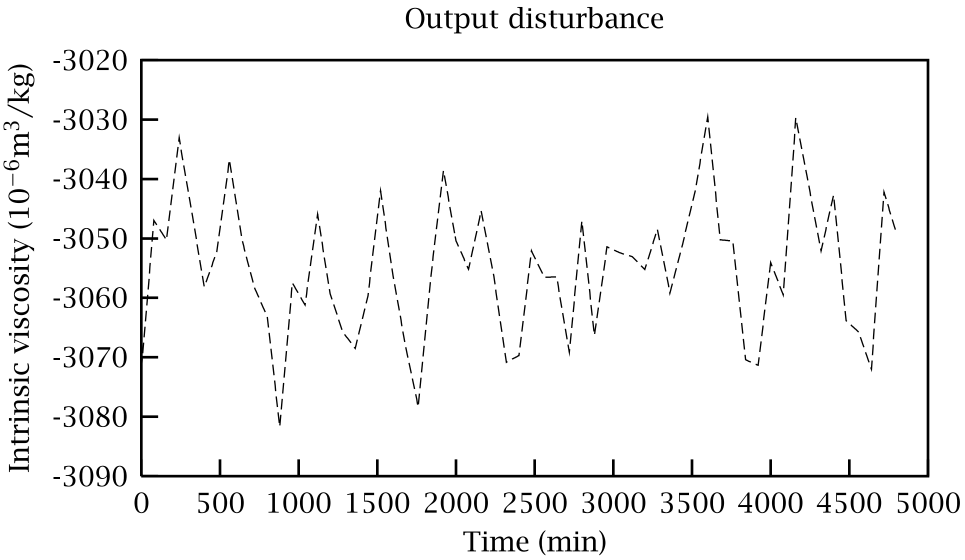

Figure 6.3: Output disturbance in copolymer viscosity

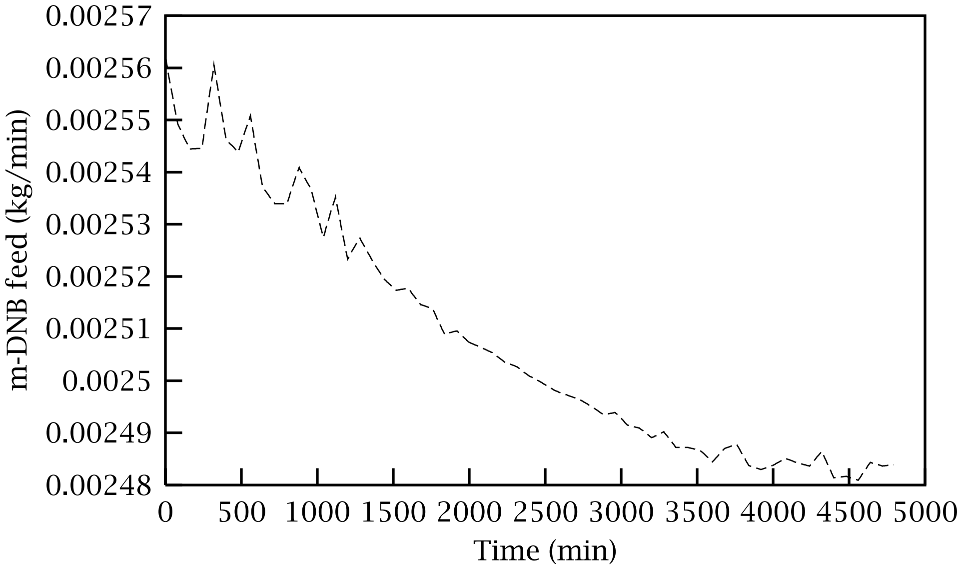

Figure 6.4: Measured disturbance due to m-DNB in feed stream

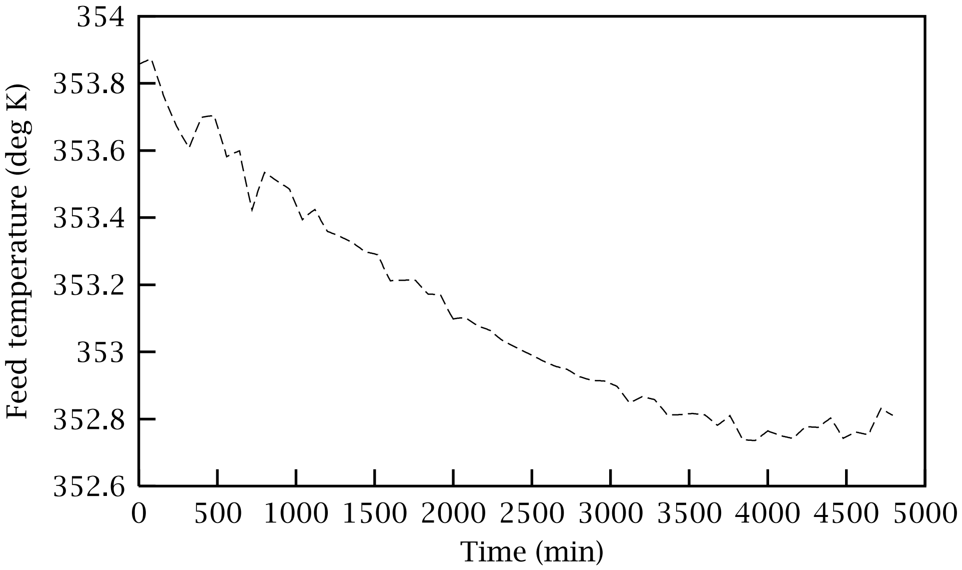

Figure 6.5: Measured disturbance of feed temperature

The quadratic penalty on the deviation of the inputs (R) from their desired values ($\bar{u}$) is set to zero

$$R = 0 \tag{6.27}$$

The values of the quadratic penalty on the rate of change of inputs (S) are set after taking into account the lower bound (u_{min}) and upper bound (u_{max}) into consideration

$$S = S_o \frac{1}{(u_{max} - u_{min})^2} \tag{6.28}$$

The rate of change penalty on inputs is then set by choosing appropriate value of S_o (Table 6.1). The output disturbance model formulation is employed with filter gain

	S_o (LMPC)	S_o (TLMPC)	u_{max}	u_{min}
Vinyl acetate feed ($G_{b,f}$)	100	10	3.0kg/min	0.15kg/min
Acetaldehyde feed ($G_{t,f}$)	100	100	0.25kg/min	0.005kg/min
Coolant temperature (T_j)	100	1000	373^oK	298^oK

Table 6.1: Input constraints and tuning for MMA-VA copolymerization

($L = [0, I]$) to account for the bias between model predictions and plant data. The augmented disturbance model provides the integral action to the controller thereby resulting in zero steady-state tracking error.

The process objective is to make copolymer grades characterized by composition and viscosity, at the required production rates. The copolymer grades specified by their desired targets that are chosen for the feedback controller simulations are listed (Table 6.2). The main characteristics and conclusions of the feedback controller simulations can be tabulated as follows (Table 6.3).

Product grade	Polymer production rate (kg/min)	Mole fraction of MMA in copolymer	Copolymer viscosity (10^{-6}m^3/kg)
A	0.25	0.75	37000
B	0.30	0.60	35000
C	0.30	0.65	36000

Table 6.2: Product grades for MMA-VA copolymerization

6.2.1 Plant Start-up

The following results show the performance of a model predictive controller during plant start-up. In each start-up, the reactor has initially been flushed with a stream that

Case Number	Plant Operation	Feedback Controller	Controller Performance	Figures
1	Start-up (No polymer to Grade A)	LMPC TLMPC	Fails Succeeds	6.6, 6.7, 6.8 6.9, 6.10, 6.11
2	Start-up (No polymer to Grade B)	LMPC TLMPC	Succeeds Succeeds	6.12, 6.13, 6.14 6.15, 6.16, 6.17
3	Grade change (Grade B to Grade A)	LMPC TLMPC	Fails Succeeds	6.18, 6.19, 6.20 6.21, 6.22, 6.23
4	Grade change (Grade B to Grade C)	LMPC TLMPC	Succeeds Succeeds	6.24, 6.25, 6.26 6.27, 6.28, 6.29
5	Regulation (Grade A)	LMPC TLMPC	Fails Succeeds	6.30, 6.31, 6.32 6.33, 6.34, 6.35
6	Regulation (Grade B)	LMPC TLMPC	Succeeds Succeeds	6.36, 6.37, 6.38 6.39, 6.40, 6.41

Table 6.3: Feedback controller performance for MMA-VA copolymerization

has dilute quantities of monomers dissolved in the solvent. There is no initiator, live polymer chains or dead polymer chains that are present in the reactor. The objective of start-up is to start making a particular grade of copolymer characterized by composition and viscosity, at a certain production rate. The production rate is available as an on-line measurement every 5 minutes whereas the copolymer composition and viscosity are measured every 25 minutes with a delay of 25 minutes. The first measurements of copolymer composition and viscosity are taken only at 100 minutes. The following two cases are outlined.

Case Number 1. The first set of simulations show a clear case where an LMPC feedback fails whereas a TLMPC feedback attains the process objectives. The closed loop outputs corresponding to the two feedback controllers are compared (Figures 6.6, 6.7 and 6.8). The polymer production rate reaches its setpoint with both LMPC and TLMPC feedback controllers. The polymer composition and viscosity oscillate around their setpoints instead of settling at the desired targets for LMPC feedback scheme. The closed loop inputs corresponding to the two feedback controllers are compared (Figures 6.9, 6.10 and 6.11). The inputs corresponding to TLMPC are smoother compared to the inputs corresponding to LMPC.

Case Number 2. The second set of simulations show a case where both LMPC and TLMPC feedback controllers attain process objectives. The performance of the two feedback controllers is examined (Figures 6.12, 6.13 and 6.14). The polymer production

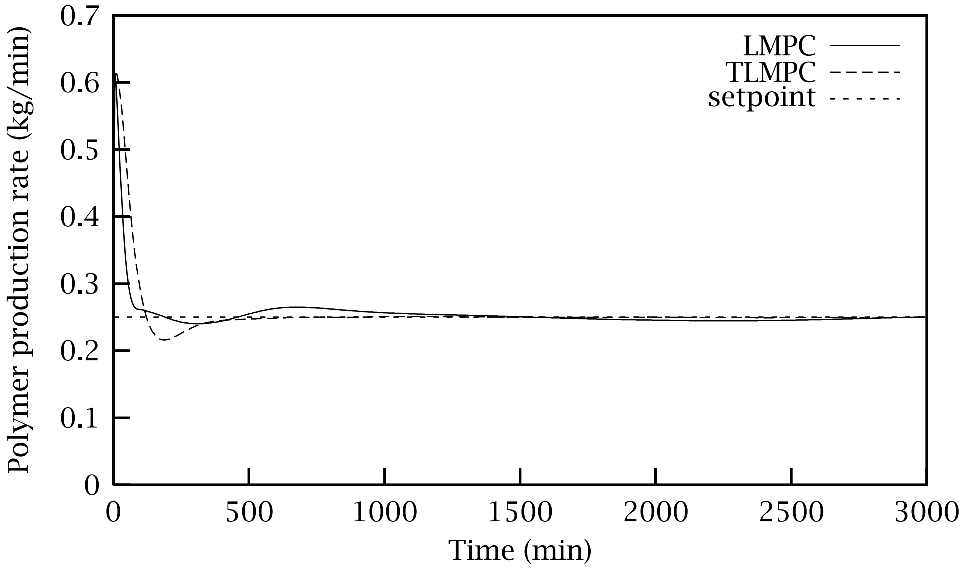

Figure 6.6: Case 1: Measured polymer production rate

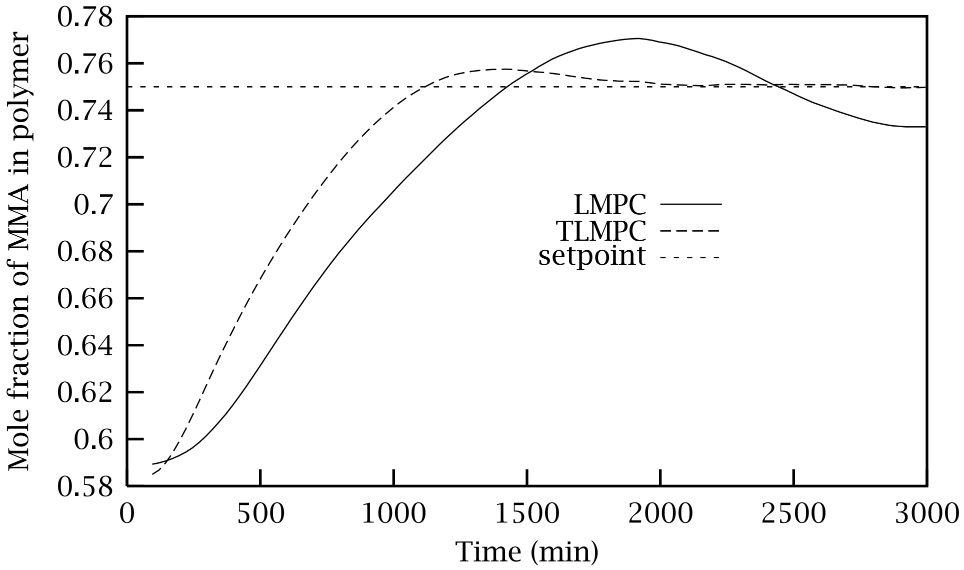

Figure 6.7: Case 1: Measured copolymer composition

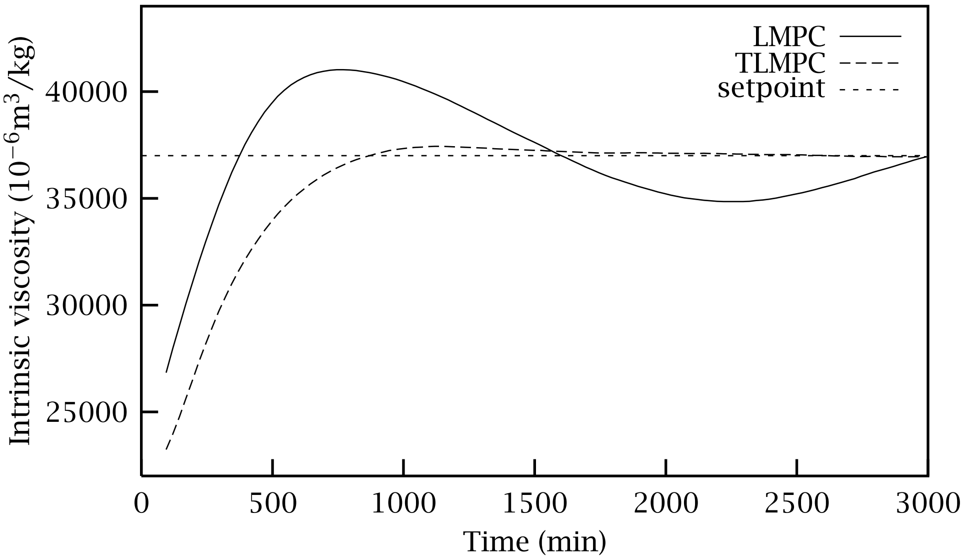

Figure 6.8: Case 1: Measured copolymer viscosity

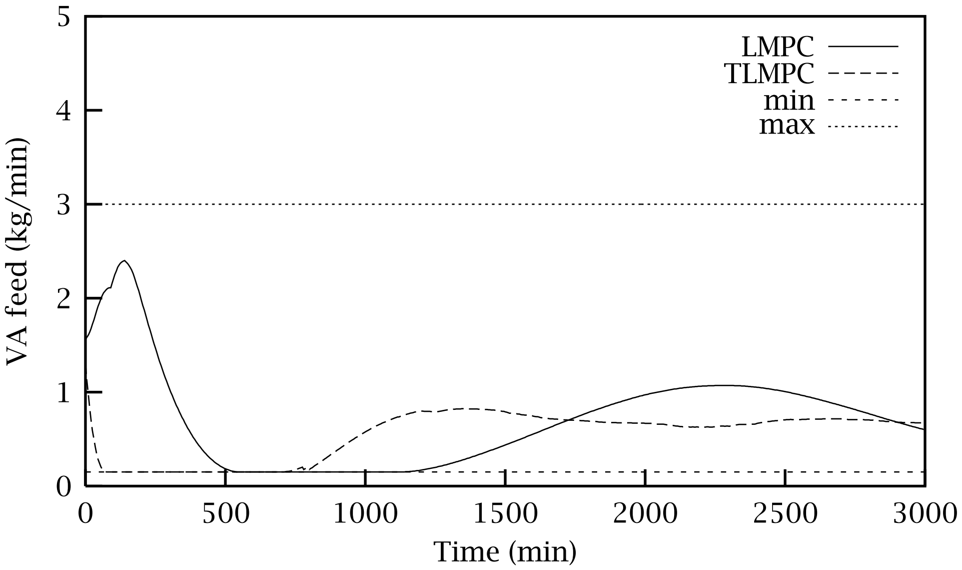

Figure 6.9: Case 1: Manipulated VA feed

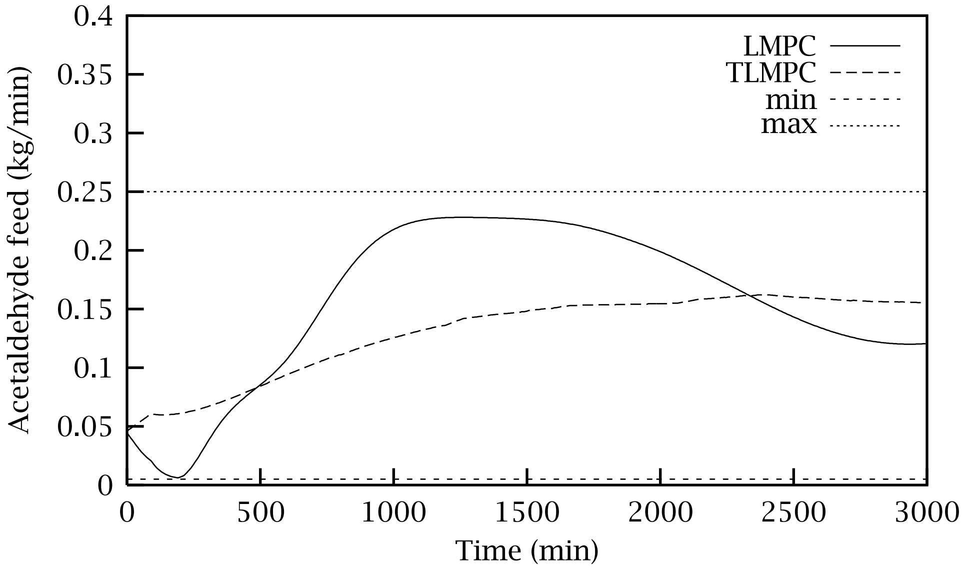

Figure 6.10: Case 1: Manipulated acetaldehyde feed

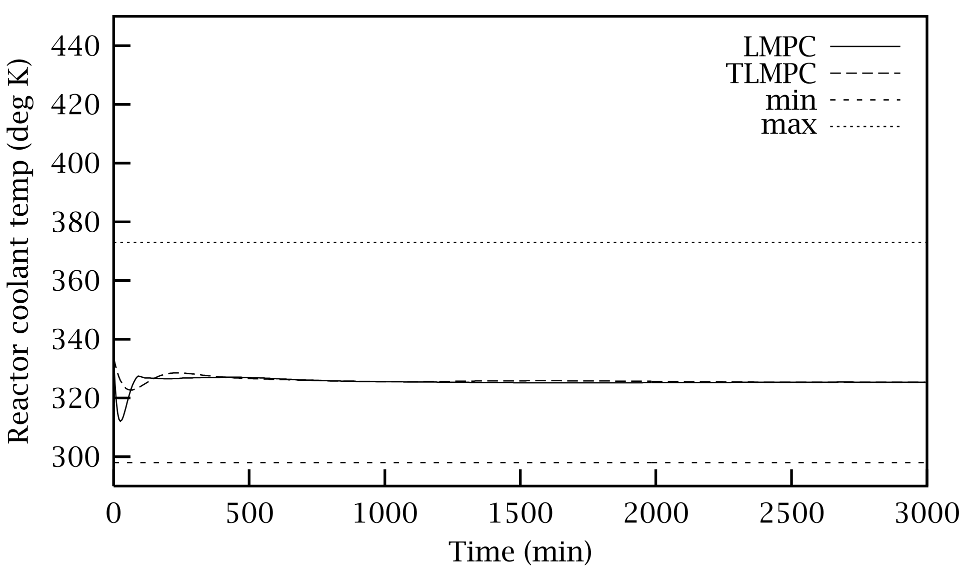

Figure 6.11: Case 1: Manipulated coolant temperature

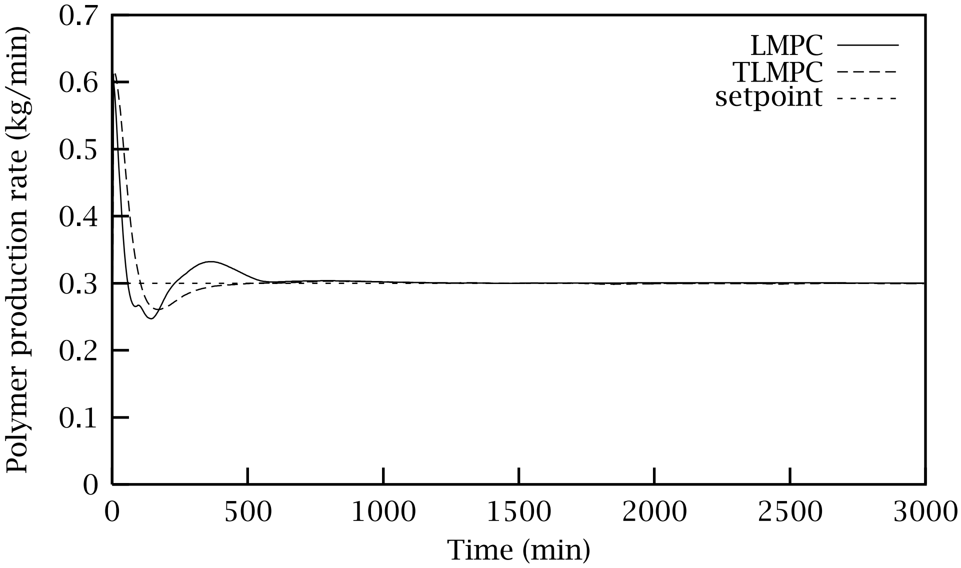

Figure 6.12: Case 2: Measured polymer production rate

rate, composition and viscosity reach their setpoints for both feedback controllers. The inputs corresponding to TLMPC are similar to the inputs corresponding to LMPC (Figures 6.15, 6.16 and 6.17).

6.2.2 Grade Change

The performance of the two model predictive controllers during polymer grade changes is studied. The product grade is characterized by the composition and viscosity of the copolymer. In each grade change, the reactor is initially making a certain grade of polymer before it is required to make a different product grade. The objective of grade change is to start making the new grade of copolymer characterized by composition and viscosity, at a certain production rate. The production rate is measured every 5 minutes whereas the copolymer composition and viscosity are measured every 25 minutes with a delay of 25 minutes. The following two cases are examined.

Case Number 3. The first grade change case exhibits conclusive failure of an LMPC feedback scheme compared to a TLMPC feedback scheme. The polymer production rate (Figure 6.18), copolymer composition (Figure 6.19) and viscosity (Figure 6.20) vary around their setpoints for LMPC in sharp contrast to TLMPC.

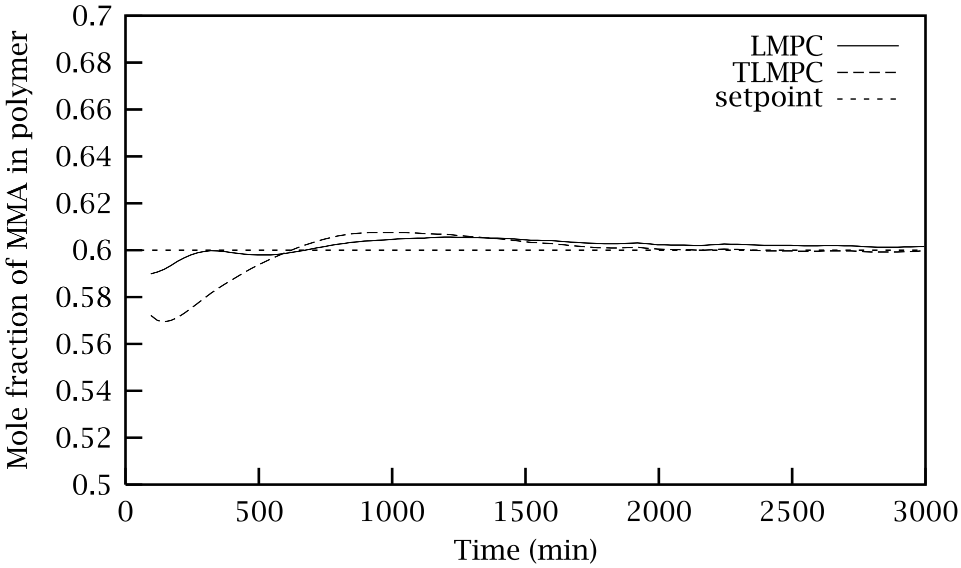

Figure 6.13: Case 2: Measured copolymer composition

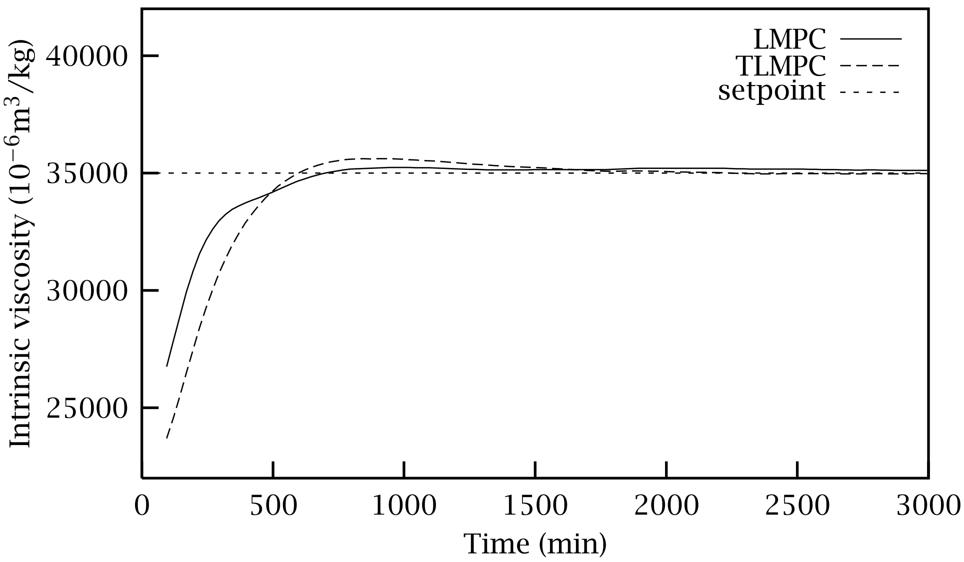

Figure 6.14: Case 2: Measured copolymer viscosity

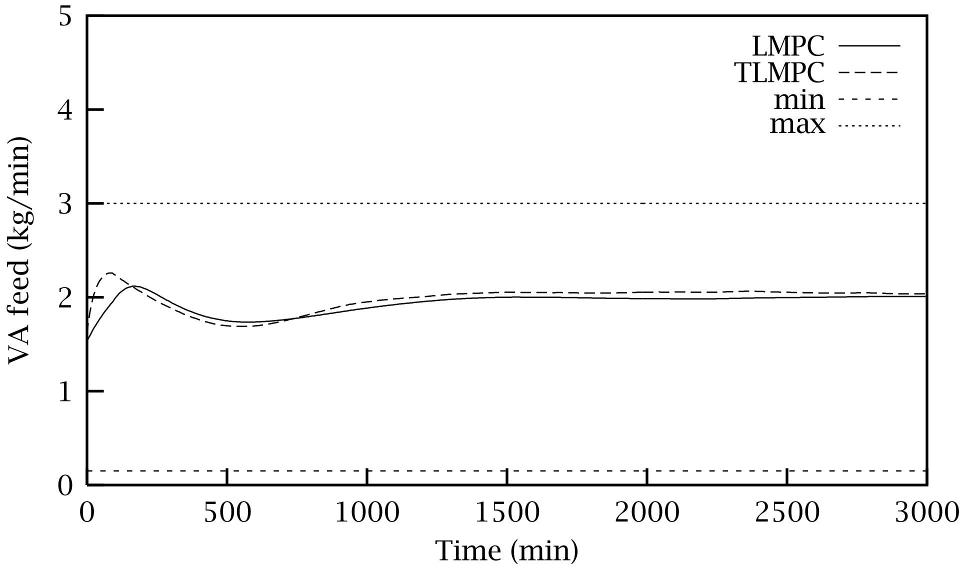

Figure 6.15: Case 2: Manipulated VA feed

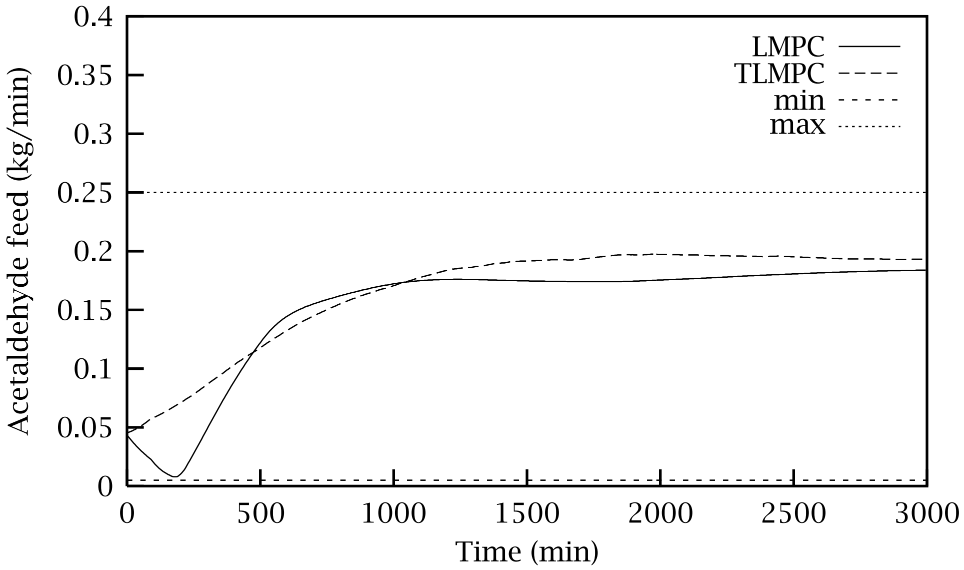

Figure 6.16: Case 2: Manipulated acetaldehyde feed

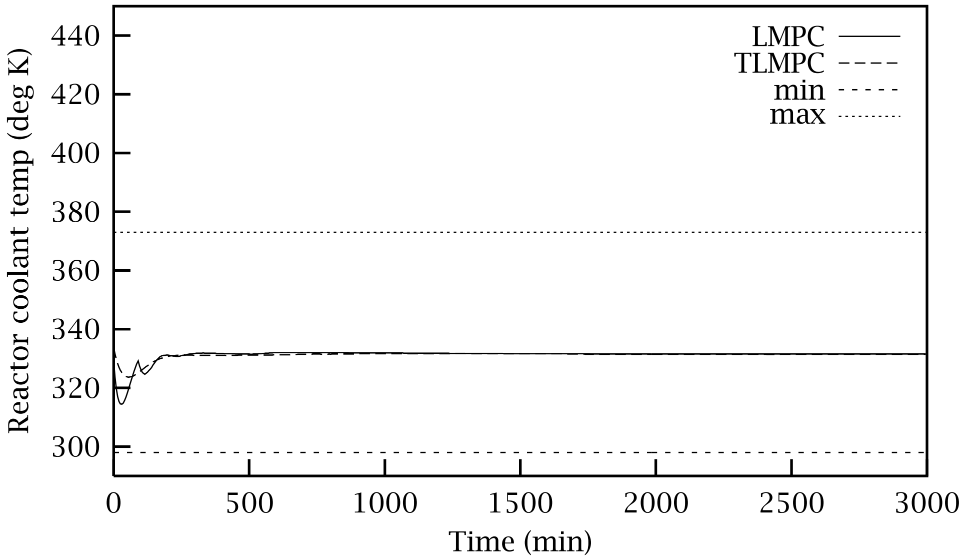

Figure 6.17: Case 2: Manipulated coolant temperature

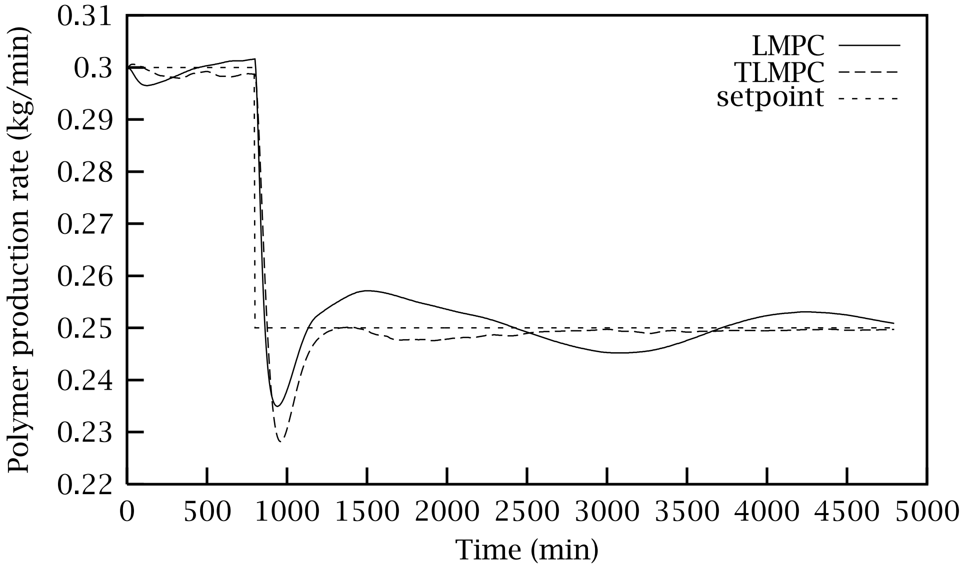

Figure 6.18: Case 3: Measured polymer production rate

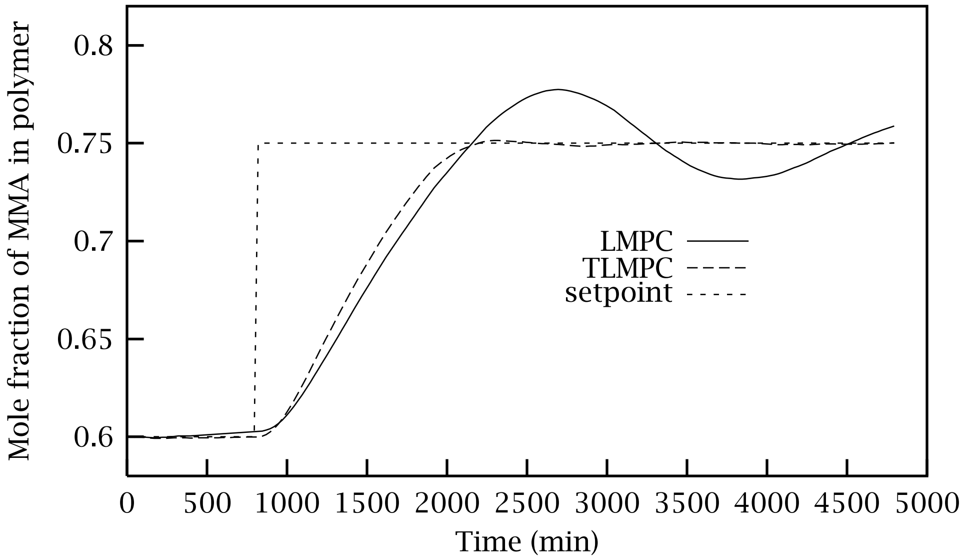

Figure 6.19: Case 3: Measured copolymer composition

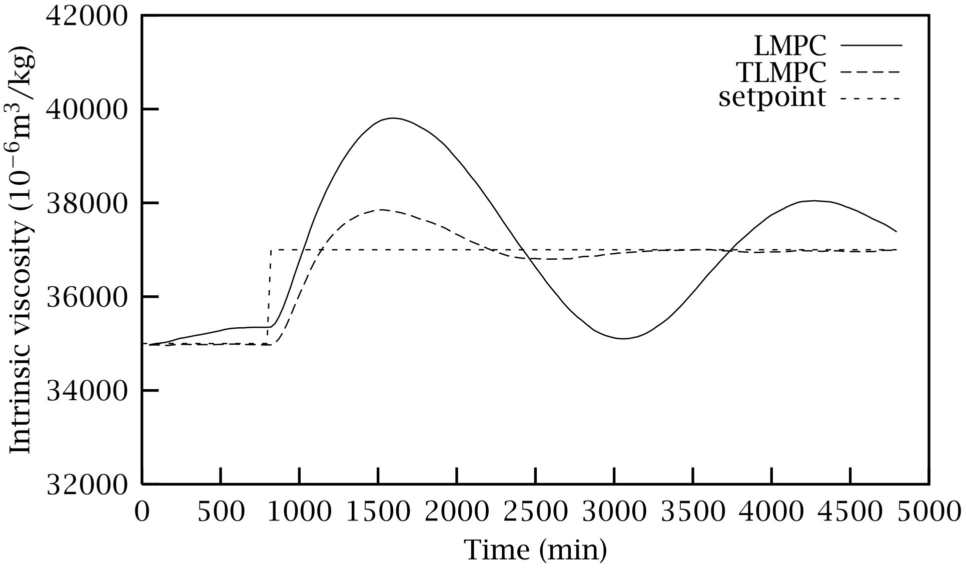

Figure 6.20: Case 3: Measured copolymer viscosity

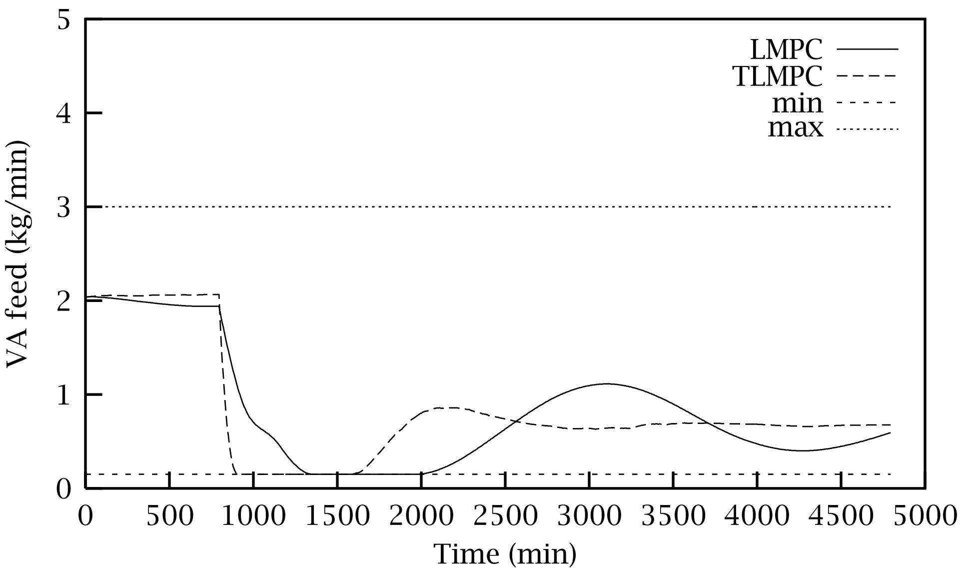

Figure 6.21: Case 3: Manipulated VA feed

The TLMPC inputs do not vary severely in contrast to those corresponding to LMPC (Figures 6.21, 6.22 and 6.23). The LMPC feedback scheme is unable to achieve process objectives even after moving the inputs significantly.

Case Number 4. The second grade change case results in good performance by LMPC and TLMPC feedback schemes. The regulated outputs corresponding to both the feedback controllers (Figures 6.24, 6.25 and 6.26) reach their targets. The manipulated inputs resulting from the two control schemes are alike (Figures 6.27, 6.28 and 6.29).

6.2.3 Regulation around a setpoint

Regulatory control around a setpoint determined by polymer requirements is performed for two different product grades. The reactor is initially around the setpoint for the polymer grade. The process goal is to keep making the particular grade of copolymer characterized by composition and viscosity, at a certain production rate. The production rate is available as an on-line measurement every 5 minutes whereas the copolymer composition and viscosity are available from the laboratory every 15 minutes with a delay of 25 minutes. Two regulation cases are studied.

Case Number 5. In the first set of simulations, the LMPC feedback fails whereas a TLMPC feedback succeeds in reaching process goals (Figures 6.30, 6.31 and 6.32). The closed-loop outputs reach their setpoints for TLMPC whereas they oscillate around the

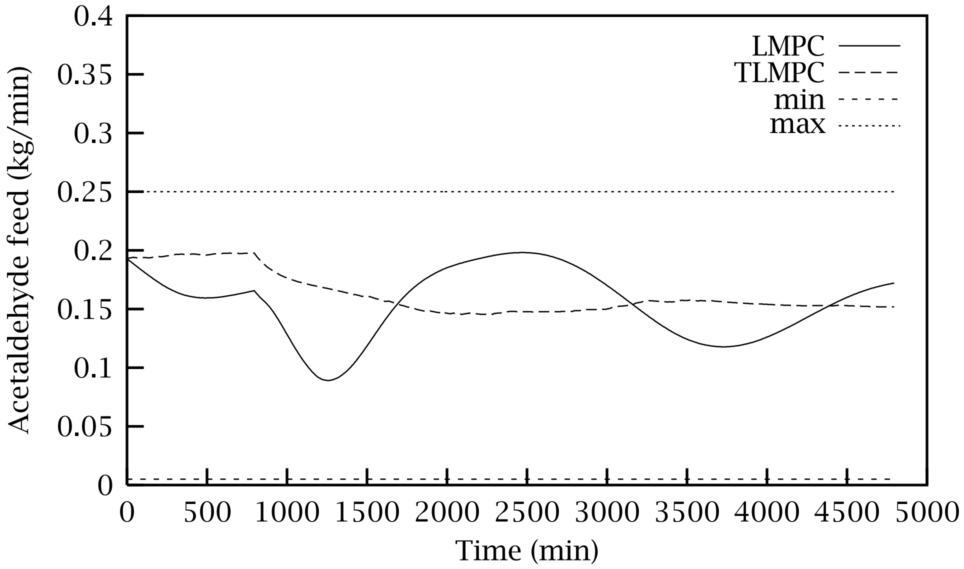

Figure 6.22: Case 3: Manipulated acetaldehyde feed

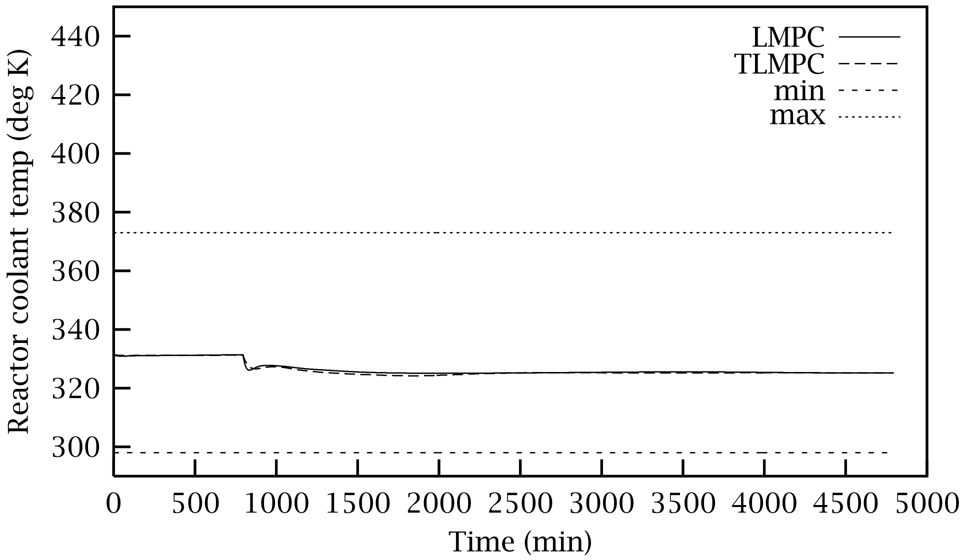

Figure 6.23: Case 3: Manipulated coolant temperature

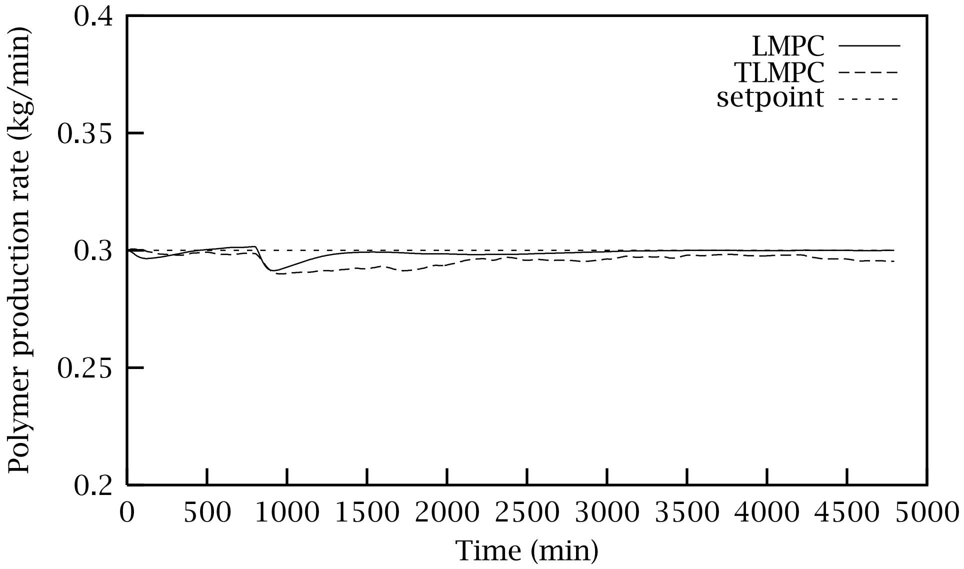

Figure 6.24: Case 4: Measured polymer production rate

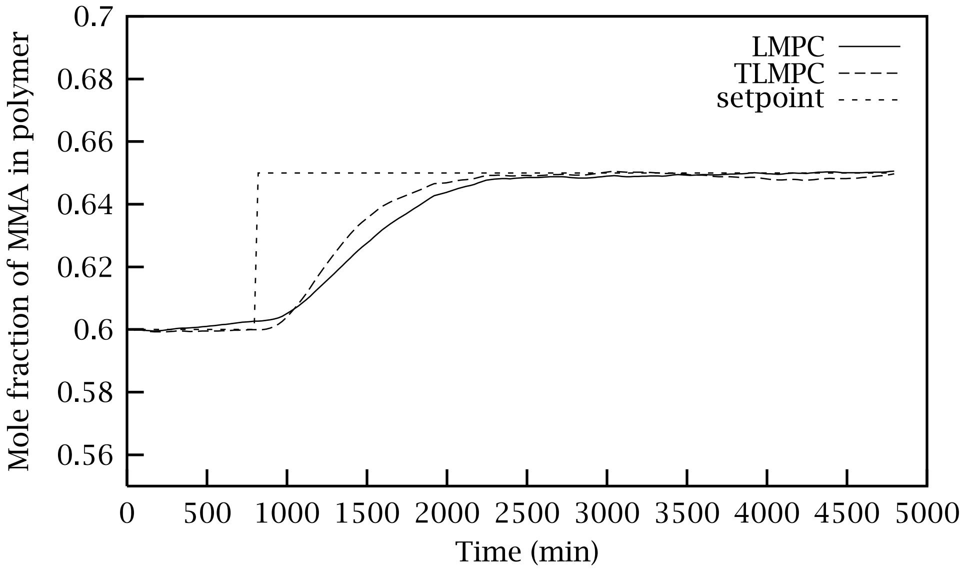

Figure 6.25: Case 4: Measured copolymer composition

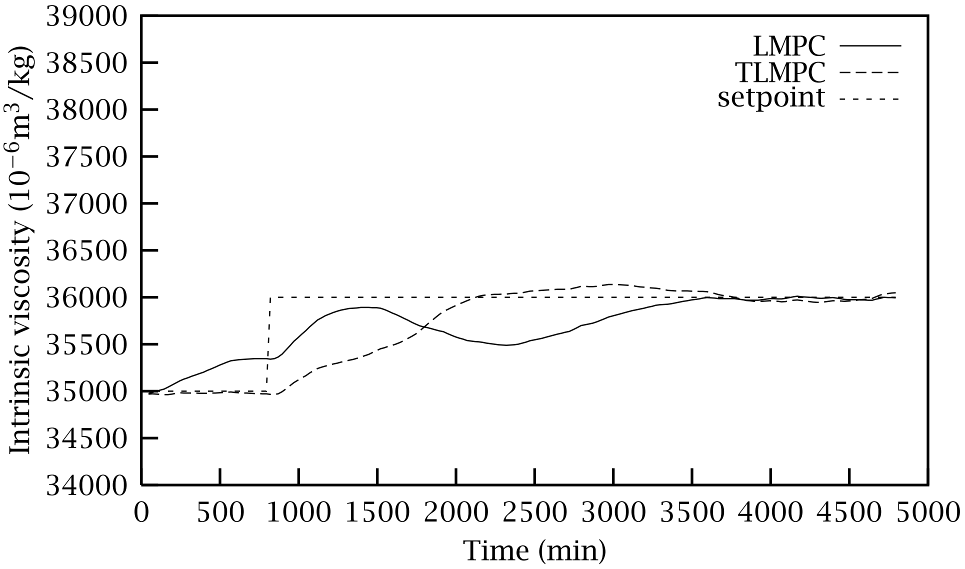

Figure 6.26: Case 4: Measured copolymer viscosity

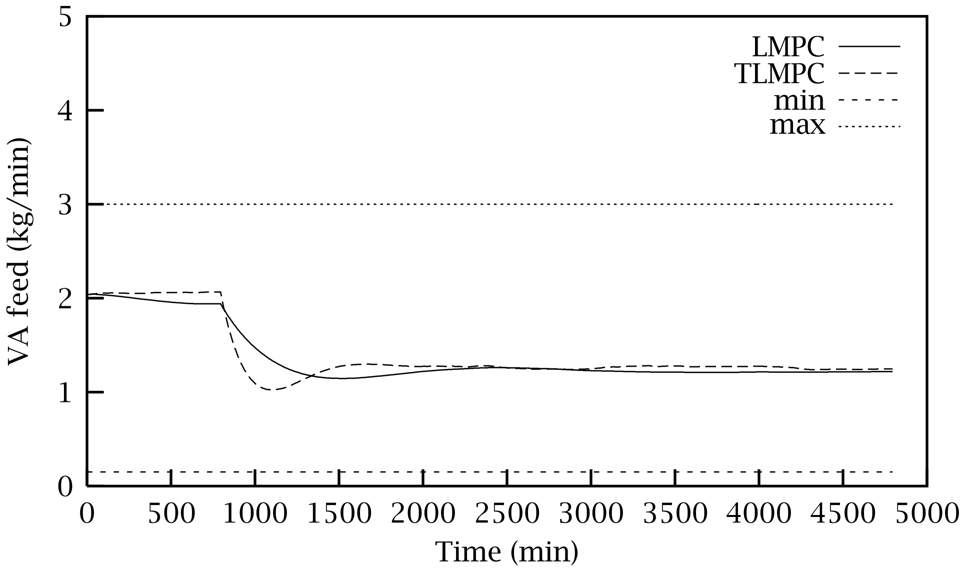

Figure 6.27: Case 4: Manipulated VA feed

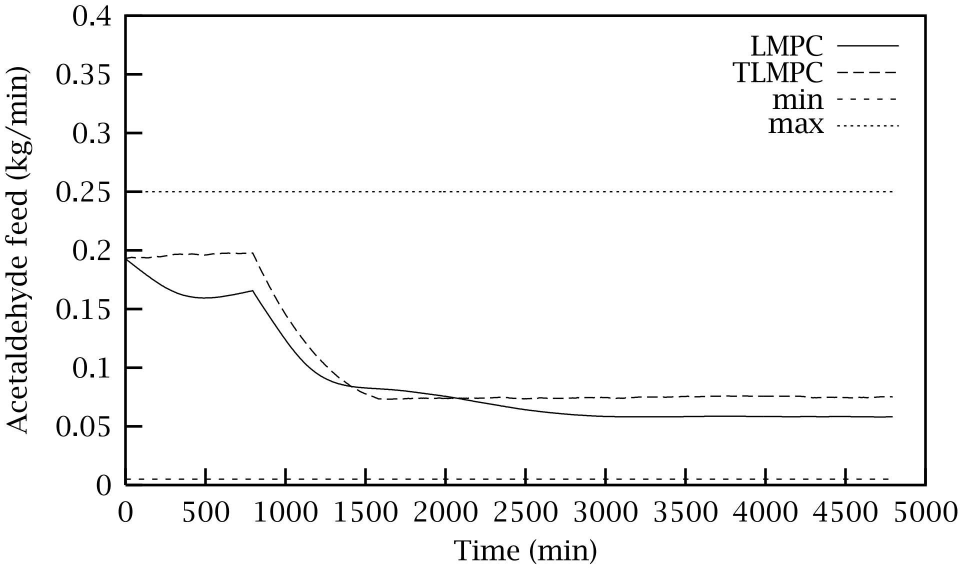

Figure 6.28: Case 4: Manipulated acetaldehyde feed

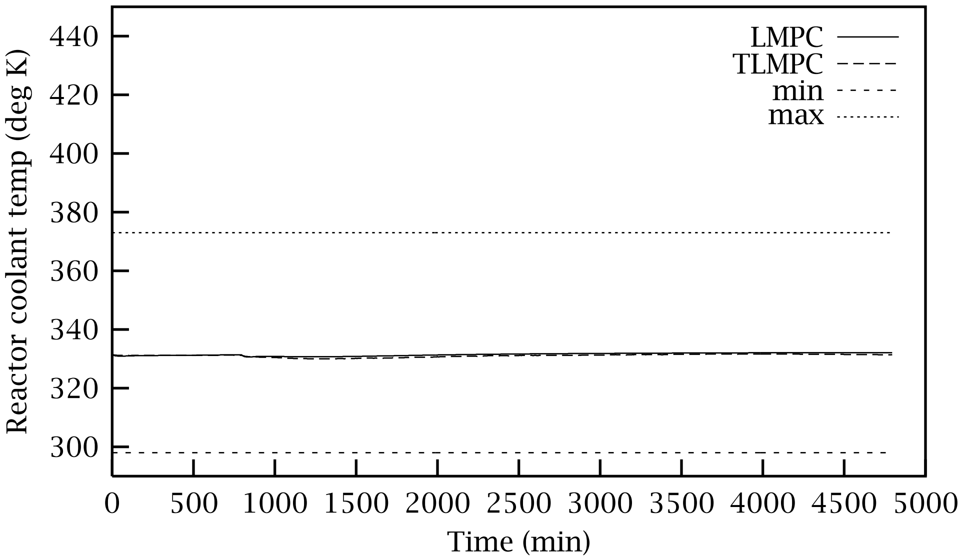

Figure 6.29: Case 4: Manipulated coolant temperature

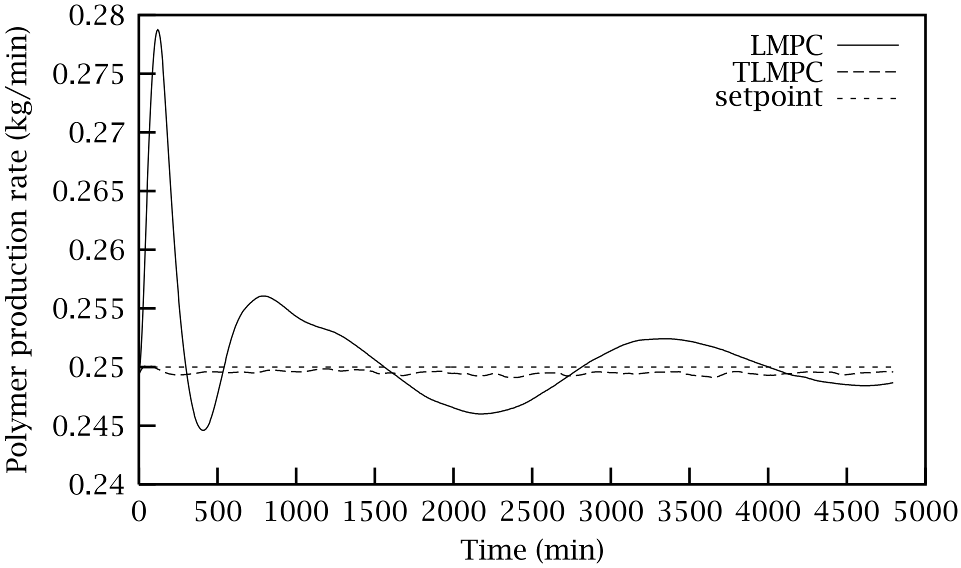

Figure 6.30: Case 5: Measured polymer production rate

setpoints for LMPC. The closed loop inputs corresponding to LMPC move around aggressively in comparison to those corresponding to TLMPC (Figures 6.33, 6.34 and 6.35).

Case Number 6. The second regulation case exhibits a case where both LMPC and TLMPC feedback controllers attain process objectives (Figures 6.36, 6.37 and 6.38). The polymer production rate, composition and viscosity reach their setpoints for both feedback controllers. The closed loop inputs of LMPC and TLMPC feedback schemes are close together (Figures 6.39, 6.40 and 6.41).

6.2.4 Comments

A TLMPC feedback controller is formulated to perform target tracking in a prototypical polymerization process and then implemented for the following scenarios:

- Plant start-up
- Polymer grade change
- Regulation at a fixed setpoint

The results of this chapter show the effectiveness of TLMPC compared to LMPC for making various grades of a copolymer. The LMPC feedback scheme is effective for a lot of polymer control cases as demonstrated in this chapter. But, the LMPC feedback

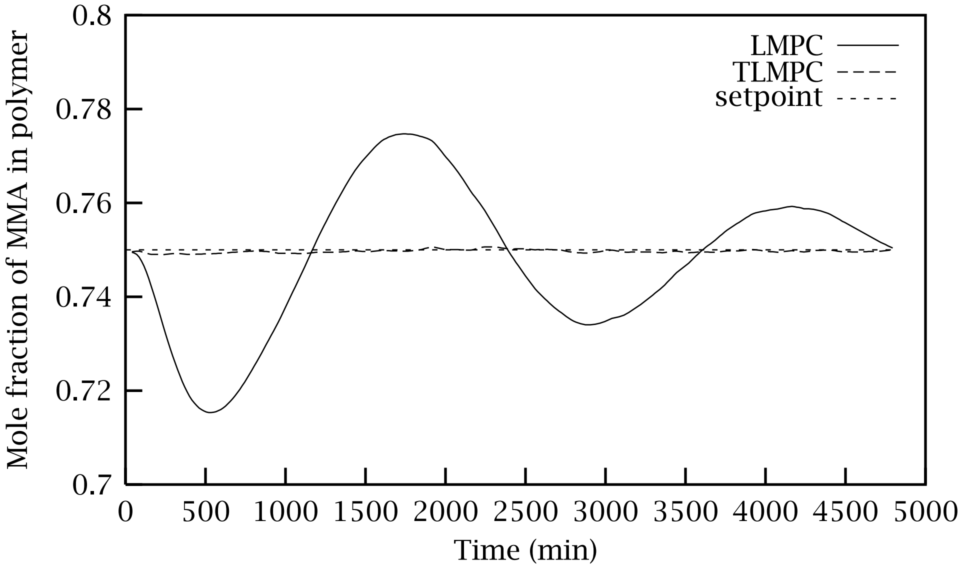

Figure 6.31: Case 5: Measured copolymer composition

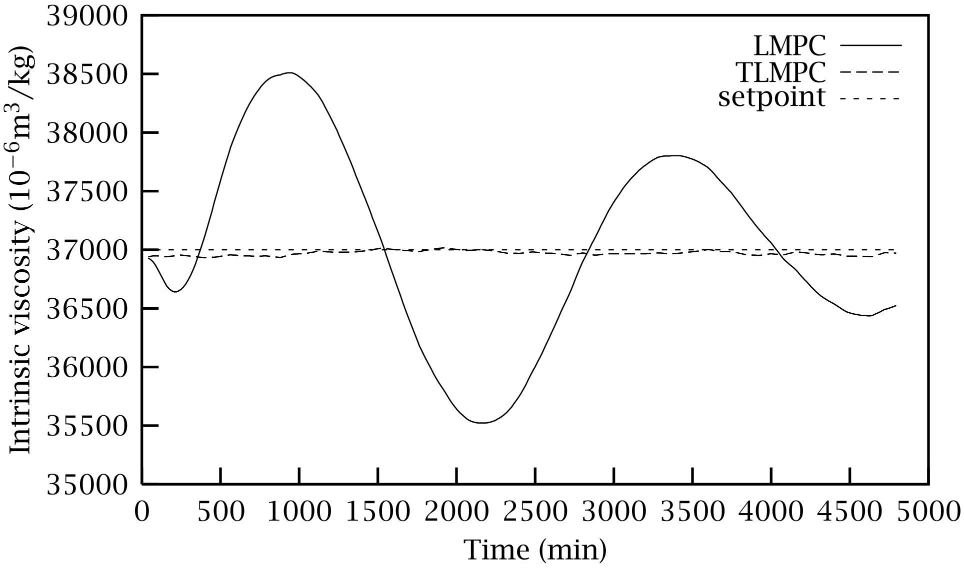

Figure 6.32: Case 5: Measured copolymer viscosity

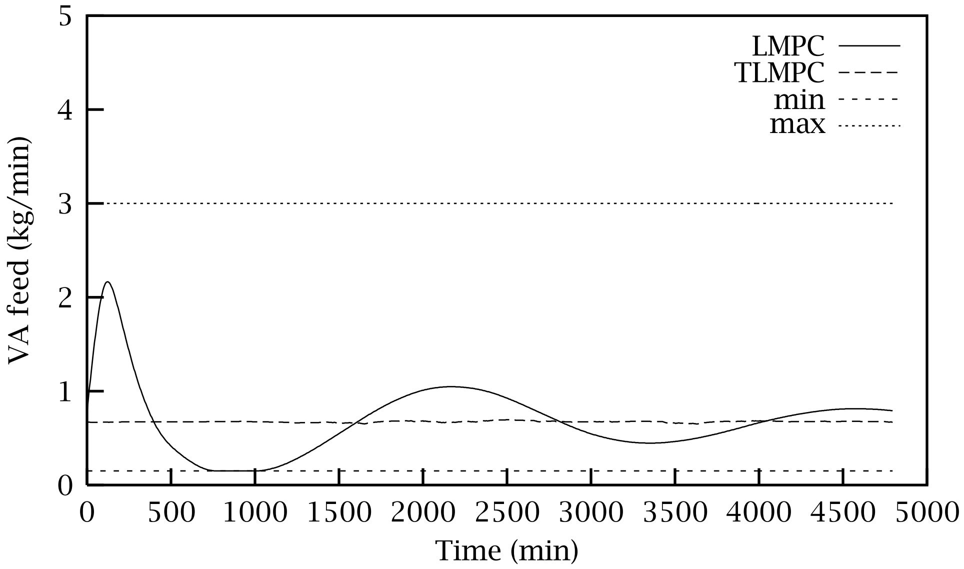

Figure 6.33: Case 5: Manipulated VA feed

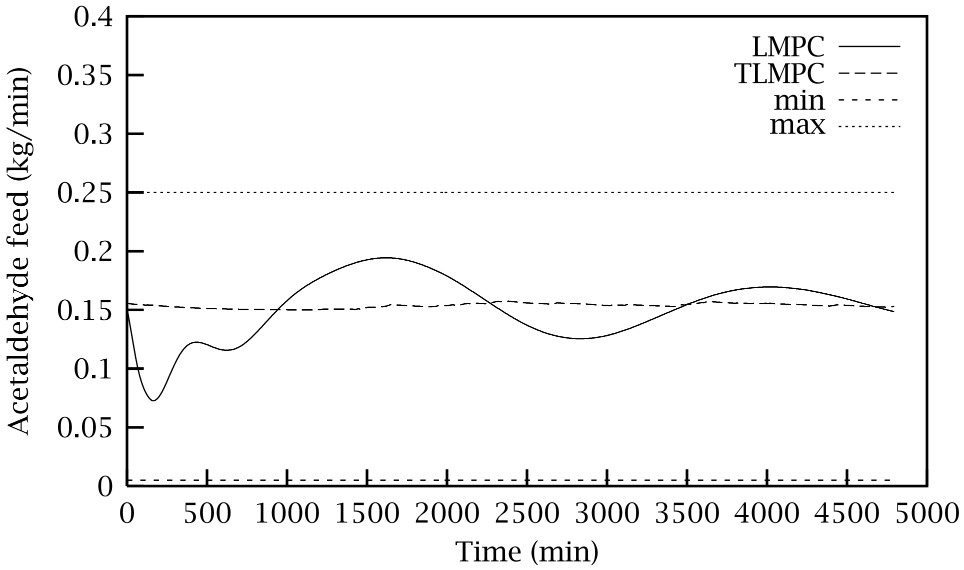

Figure 6.34: Case 5: Manipulated acetaldehyde feed

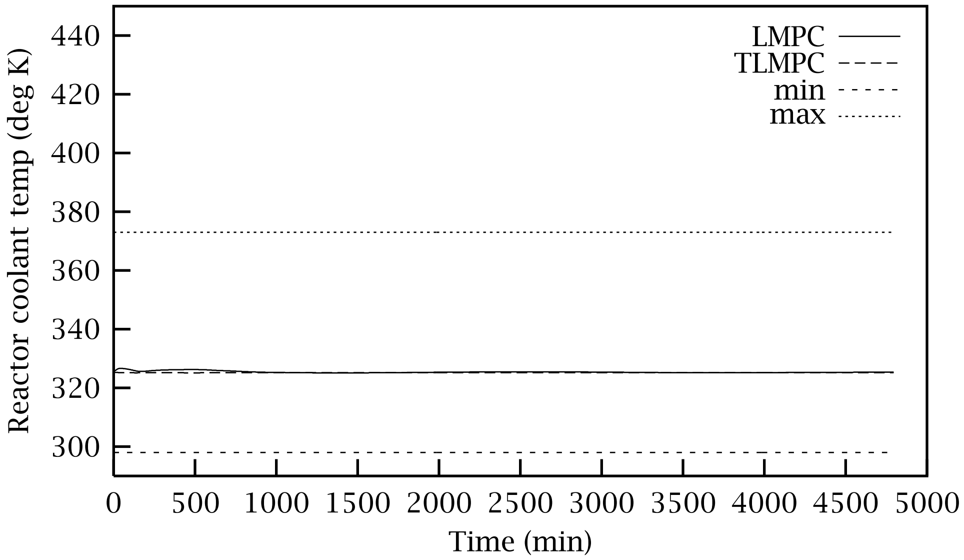

Figure 6.35: Case 5: Manipulated coolant temperature

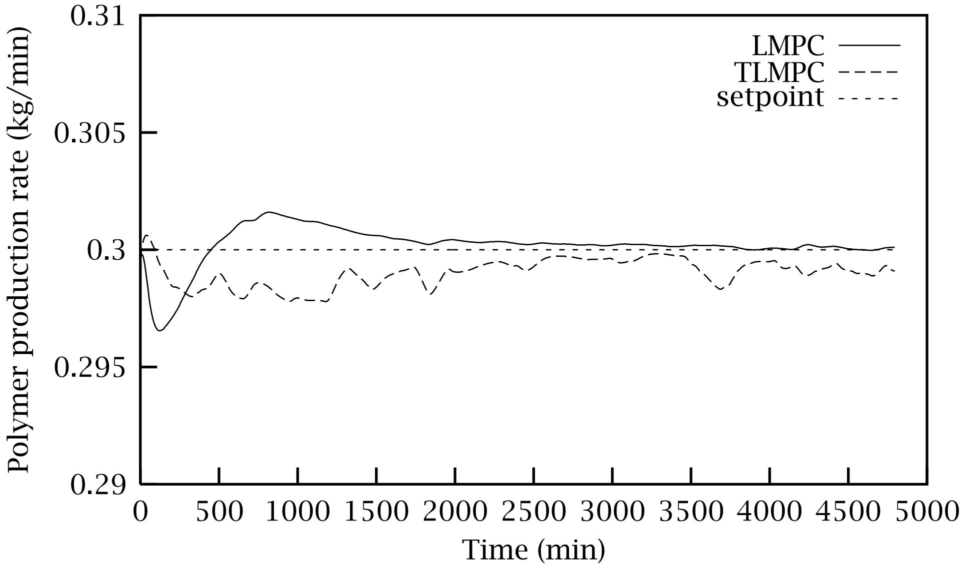

Figure 6.36: Case 6: Measured polymer production rate

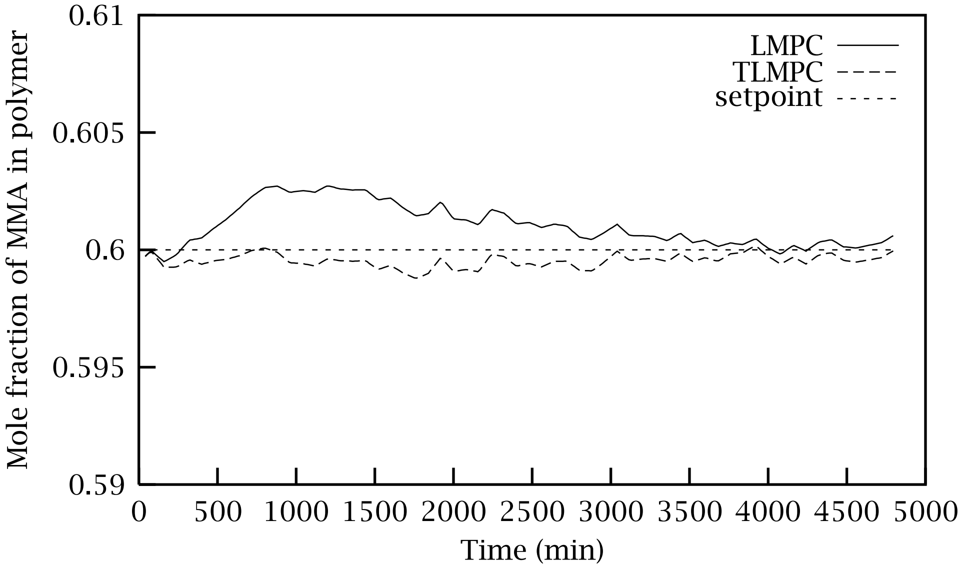

Figure 6.37: Case 6: Measured copolymer composition

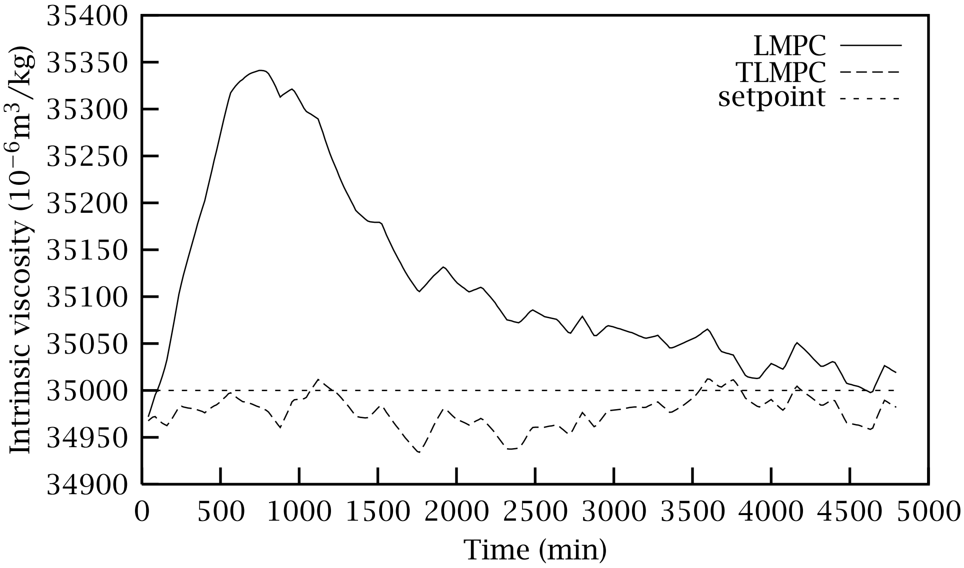

Figure 6.38: Case 6: Measured copolymer viscosity

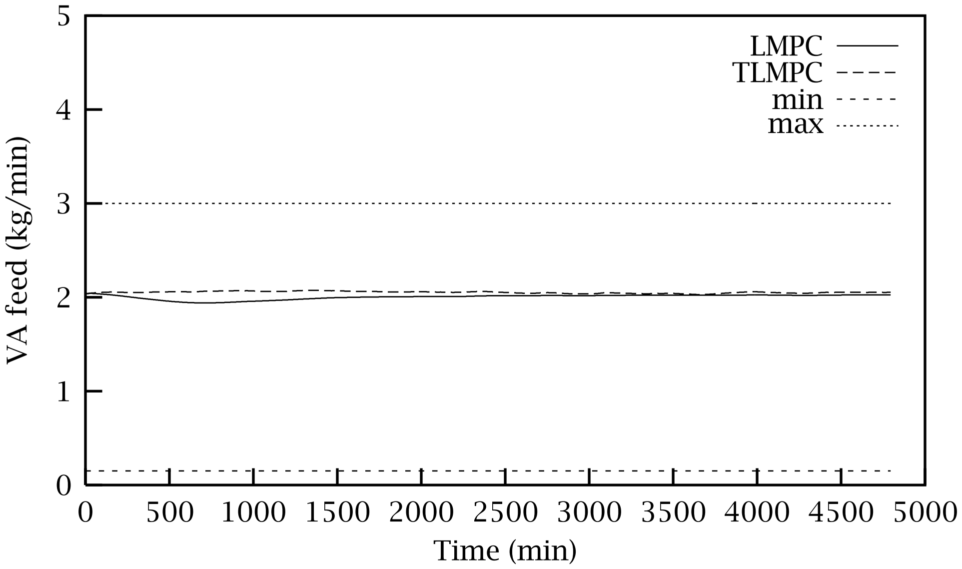

Figure 6.39: Case 6: Manipulated VA feed

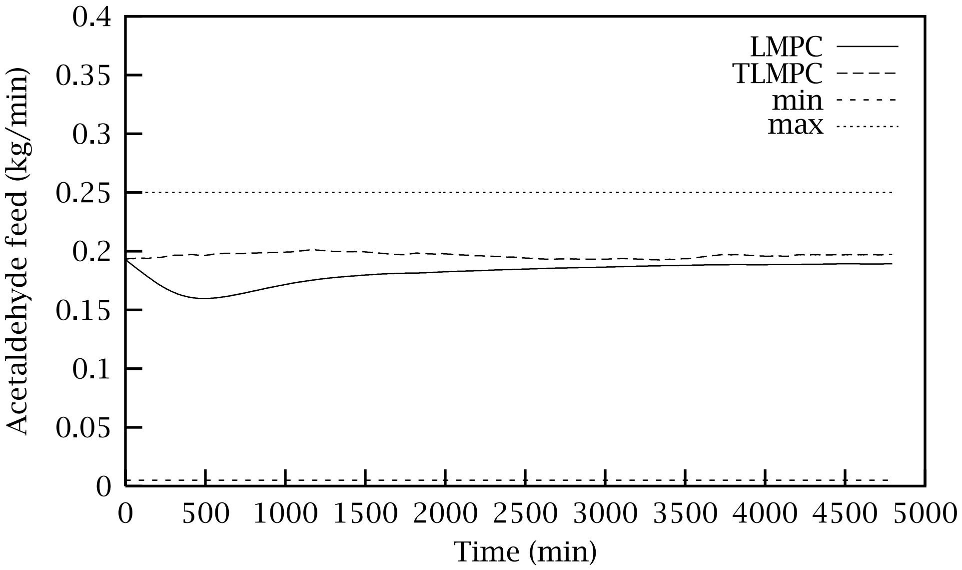

Figure 6.40: Case 6: Manipulated acetaldehyde feed

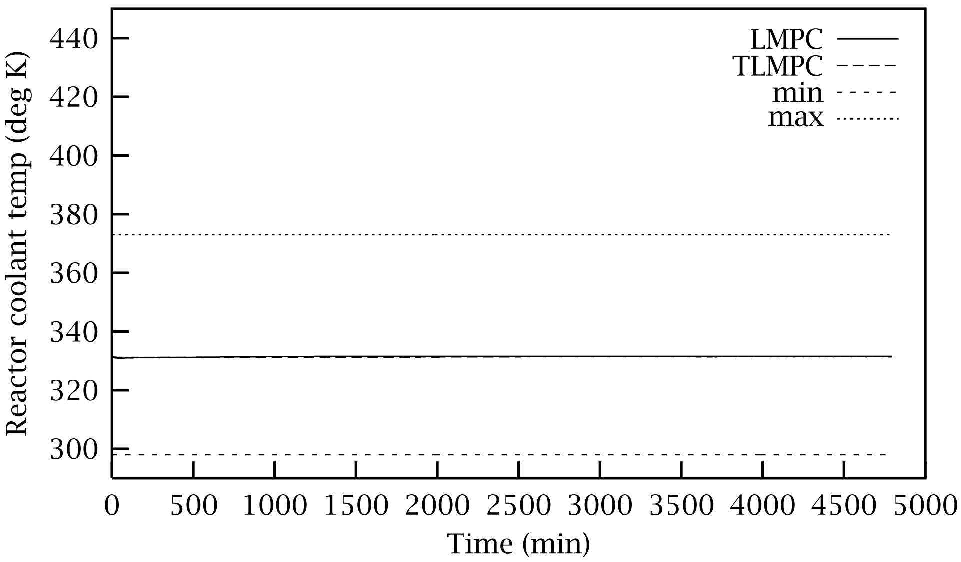

Figure 6.41: Case 6: Manipulated coolant temperature

scheme can easily fail for a realistic case to make a certain polymer grade. LMPC does not ensure that process objectives can be achieved with a fixed linear model (Grade A for cases 1, 3 and 5) for different product grades. It is observed that the linear model obtained around the conditions for grade A is able to achieve the process objectives for cases 1, 3 and 5. Hence, LMPC can work if linear models are swapped and maintained for different grades. The TLMPC does not require any such extensive bookkeeping and is able to attain the varied goals of polymerization control effectively. Similar results are also obtained using another disturbance set that is also based on our experience with industrial datasets. These results demonstrate the effectiveness of TLMPC feedback over LMPC feedback to attain improved plant operation for a prototypical industrial polymerization process.

The LMPC feedback controller is properly tuned before implementing it for all the above cases. The tuning for LMPC is demonstrated for the second grade change (case 4). The quadratic penalty on the deviation of the outputs (Q) and the quadratic penalty on the deviation of the inputs (R) are fixed at their nominal values. S values are altered by varying S_o.

$$S = S_o \frac{1}{(u_{max} - u_{min})^2} \tag{6.29}$$

The inputs corresponding to different tunings for LMPC are shown (Figures 6.42, 6.43 and 6.44). The inputs are well tuned for $S_o = 100$ in comparison to the inputs corresponding to $S_o = 10$ or $S_o = 1000$. The regulated outputs (Figures 6.45, 6.46 and 6.47)

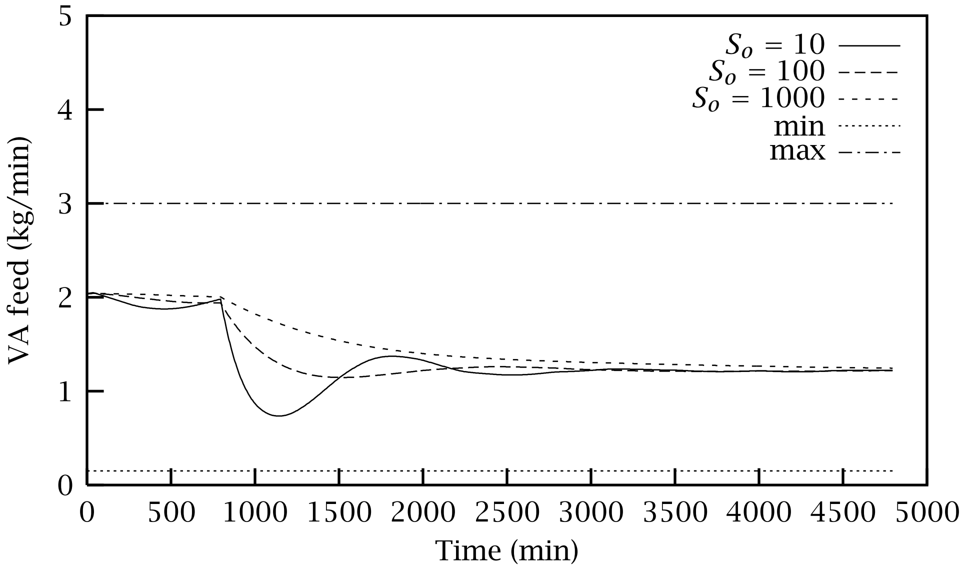

Figure 6.42: Manipulated VA feed (LMPC tuning)

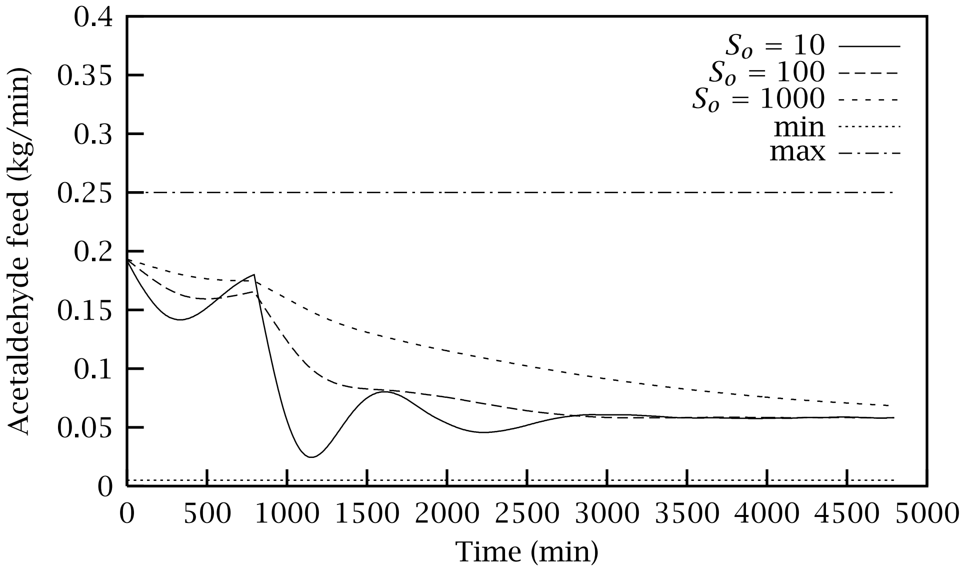

Figure 6.43: Manipulated acetaldehyde feed (LMPC tuning)

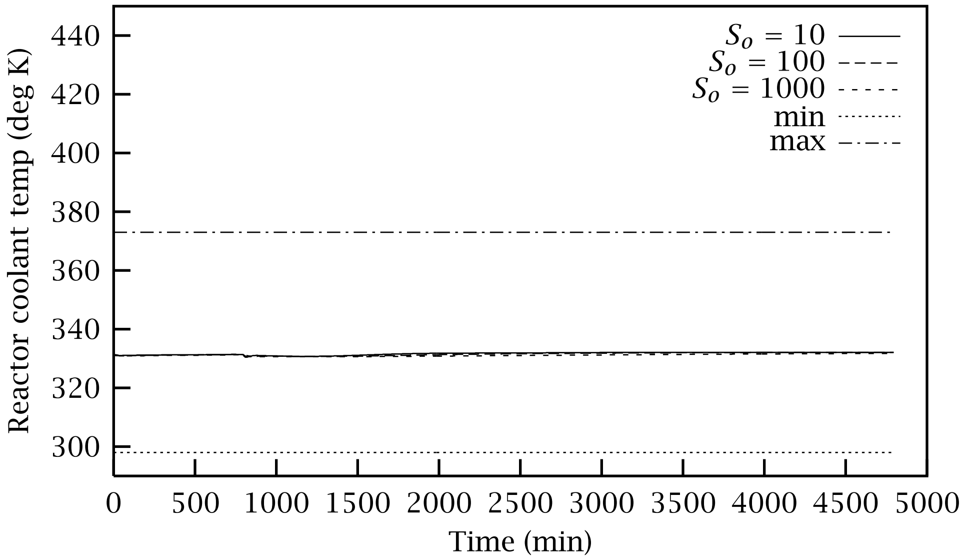

Figure 6.44: Manipulated coolant temperature (LMPC tuning)

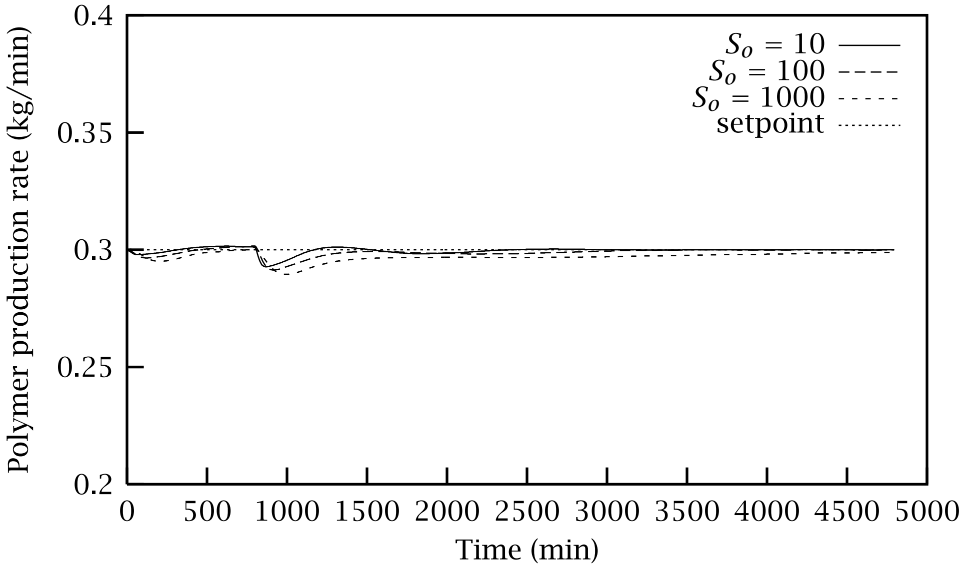

Figure 6.45: Measured polymer production rate (LMPC tuning)

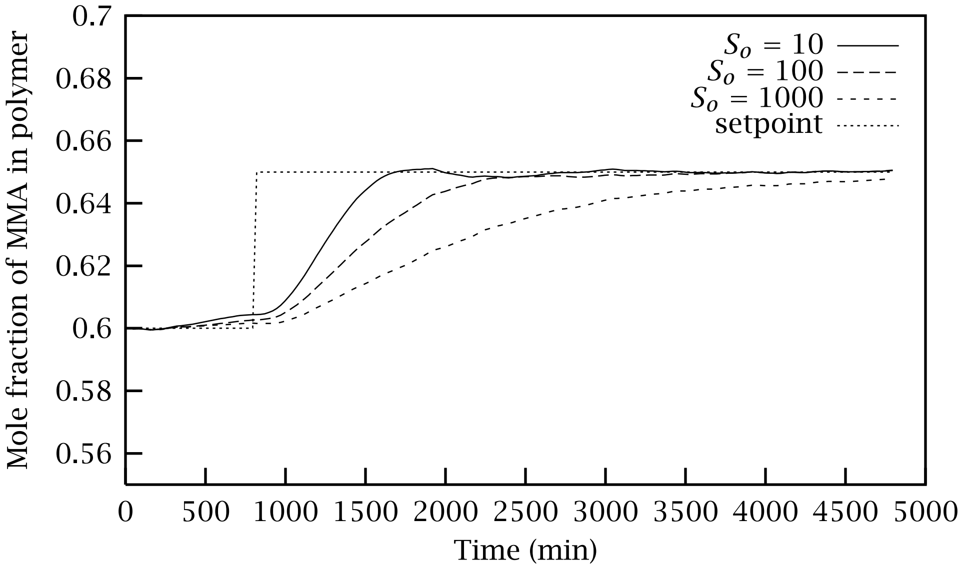

Figure 6.46: Measured copolymer composition (LMPC tuning)

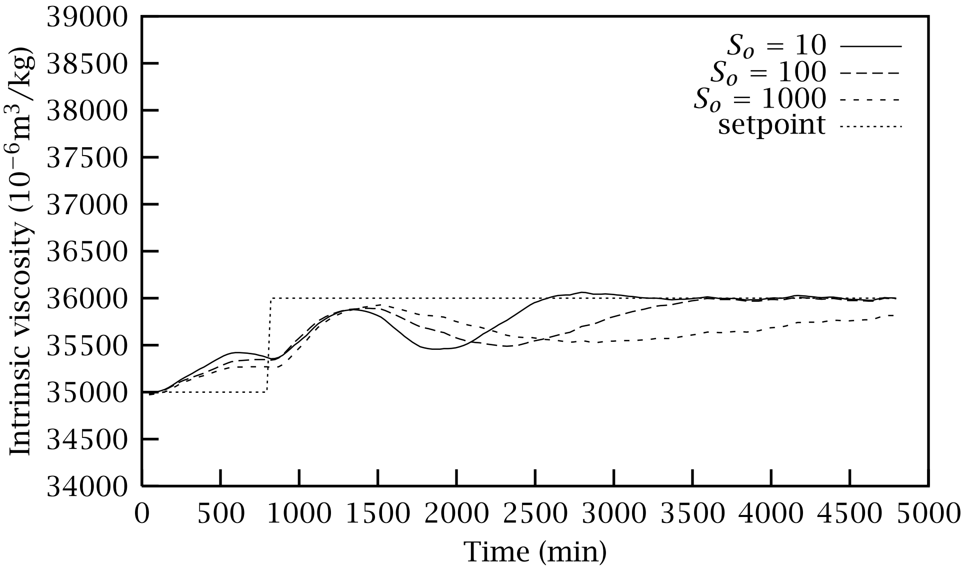

Figure 6.47: Measured copolymer viscosity (LMPC tuning)

for $S_o = 100$ also show acceptable performance. Hence, the lack of performance of LMPC for all the feedback control cases is not due to poor tuning.

The performance of the model predictive controllers is also examined for different kinetic parameters and initial states for prediction model in comparison to the plant for the first regulation case (case 5). In this case, the filter gain ($L = [L_x, L_p]$) is tuned based on the covariances of state noise (w_k), noise in sensor measurement (v_k) and noise in output disturbance (ξ_k) resulting in an extended Kalman filter for the nonlinear system to evaluate estimates of the states ($\hat{x}$) and the output disturbances ($\hat{p}$). The kinetic parameters are varied based on results obtained for an actual copolymerization process (Table 5.2 in Chapter 5). The pre-exponential factors for the propagation rate constants are varied for predictive model simulations from their nominal values corresponding to the plant simulations (Table 6.4). Modeling discrepancy is also introduced

	Model	Plant
A_{paa}	$f \cdot 3.207 \times 10^6$ $\text{m}^3/\text{kmol}\cdot\text{s}$	3.207×10^6 $\text{m}^3/\text{kmol}\cdot\text{s}$
A_{pab}	$f \cdot 1.233 \times 10^5$ $\text{m}^3/\text{kmol}\cdot\text{s}$	1.233×10^5 $\text{m}^3/\text{kmol}\cdot\text{s}$
A_{pba}	$f \cdot 2.103 \times 10^8$ $\text{m}^3/\text{kmol}\cdot\text{s}$	2.103×10^8 $\text{m}^3/\text{kmol}\cdot\text{s}$
A_{pbb}	$f \cdot 6.308 \times 10^6$ $\text{m}^3/\text{kmol}\cdot\text{s}$	6.308×10^6 $\text{m}^3/\text{kmol}\cdot\text{s}$

Table 6.4: Plant-model mismatch for pre-exponential factors of propagation rate constants

for the initial state estimates ($\hat{x_0}$) compared to the initial plant states (x_0).

$$\hat{x}_0 = f \cdot x_0 \tag{6.30}$$

The inputs are tuned by setting $S_o = [100, 1000, 10000]$ to make the controller less aggressive in presence of plant-model mismatch for kinetic parameters and initial states. The closed-loop response for the regulated outputs (Figures 6.48, 6.49 and 6.50) shows the performance in presence of disturbances, plant-model mismatch and modeling errors. The performance of TLMPC is better for $f = 1.05$ and $f = 1.1$, in comparison to $f = 1.5$ and $f = 2.0$. The corresponding inputs for the TLMPC feedback scheme are shown (Figures 6.51, 6.52 and 6.53). The closed-loop inputs for $f = 1.05$ and $f = 1.1$ move around less in comparison to those for $f = 1.5$ and $f = 2.0$. The closed-loop inputs and outputs for $f = 2.0$ exhibit lack of performance by the feedback controller in presence of extreme uncertainty in the process model. In conclusion, the proposed target linearization model predictive controller is able to handle realistic disturbances, plant-model mismatch and modeling errors.

The use of non-zero L_x is compared to the performance of the open-loop observer in state estimates with $L_x = 0$ for $f = 1.5$. The closed-loop response for the regulated

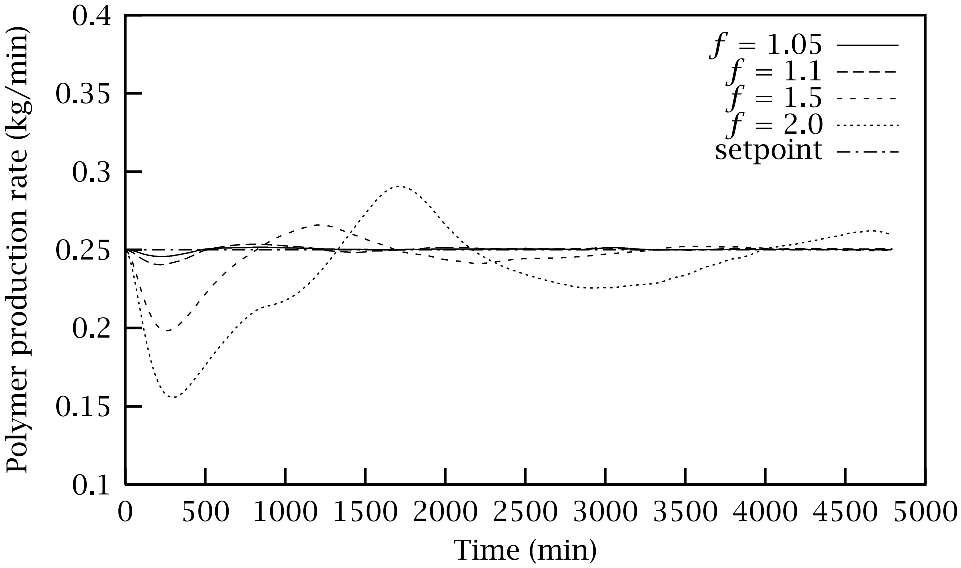

Figure 6.48: Measured polymer production rate (plant-model mismatch for kinetic parameters and initial states)

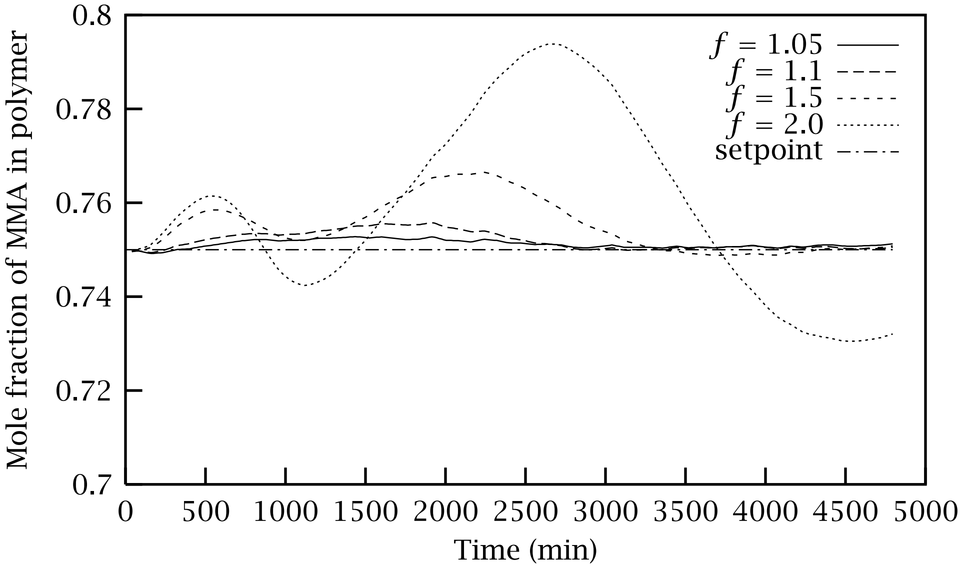

Figure 6.49: Measured copolymer composition (plant-model mismatch for kinetic parameters and initial states)

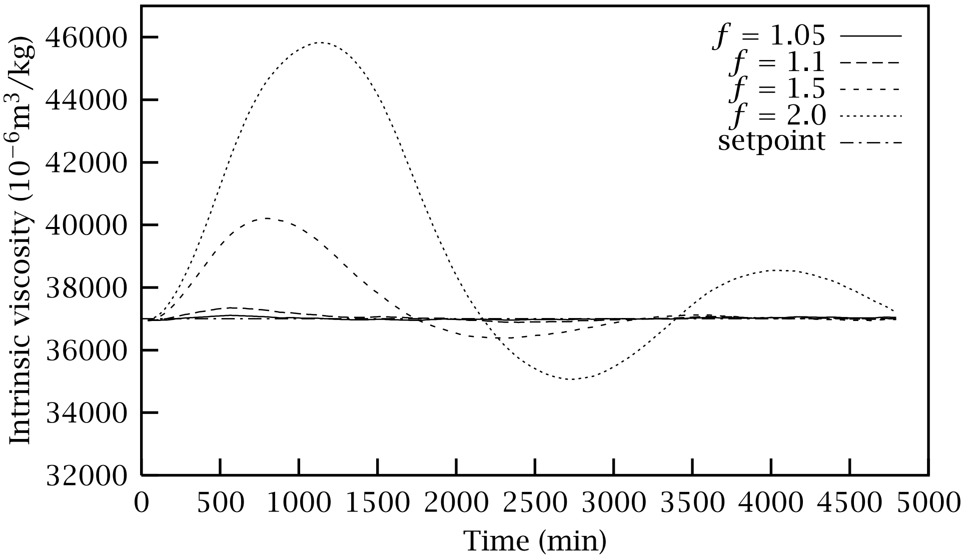

Figure 6.50: Measured copolymer viscosity (plant-model mismatch for kinetic parameters and initial states)

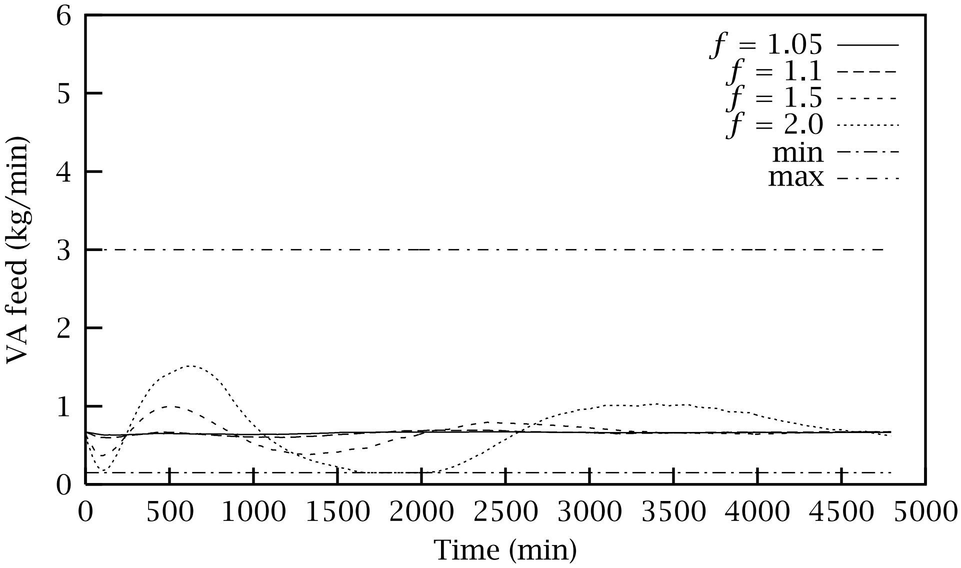

Figure 6.51: Manipulated VA feed (plant-model mismatch for kinetic parameters and initial states)

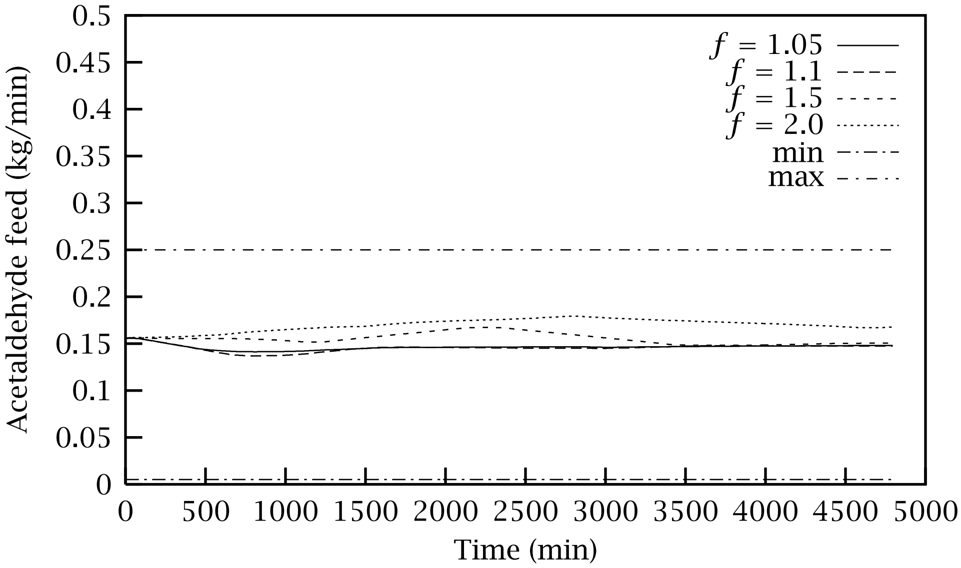

Figure 6.52: Manipulated acetaldehyde feed (plant-model mismatch for kinetic parameters and initial states)

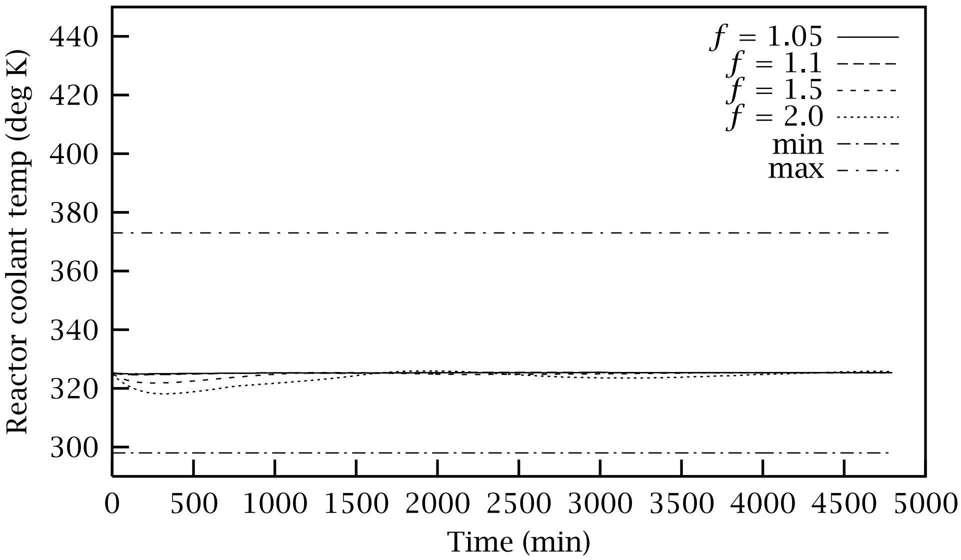

Figure 6.53: Manipulated coolant temperature (plant-model mismatch for kinetic parameters and initial states)

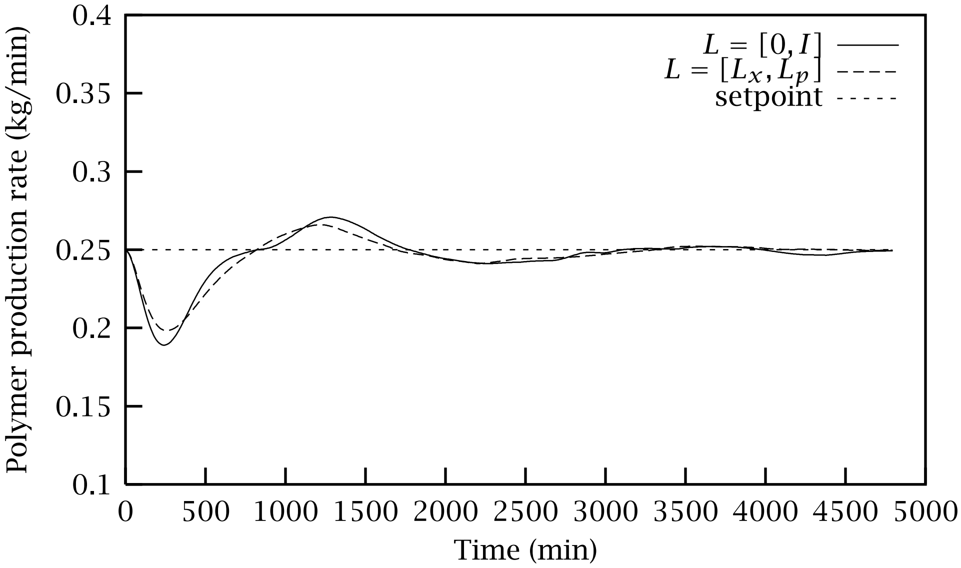

Figure 6.54: Effect of state estimator on regulated polymer production rate

outputs (Figures 6.54, 6.55 and 6.56) shows the effect of state estimator to improve feedback controller performance. The performance of closed-loop outputs is better for $L = [L_x, L_p]$ in comparison to $L = [0, I]$. The corresponding closed-loop inputs for the two feedback control schemes are also shown (Figures 6.57, 6.58 and 6.59).

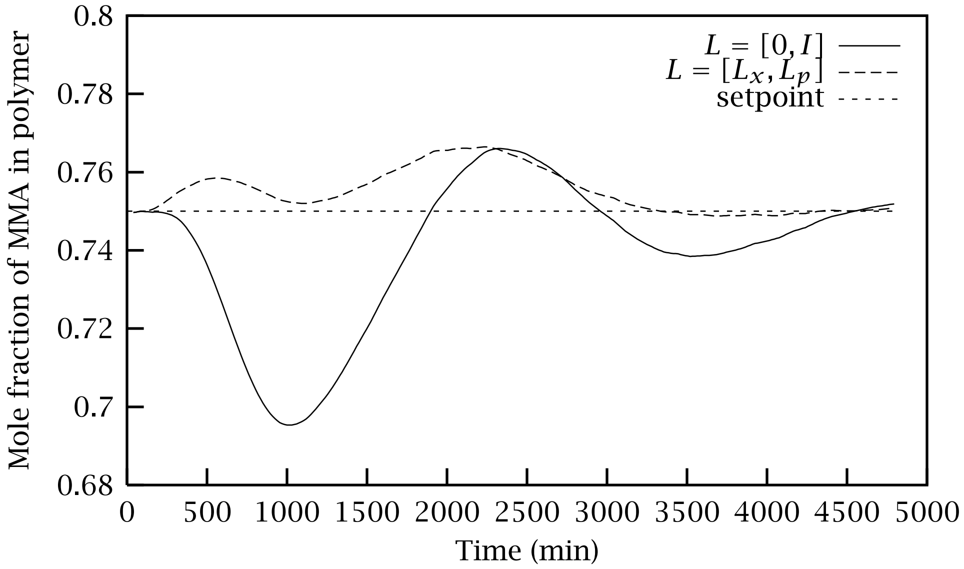

Figure 6.55: Effect of state estimator on regulated copolymer composition

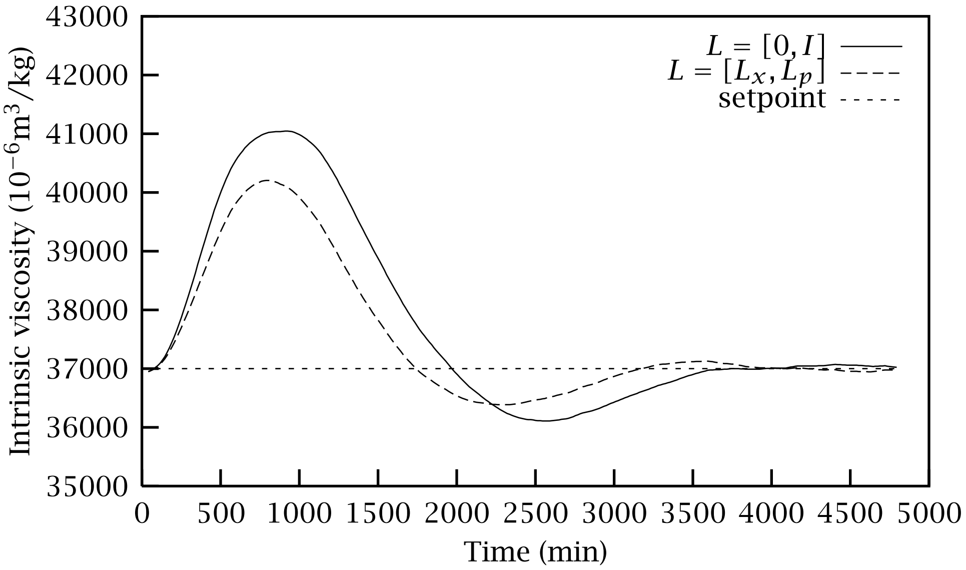

Figure 6.56: Effect of state estimator on regulated copolymer viscosity

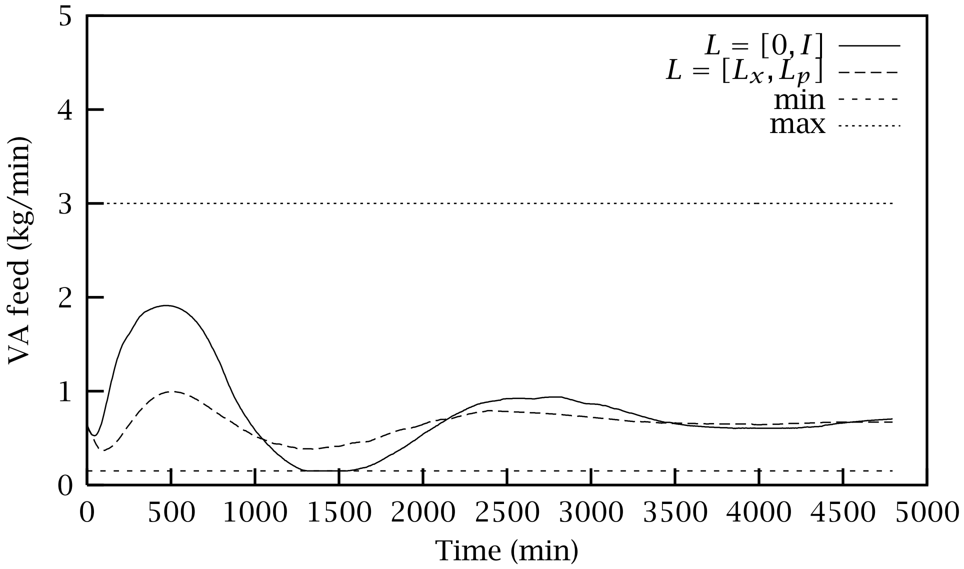

Figure 6.57: Effect of state estimator on manipulated VA feed

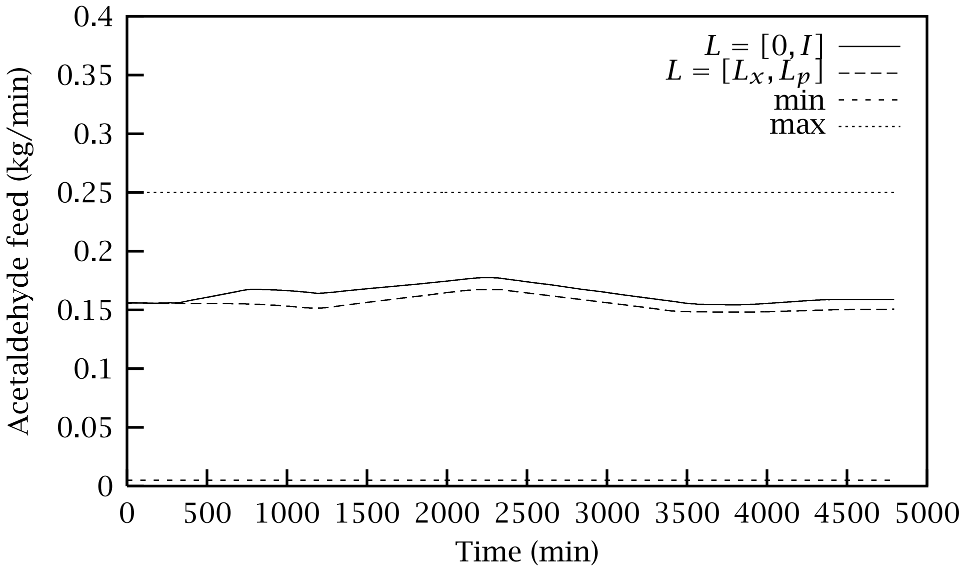

Figure 6.58: Effect of state estimator on manipulated acetaldehyde feed

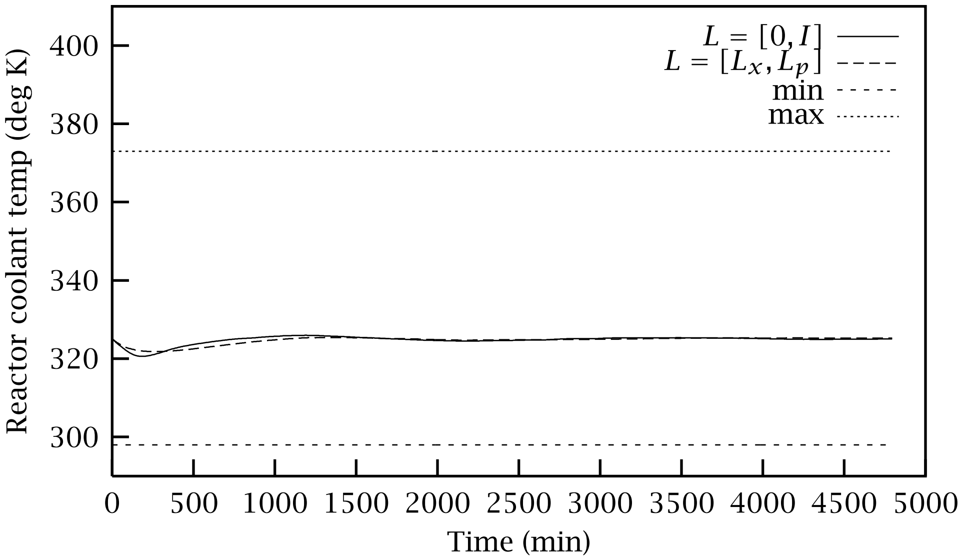

Figure 6.59: Effect of state estimator on manipulated coolant temperature

Chapter 7

Controller Performance Assessment

The performance of the TLMPC feedback controller is better than that of the LMPC feedback controller (Chapter 6) to achieve different process objectives during plant start-up, product grade change and regulation around a setpoint. The comparison of the feedback controllers against minimum variance controller enables one to justify the development and implementation of advanced control schemes for polymerization processes. The following minimum variance controller for the process is used as a benchmark to evaluate feedback controller performance.

7.1 Minimum Variance Controller

The polymerization process to be regulated is the following non-linear dynamical system

$$\frac{dx}{dt} = f(x, u, d, t) \tag{7.1}$$

$$y = h(x) + p(t) \tag{7.2}$$

where

$$x = [c_a, c_b, c_i, c_s, c_t, c_z, \lambda_a, \lambda_b, T_r, \psi_0^p, \psi_1^p, \psi_2^p, c_{a,s}, c_{b,s}, c_{s,s}]^T \tag{7.3}$$

$$u = [G_{b,f}, G_{t,f}, T_j]^T \tag{7.4}$$

$$d = [G_{a,f}, G_{i,f}, G_{s,f}, G_{z,f}, T_f]^T \tag{7.5}$$

$$y = [c_{a,s}, c_{b,s}, c_{s,s}, T_r, G_{pi}, Y_{ap}, [\eta]]^T \tag{7.6}$$

and $p(t)$ is the output disturbance in the process measurements. The discretized process can be represented as

$$x_{k+1} = F(x_k, u_k, d_k) \tag{7.7}$$

$$p_{k+1} = p_k + a_k \tag{7.8}$$

$$y_{k+1} = H(x_{k+1}) + p_{k+1} \tag{7.9}$$

where a_k is independent normally distributed residual in the output disturbances (p_k) for the process measurements. It is assumed that the measured disturbances (d_k) and manipulated variables (u_k) affecting the process have no unmeasured residuals present in them. The objective of the control law is to minimize the variance of the output y. The control law should be a function of observed outputs up to and including time k ($y_k, y_{k-1}, \cdots$), observed measured disturbances up to and including time k ($d_k, d_{k-1}, \cdots$), and of all past control moves ($u_{k-1}, u_{k-2}, \cdots$). Using equations 7.7, 7.8 and 7.9 the output at time $k+1$ can be expressed as

$$y_{k+1} = H(F(x_k, u_k, d_k)) \quad + p_k \quad + a_k \tag{7.10}$$

Minimizing the expectation of the squared output $Ey^2(k+1)$ minimizes the variance of the output. For a given u_k the expectation of the squared output can be written as

$$Ey_{k+1}^2 = Ea_k^2 \quad + E[H(F(x_k, u_k, d_k)) \quad + p_k]^2 \tag{7.11}$$

The mixed terms vanish because a_k is independentally distributed. In the general case, equation 7.11 can be solved with the constraints on manipulated variables (u_k) to obtain the minimum variance control law. Hence

$$Ey_{k+1}^2 \geq Ea_k^2 \tag{7.12}$$

where the equality holds for

$$H(F(x_k, u_k, d_k)) \quad + p_k = 0 \tag{7.13}$$

Substituting for p_k in equation 7.13 gives

$$H(F(x_k, u_k, d_k)) \quad + y_k - H(x_{k-1}) = 0 \tag{7.14}$$

Equation 7.14 can be numerically solved for the minimum variance controller action (u_k). If the equality in the equation 7.14 can be attained, then the output variance of this controller for the given data can be written as

$$\text{variance}(y_k) = \text{variance}(a_k) \tag{7.15}$$

The performance of the feedback controllers (LMPC and TLMPC) for case 5 in Chapter 6 is evaluated against the minimum variance controller for the given data. The variance of the residuals (a) in the output disturbances (p) for the process measurements is calculated to obtain the theoretical minimum variance that can be attained by any control scheme. The mean and scaled standard deviation for the different controllers is shown in Table 7.1. The total scaled variance of the regulated outputs is 13.59×10^{-4} for LMPC and 9.65×10^{-7} for TLMPC. The target linearization MPC performs far better than the LMPC feedback scheme. The performance of the feedback controllers compared to the minimum variance controller suggests that better performance may not be realizable due to model inadequacies.

Output	Control law	Mean	Scaled standard deviation	Setpoint
Polymer production rate (kg/min)	LMPC	0.2510	2.03×10^{-2}	0.2500
	TLMPC	0.2495	6.81×10^{-4}	
	Min variance	0.2500	3.89×10^{-6}	
Mole fraction of MMA in copolymer	LMPC	0.7482	2.09×10^{-2}	0.7500
	TLMPC	0.7497	4.66×10^{-4}	
	Min variance	0.7500	6.93×10^{-5}	
Copolymer viscosity (10^{-6}m^3/kg)	LMPC	37034	2.26×10^{-2}	37000
	TLMPC	36970	5.35×10^{-4}	
	Min variance	37000	6.69×10^{-5}	

Table 7.1: Performance of feedback controllers for case 5 in Chapter 6

7.2 Diagnostic Checking of Models

Model inadequacies can be determined by examining the following correlations of the residuals [17].

- The autocorrelation function ($r_{aa}(m)$) of the residuals from the fitted model at lag m
- The cross correlation function ($r_{\alpha a}(m)$) between the input (α_k) and the residuals at lag m

The input vector (α_k) consists of the predicted outputs ($\hat{y}_k$). If the autocorrelation function ($r_{aa}(m)$) shows marked correlation patterns then that suggests model inadequacy. The model inadequacies may be present in the process and/or noise model. If the residuals are not cross correlated with the inputs (α), but are autocorrelated, then the process model is correct and the noise model is incorrect. If the residuals show cross correlation with the inputs then there is inadequacy in the process model.

7.2.1 Autocorrelation checks

The autocorrelation function ($r_{aa}(m)$) of the residuals at lag m can be evaluated using the following expression

$$r_{aa}(m) = \frac{c_{aa}(m)}{c_{aa}(0)} \tag{7.16}$$

where

$$c_{aa}(m) = \frac{1}{N} \sum_{k=1}^{N-m} (a_k - \bar{a})(a_{k+m} - \bar{a}) \quad m = 0, 1, 2, \cdots, M \tag{7.17}$$

An overall check that takes into account distributional effects produced by fitting is as follows. If the functional form of the model is adequate, then the quantity

$$\bar{Q} = N(N+2)\sum_{m=1}^{M}\frac{r_{aa}^2(m)}{N-m} \quad \text{where} \quad M < N/4 \tag{7.18}$$

is approximately distributed as χ^2 with $M - p - q$ degrees of freedom. If the model is inappropriate, then the average value of $\bar{Q}$ will be inflated. In this case, $p = 1$ because the output is dependent only on the previous value of the output and $q = 0$ because the output is not dependent on any of the previous values of the residual.

7.2.2 Cross correlation checks

The cross correlation function $(r_{\alpha a}(m))$ between the inputs (α) and the residuals at lag m can be evaluated using the following expression

$$r_{\alpha a}(m) = \frac{c_{\alpha a}(m)}{s_\alpha s_a} \tag{7.19}$$

where $s_\alpha = \sqrt{c_{\alpha\alpha}(0)}$, $s_a = \sqrt{c_{aa}(0)}$ and $c_{\alpha a}(m)$ is provided by

$$c_{\alpha a}(m) = \frac{1}{N}\sum_{k=1}^{N-m}(\alpha_k - \bar{\alpha})(a_{k+m} - \bar{a}) \quad m = 0, 1, 2, \cdots, M \tag{7.20}$$

An overall test of the hypothesis of model adequacy, similar to the autocorrelation test, is as follows. If the functional form of the model is adequate, then the quantity

$$\bar{S} = N(N+2)\sum_{m=0}^{M}\frac{r_{\alpha a}^2(m)}{N-m} \quad \text{where} \quad M < N/4 \tag{7.21}$$

is approximately distributed as χ^2 with $M + 1 - (r + s + 1)$ degrees of freedom. In this case, $r = 1$ because the output is dependent only on the previous output and $s = 0$ because the output is dependent only on the previous input.

7.2.3 Linear example

The correlation checks are first demonstrated for a simple linear example. The plant representation for the process is

$$y_{k,p} = 0.5y_{k-1,p} + 0.5u_{k-1} + b_k + w_{k,p} \tag{7.22}$$

where $y_{k,p}$ is the measured plant output at sample time k, u and b are measured inputs, and w is the nominal white noise in the output. Two model representations are chosen for the process.

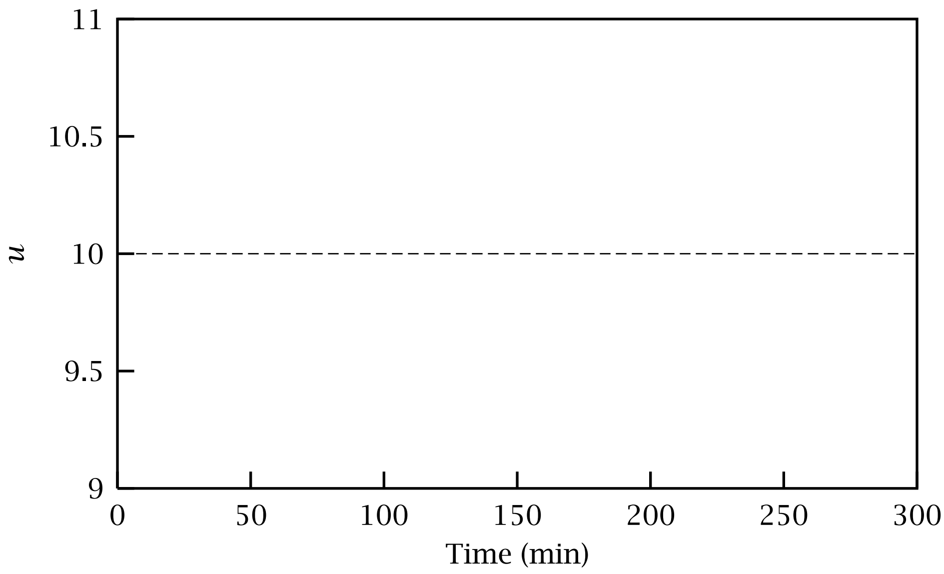

Figure 7.1: Input u (linear example 1)

- Model 1

$$y_{k,1} = 0.5y_{k-1,1} + 0.5u_{k-1} + b_k \tag{7.23}$$
$$a_{k,1} = y_{k,p} - y_{k,1} \tag{7.24}$$

- Model 2

$$y_{k,2} = 0.5y_{k-1,1} + u_{k-1} + b_k \tag{7.25}$$
$$a_{k,2} = y_{k,p} - y_{k,2} \tag{7.26}$$

The first model (model 1) is an appropriate representation of the process whereas the second model (model 2) is substantially different from the actual process. This simple linear example will demonstrate the application of correlation checks to the two models to identify model inadequacies. Two different trends of input variable (u_k) are used for the correlation checks. The input u is nearly constant in the first linear example (Figure 7.1), whereas it is a ramp for the second linear example (Figure 7.2). The input b is a ramp for both examples

The correlation checks are performed using the first 300 measurements (N = 300) for the output (y_k) to evaluate the correlation functions at the first 75 lags (M = 75).

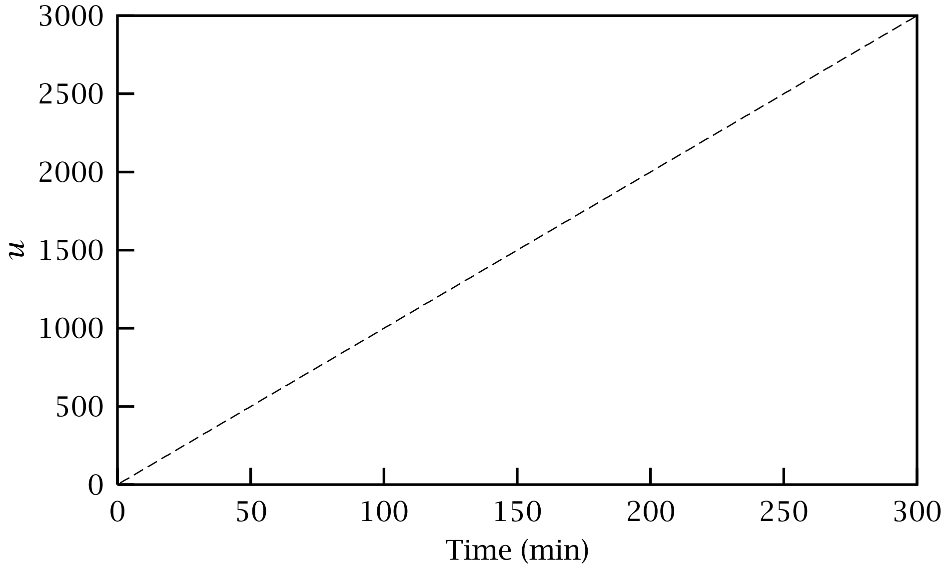

Figure 7.2: Input u (linear example 2)

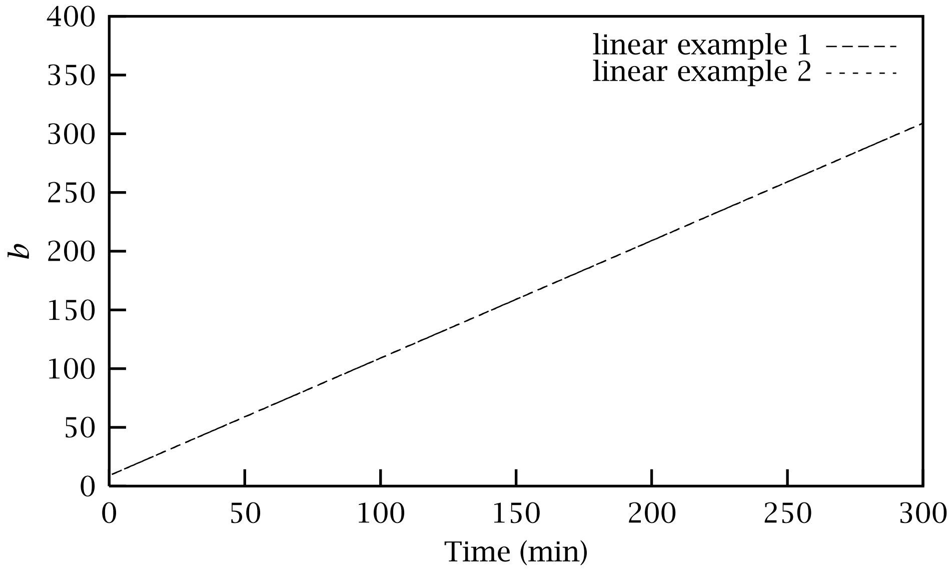

Figure 7.3: Input b

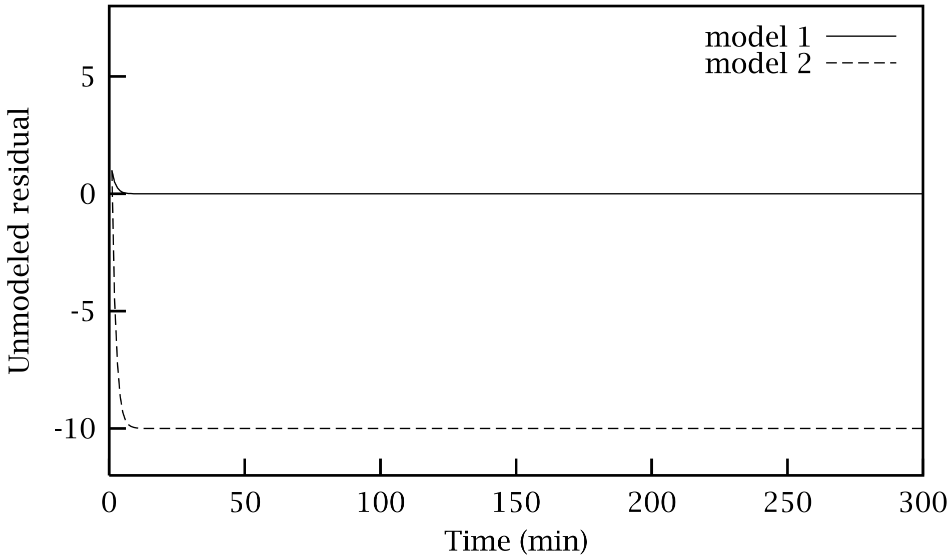

Figure 7.4: Residuals in output measurement (linear example 1)

Linear example 1. The residuals (a) corresponding to the measurements (y) that are used in the correlation checks for linear example 1 are shown (Figure 7.4). The residuals for model 1 or model 2 do not indicate significant modeling errors. The autocorrelation function for residuals corresponding to the measurements at different lags is also examined (Figure 7.5). The values of the autocorrelation function in Figure 7.5 are same for the two models and mostly inside the bounds of error ($\pm 1/\sqrt{N} = \pm 0.05774$). The $\bar{Q}$ criterion for the residuals in outputs has been calculated and tabulated (Table 7.2). $\bar{Q}$ statistic is similar for model 1 and model 2. The 1% point for χ^2 with 74 degrees of

Model	$\bar{Q}$
Model 1	101.12
Model 2	101.13

Table 7.2: $\bar{Q}$ statistic for autocorrelation of residuals in output measurements (linear example 1)

freedom is 105.20 and 99% point for χ^2 with 74 degrees of freedom is 48.67. The $\bar{Q}$ statistic does not indicate that there are any significant modeling inadequacies in either model. The residuals (Figure 7.4), autocorrelation function (Figure 7.5) and $\bar{Q}$ statistic (Table 7.2) together fail to indicate modeling deficiencies in model 2 compared to model 1.

The model inadequacies may be further diagnosed by performing cross correla-

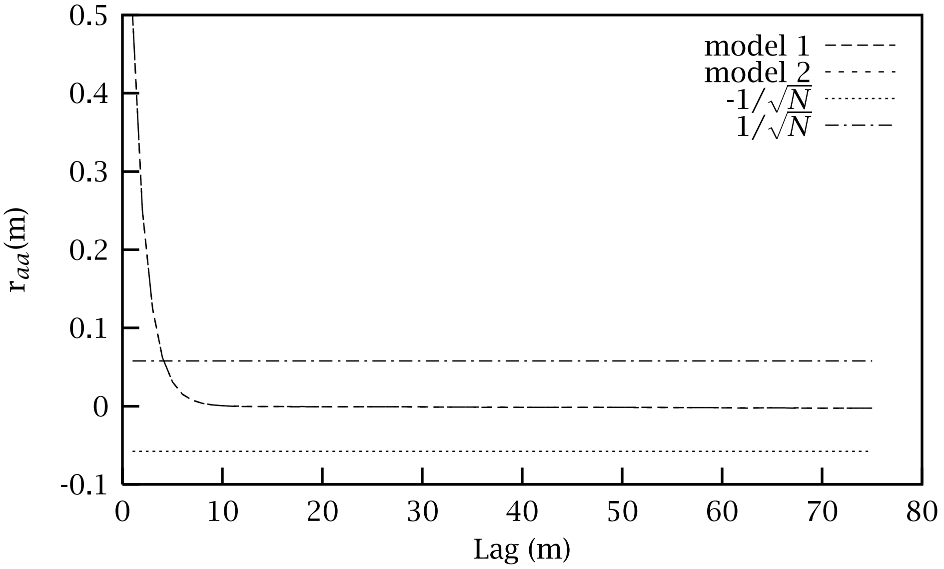

Figure 7.5: Autocorrelation of residuals (linear example 1)

tion checks between predicted outputs and residuals (a). The cross correlation function for residuals with the predicted outputs for the two models at different lags is shown in Figure 7.6. Cross correlation function (Figure 7.6) is inside the bounds of error ($\pm 1/\sqrt{N} = \pm 0.05774$) for model 1 as well as model 2. The $\bar{S}$ criterion for cross correlation of residuals with predicted outputs has been evaluated and shown in Table 7.3. Comparison of $\bar{S}$ with the χ^2 value for 74 degrees of freedom clearly suggests

Model	$\bar{S}$
Model 1	24.50
Model 2	25.13

Table 7.3: $\bar{S}$ statistic for cross correlation of residuals with predicted outputs (linear example 1)

that there is no model inadequacy for model 1 and model 2. The cross correlation function (Figure 7.6) and the $\bar{S}$ statistic (Table 7.3) both indicate that there are no modeling errors in the process model for model 1 or model 2. In this example, there is modeling error for model 2 with respect to input u. Examination of cross correlation function for residuals with the input u (Figure 7.7) does not show any modeling deficiencies in model 2 with respect to that input. The corresponding $\bar{S}$ criterion for cross correlation of output residuals with input u is also calculated (Table 7.4). The $\bar{S}$ criterion suggests no model inadequacy for model 2 compared to model 1. The cross correlation function

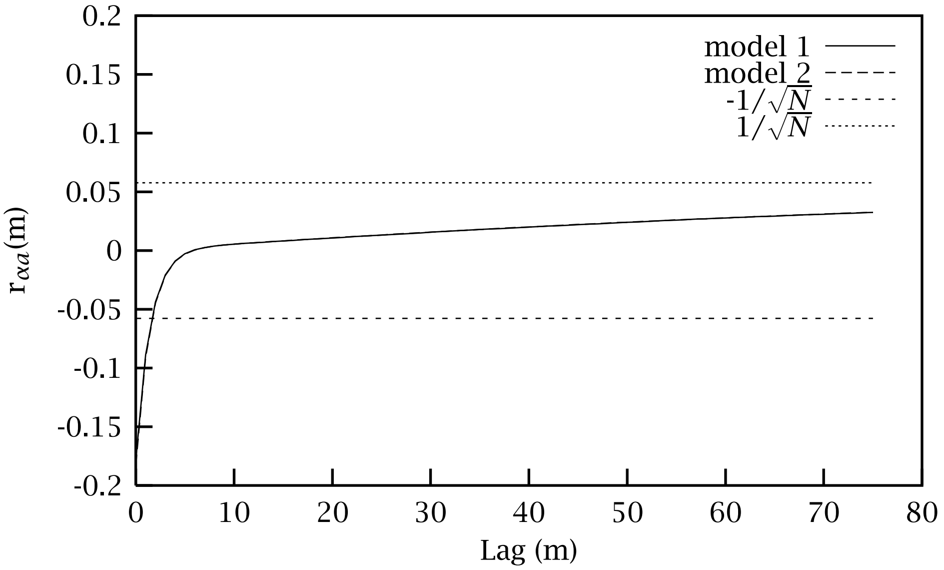

Figure 7.6: Cross correlation of residuals with predicted outputs (linear example 1)

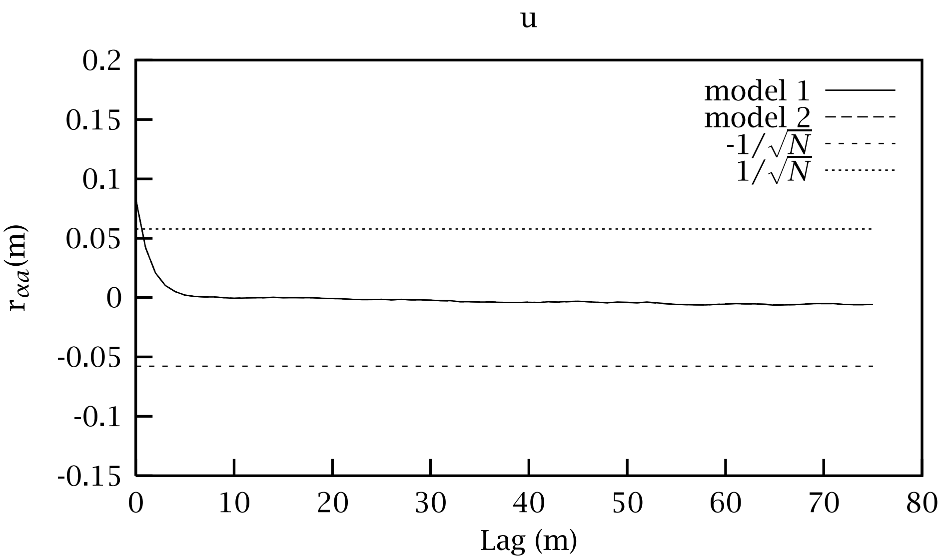

Figure 7.7: Cross correlation of residuals with input u (linear example 1)

Model	$\bar{S}$
Model 1	3.18
Model 2	3.19

Table 7.4: $\bar{S}$ statistic for cross correlation of residuals with input u (linear example 1)

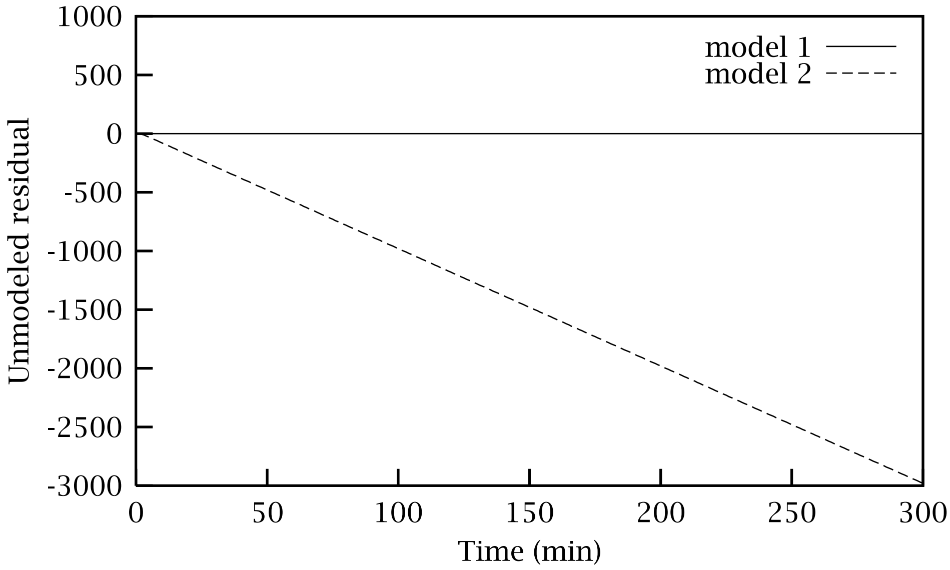

Figure 7.8: Residuals in output measurement (linear example 2)

(Figure 7.7) and the $\bar{S}$ statistic (Table 7.4) together do not indicate extreme modeling errors with respect to the variable u for model 2. These correlations of residuals are unable to diagnose the extent of modeling deficiencies because the input u does not vary significantly. Hence, if the input u does not have a substantial effect on the output y then model 2 will also be an appropriate representation of the process.

Linear example 2. The correlation analysis is performed for the same process and models with a ramp input (u) to see how the ramp variation affects the analysis. The residuals (a) corresponding to the ramp u show extreme modeling deficiencies for model 2 in comparison to model 1 (Figure 7.8). The autocorrelation function for residuals at different lags (Figure 7.9) also shows great correlation for model 2 in contrast to model 1 (Figure 7.9). $\bar{Q}$ criterion for the residuals in outputs has been evaluated (Table 7.5). The $\bar{Q}$ statistic also indicates that the modeling inadequacies in model 2 are far more than those in model 1. The residuals (Figure 7.8), autocorrelation function (Figure 7.9) and $\bar{Q}$ statistic (Table 7.5) together indicate modeling inadequacies for

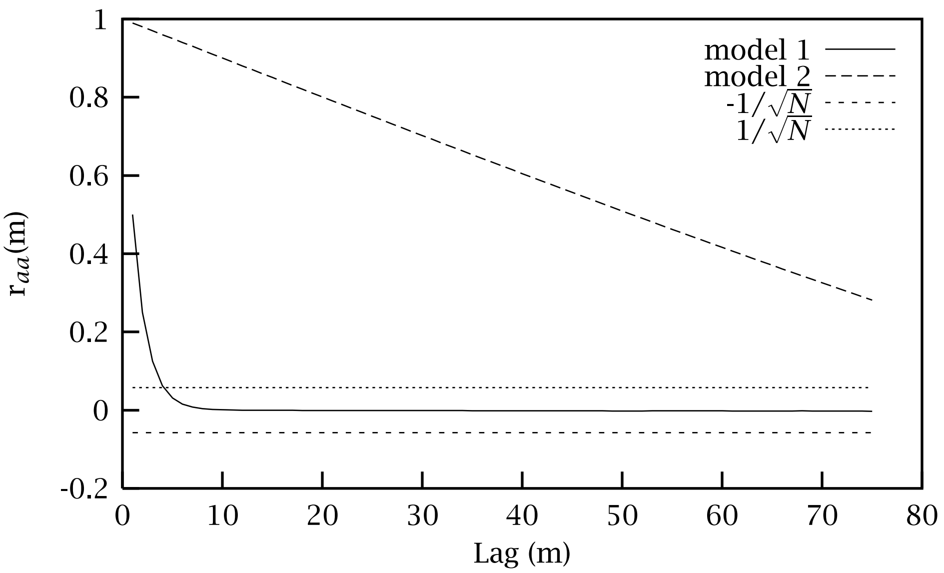

Figure 7.9: Autocorrelation of residuals (linear example 2)

Model	$\bar{Q}$
Model 1	101.24
Model 2	10871

Table 7.5: $\bar{Q}$ statistic for autocorrelation of residuals in output measurements (linear example 2)

model 2 compared to model 1.

The modeling inadequacies in model 2 may be in the process and/or noise model. As in example 1, the modeling deficiencies are further checked by examining the cross correlation between predicted outputs and residuals (Figure 7.10). The cross correlation pattern (Figure 7.10) shows modeling inadequacies for model 2 in contrast to model 1. $\bar{S}$ criterion values for cross correlation of residuals with predicted outputs have also been calculated (Table 7.6). $\bar{S}$ criterion clearly suggests model inadequacy for model

Model	$\bar{S}$
Model 1	23.58
Model 2	11173

Table 7.6: $\bar{S}$ statistic for cross correlation of residuals with predicted outputs (linear example 2)

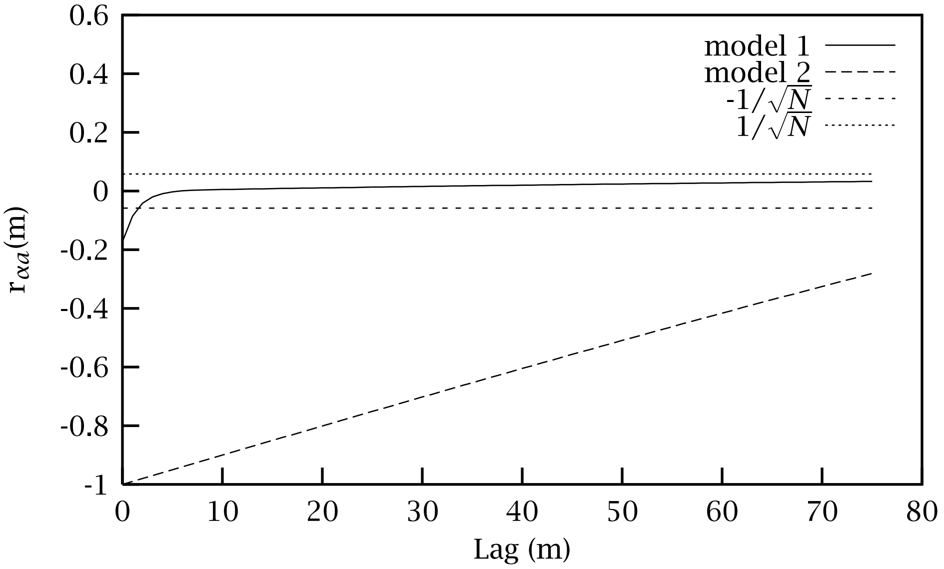

Figure 7.10: Cross correlation of residuals with predicted outputs (linear example 2)

2 and no model inadequacy for model 1. The cross correlation function (Figure 7.10) and the $\bar{S}$ statistic (Table 7.6) for example 2 indicate modeling errors in process model for model 2. As in example 1, an attempt to identify these modeling errors may be made by evaluating the cross correlation between the input variable (u) and the output residual (a). Examination of cross correlation function for residuals corresponding to the actual outputs with the inputs u (Figure 7.11) shows modeling deficiencies in model 2 in sharp contrast to model 1. The corresponding $\bar{S}$ criterion for cross correlation of output residuals with u is calculated (Table 7.7). The $\bar{S}$ criterion suggests great

Model	$\bar{S}$
Model 1	23.59
Model 2	11174

Table 7.7: $\bar{S}$ statistic for cross correlation of residuals with input u (linear example 2)

model inadequacy for model 2 compared to model 1. The cross correlation function (Figure 7.11) and the $\bar{S}$ statistic (Table 7.7) together indicate grave modeling errors with respect to the variable u for model 2.

The cross correlation between b (Figure 7.3) and the output residual (a) is also analyzed. Examination of cross correlation function for residuals corresponding to the actual outputs with b (Figure 7.12) shows modeling deficiencies in model 2 in sharp contrast to model 1. The corresponding $\bar{S}$ criterion for cross correlation of output residuals

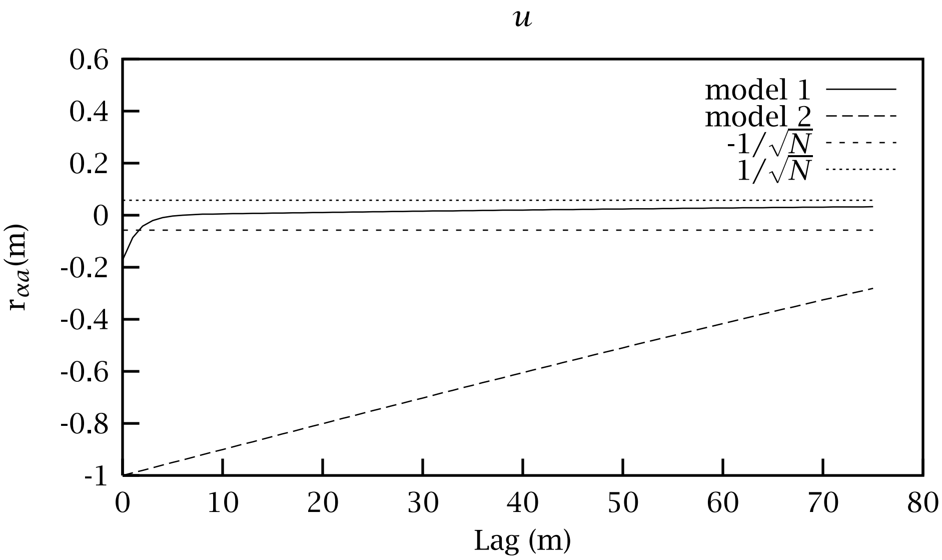

Figure 7.11: Cross correlation of residuals with input u (linear example 2)

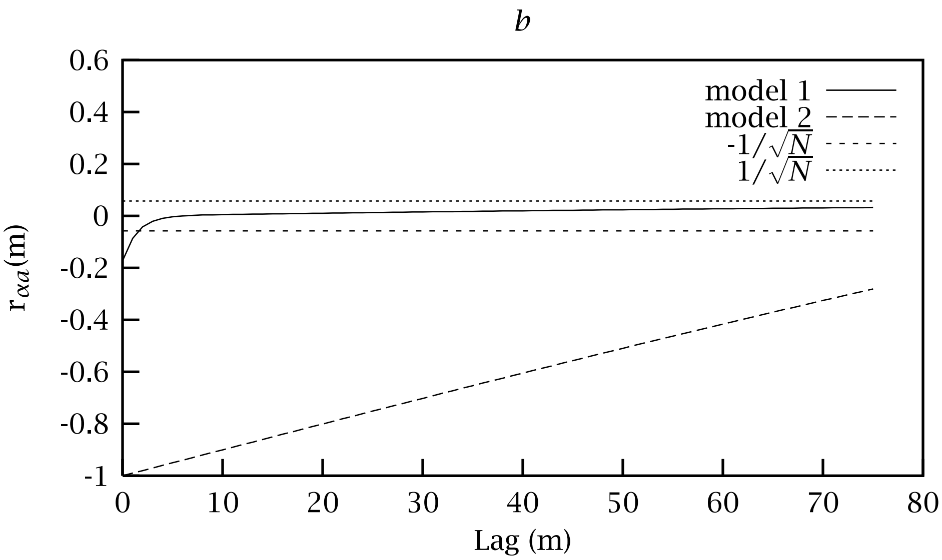

Figure 7.12: Cross correlation of residuals with input b (linear example 2)

with b is calculated (Table 7.8). The $\bar{S}$ criterion suggests great model inadequacy for

Model	$\bar{S}$
Model 1	23.59
Model 2	11174

Table 7.8: $\bar{S}$ statistic for cross correlation of residuals with input b (linear example 2)

model 2 compared to model 1. The cross correlation function (Figure 7.12) and the $\bar{S}$ statistic (Table 7.8) both indicate grave modeling errors with respect to the input b for model 2 even when there are no modeling errors with respect to b. The suggested correlation can be explained by examining the residuals for model 2 (Figure 7.8) and, inputs u (Figure 7.2) and b (Figure 7.3) for model 2. Hence, the second example indicates that the modeling inadequacies cannot be pinpointed even for a simple linear case with two inputs. These linear examples also demonstrate that the inadequacies can only be identified if there is a significant variation in the input. In the non-linear case also, the cross correlation checks can only indicate whether there is any modeling inadequacy in the process model without clear identification.

7.2.4 Polymerization model

The correlation checks are done for the MMA-VA polymerization process. Correlation analysis is performed using the first 300 measurements ($N = 300$) for each regulated output and evaluating the correlation functions at the first 75 lags ($M = 75$). The residuals (a) for the outputs with respect to the linear and non-linear model used for feedback control that are used in the correlation checks are shown (Figures 7.13, 7.14 and 7.15).

A visual inspection of the residuals suggests greater modeling deficiencies for the linear model as compared to the non-linear model. The autocorrelation function for residuals corresponding to the regulated measurements (polymer production rate, copolymer composition and viscosity) at different lags is shown for the linear model (Figure 7.16) and non-linear model (Figure 7.17). The autocorrelation function corresponding to the linear model (Figure 7.16) shows greater modeling inadequacies in contrast to the autocorrelation function for non-linear model (Figure 7.17). The $\bar{Q}$ criterion for the outputs has been evaluated for the two models (Table 7.9). The modeling deficiencies for the linear model are significantly higher than that of the non-linear model for the controlled outputs.

The modeling inadequacies can be attributed to the process and/or noise model

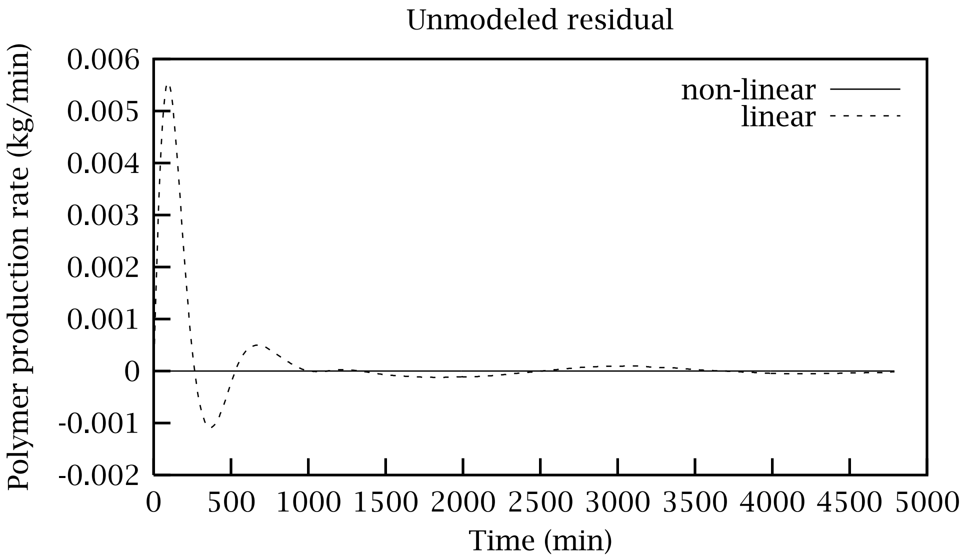

Figure 7.13: Residual in polymer production rate (polymer data)

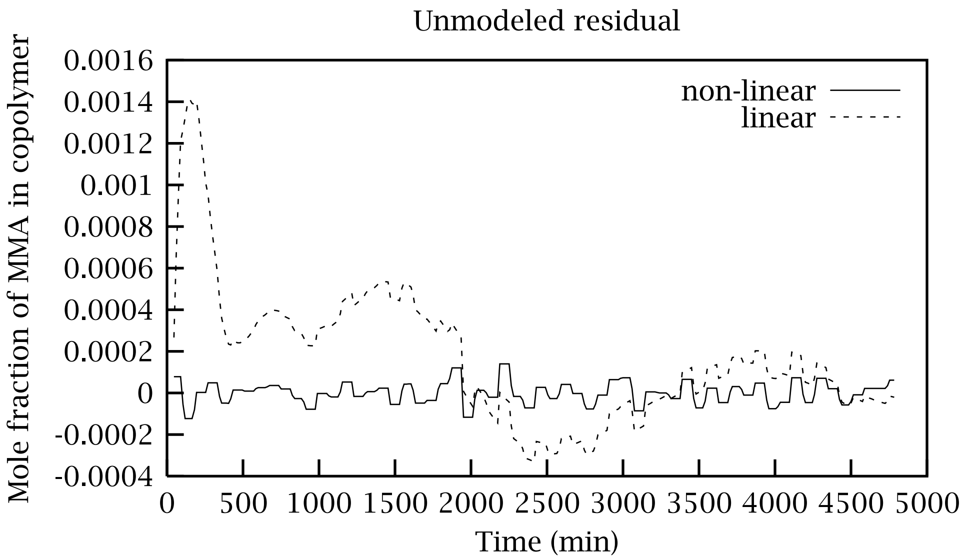

Figure 7.14: Residual in copolymer composition (polymer data)

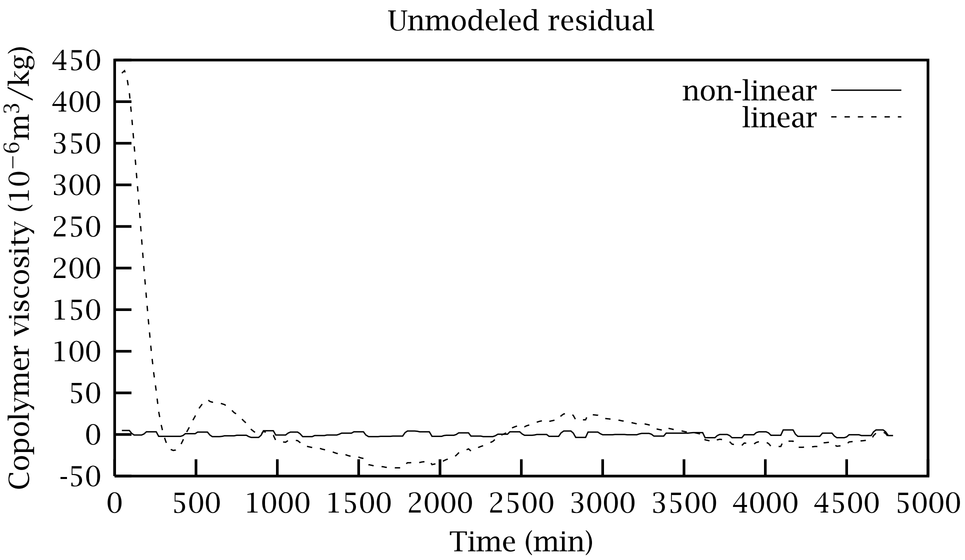

Figure 7.15: Residual in copolymer viscosity (polymer data)

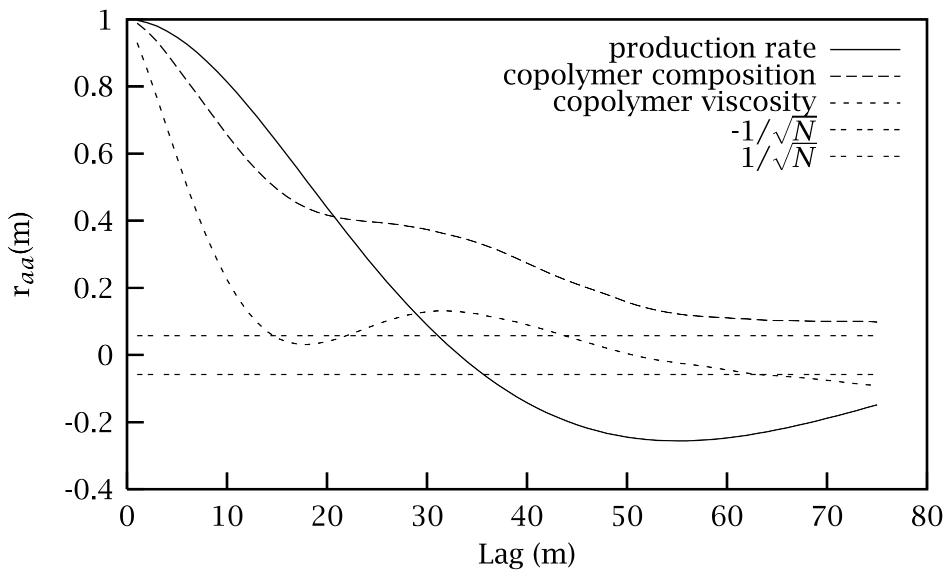

Figure 7.16: Autocorrelation of residuals from linear model corresponding to regulated outputs (polymer data)

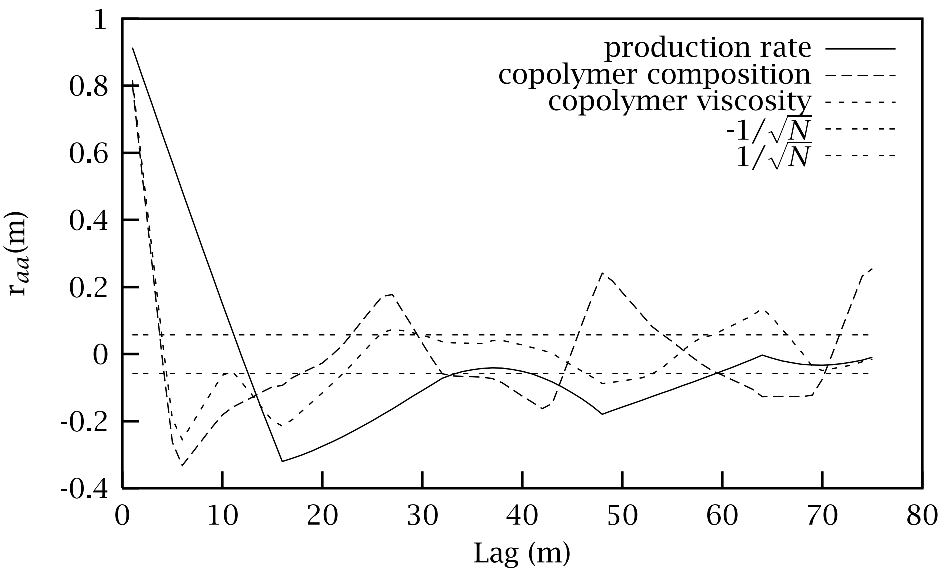

Figure 7.17: Autocorrelation of residuals from non-linear model corresponding to regulated outputs (polymer data)

Output measurement	Non-linear	Linear
Polymer production rate	1455	4742
Copolymer composition	742	4112
Copolymer viscosity	526	1261

Table 7.9: $\bar{Q}$ statistic for autocorrelation of residuals in output measurements (polymer data)

by examining the cross correlation patterns. Cross correlation functions between predictions and residuals corresponding to the measurements (Figures 7.18 and 7.19) are evaluated. Modeling inadequacies are greater for the linear model based on cross correlation plots (Figures 7.18 and 7.19). $\bar{S}$ statistic values for the two models are tabulated (Table 7.10). According to the cross correlation calculations also, the modeling inadequacies for the linear process model are significantly higher than that of the non-linear process model for the regulated outputs.

The cross correlation of residuals with disturbances is examined to further diagnose modeling deficiencies. The effect of the inhibitor feed and feed temperature along with the corresponding output disturbance (p) is first studied for polymer production rate (Figures 7.20 and 7.21). Similarly, the cross correlation function for the copolymer composition is also shown (Figures 7.22 and 7.23). The cross correlation function values for the copolymer viscosity are evaluated for the two models (Figures 7.24 and 7.25).

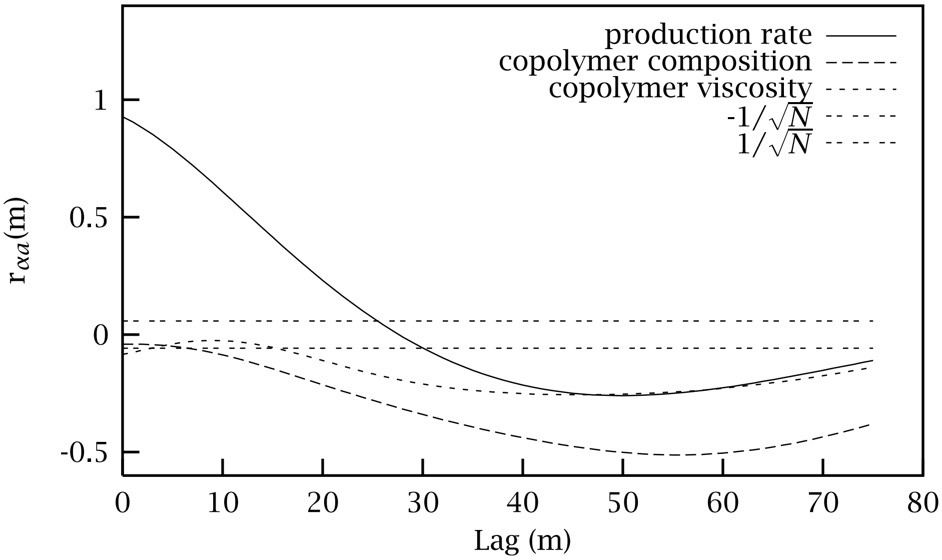

Figure 7.18: Cross correlation of residuals from linear model with corresponding output predictions (polymer data)

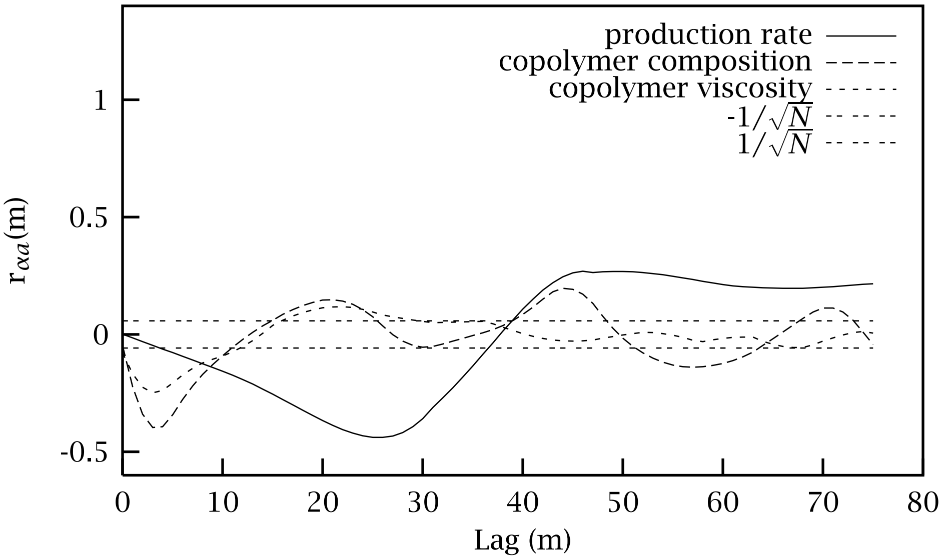

Figure 7.19: Cross correlation of residuals from non-linear model with corresponding output predictions (polymer data)

Output measurement	Non-linear	Linear
Polymer production rate	1608	3364
Copolymer composition	452	3866
Copolymer viscosity	162	968

Table 7.10: $\bar{S}$ statistic for cross correlation of residuals with predictions (polymer data)

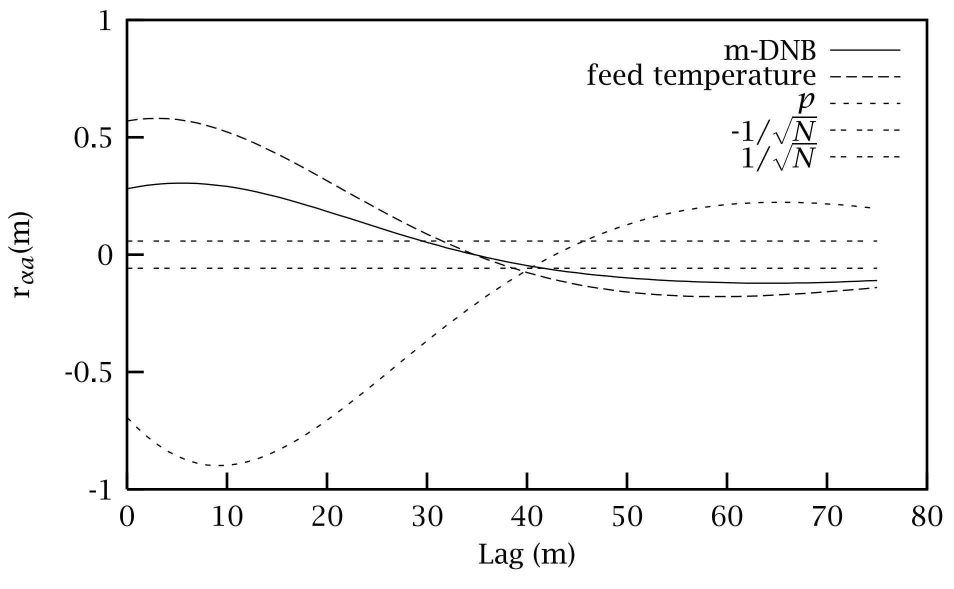

Figure 7.20: Cross correlation of residuals from linear model with disturbances for polymer production rate (polymer data)

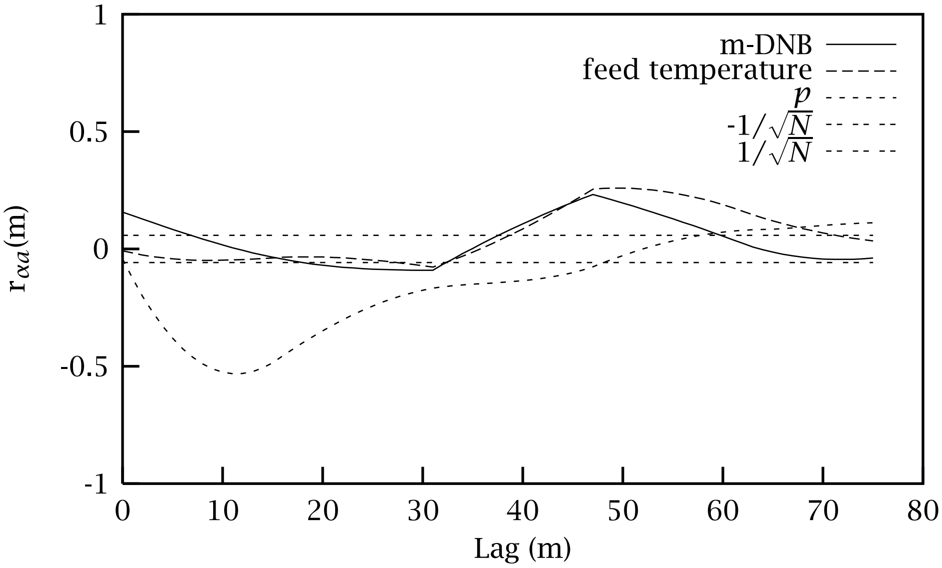

Figure 7.21: Cross correlation of residuals from non-linear model with disturbances for polymer production rate (polymer data)

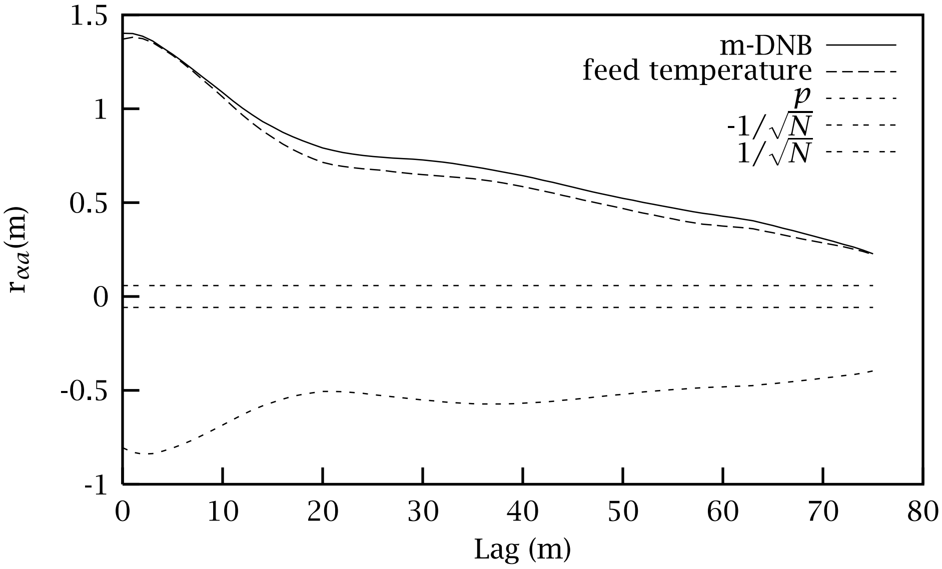

Figure 7.22: Cross correlation of residuals from linear model with disturbances for copolymer composition (polymer data)

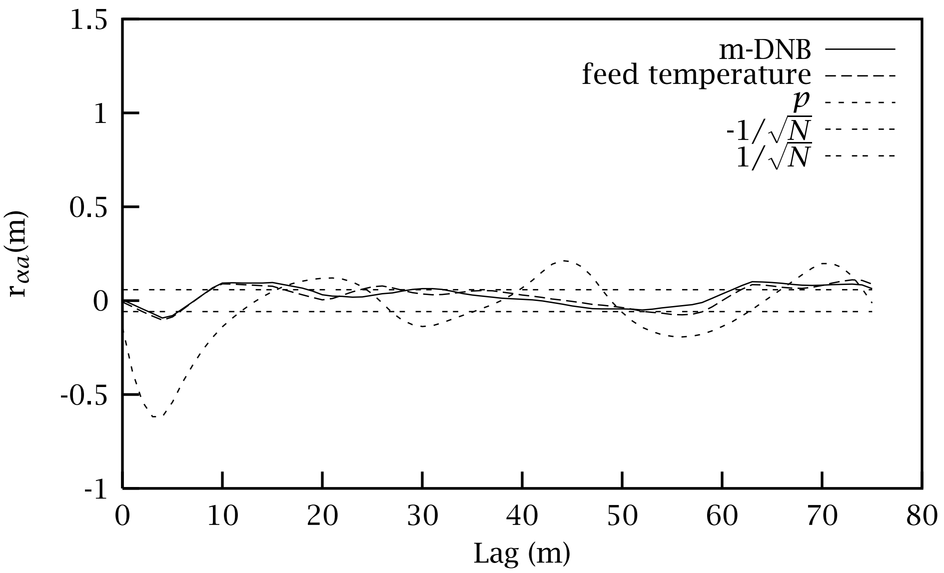

Figure 7.23: Cross correlation of residuals from non-linear model with disturbances for copolymer composition (polymer data)

Disturbance	Non-linear	Linear
m-DNB feed	272	680
Feed temperature	446	2100
Output disturbance (p)	1528	5985

Table 7.11: $\bar{S}$ statistic for cross correlation of residuals with disturbances for polymer production rate (polymer data)

Modeling inadequacies are there for the unmeasured output disturbance (p) compared to measured disturbances for the non-linear model. The linear model representation has significant modeling deficiencies for both measured disturbances, and the unmeasured output disturbance. $\bar{S}$ statistic values for the two models are tabulated for polymer production rate (Table 7.11), copolymer composition (Table 7.12) and copolymer viscosity (Table 7.13). There are modeling limitations with respect to the measured disturbances for the linear process model compared to the non-linear process model according to cross correlation functions. Modeling inadequacies with respect to output disturbance are present for both models.

The correlation analysis is also carried out with respect to tracking error for the two feedback controllers. The autocorrelation and cross correlation patterns indicate controller performance limitations for both linear and target linearization model predictive controllers. The tracking error shows cross correlation with respect to measured

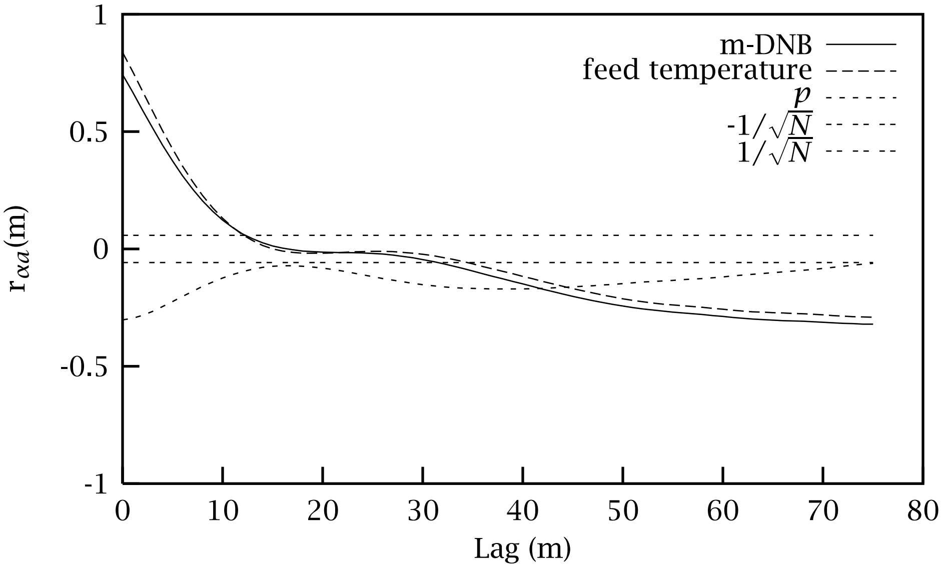

Figure 7.24: Cross correlation of residuals from linear model with disturbances for copolymer viscosity (polymer data)

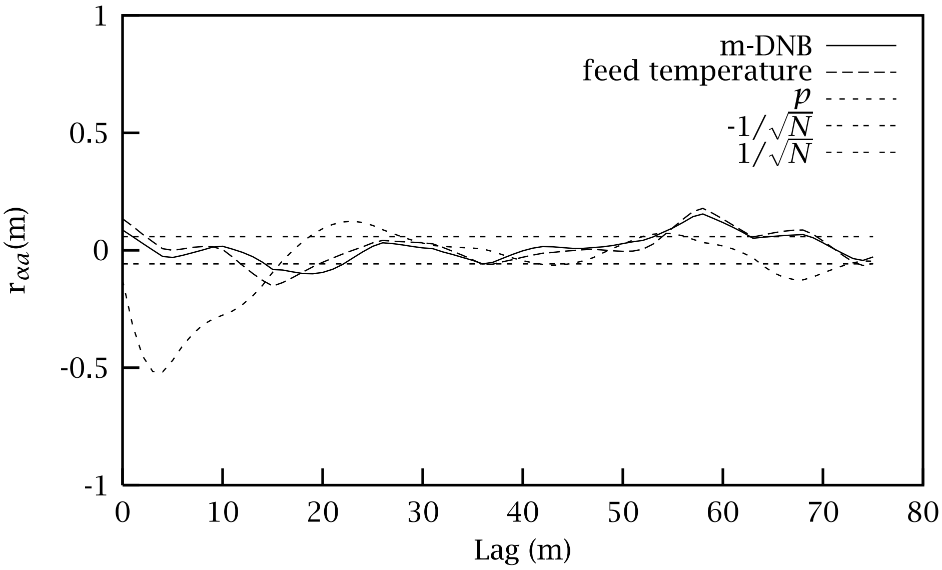

Figure 7.25: Cross correlation of residuals from non-linear model with disturbances for copolymer viscosity (polymer data)

Disturbance	Non-linear	Linear
m-DNB feed	93	14225
Feed temperature	98	12641
Output disturbance (p)	934	8252

Table 7.12: $\bar{S}$ statistic for cross correlation of residuals with disturbances for copolymer composition (polymer data)

Disturbance	Non-linear	Linear
m-DNB feed	90	1694
Feed temperature	128	1652
Output disturbance (p)	651	546

Table 7.13: $\bar{S}$ statistic for cross correlation of residuals with disturbances for copolymer viscosity (polymer data)

disturbances and unmeasured output disturbance (p) for the two models. The limitations in setpoint tracking for the linear model arise from the deficiencies present in the predictive capabilities as seen from the analysis of the residuals in prediction error. In the case of target linearization model predictive controller, the tracking errors for polymer production rate (Figure 7.26), copolymer composition (Figure 7.27) and copolymer viscosity (Figure 7.28) exhibit cross correlation with measured disturbances in contrast to the prediction errors. The $\bar{S}$ criterion values for the TLMPC are tabulated for polymer production rate, copolymer composition and copolymer viscosity (Table 7.14). The tracking error shows cross correlation with respect to the measured disturbances in contrast to the prediction error for the non-linear model. This cross correlation can be due to the following reasons

- Disturbance model limitations

Measured disturbance	Polymer production rate	Copolymer composition	Copolymer viscosity
m-DNB feed	2988	5731	9702
Feed temperature	4356	4761	7597

Table 7.14: $\bar{S}$ statistic for cross correlation of tracking error from TLMPC with measured disturbances (polymer data)

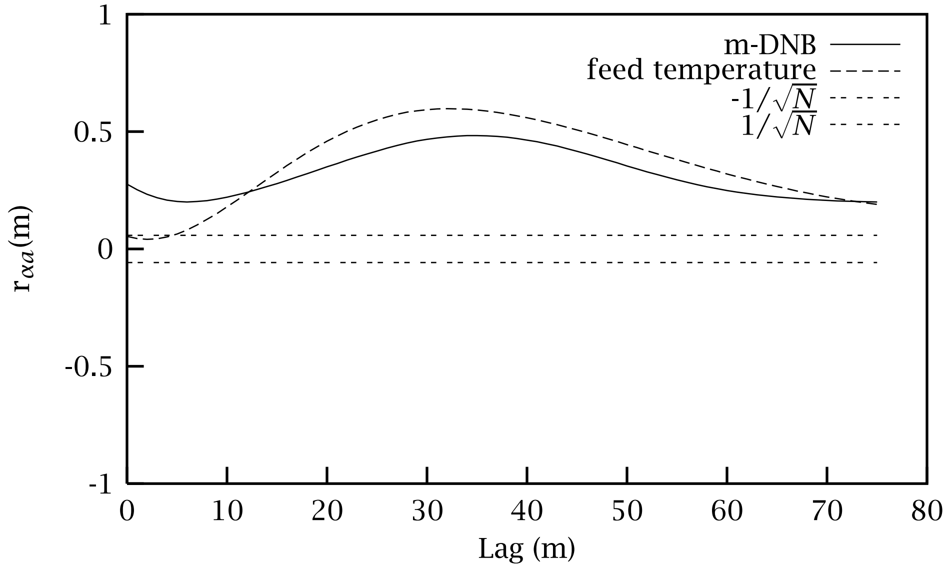

Figure 7.26: Cross correlation of tracking error from TLMPC with measured disturbances for polymer production rate (polymer data)

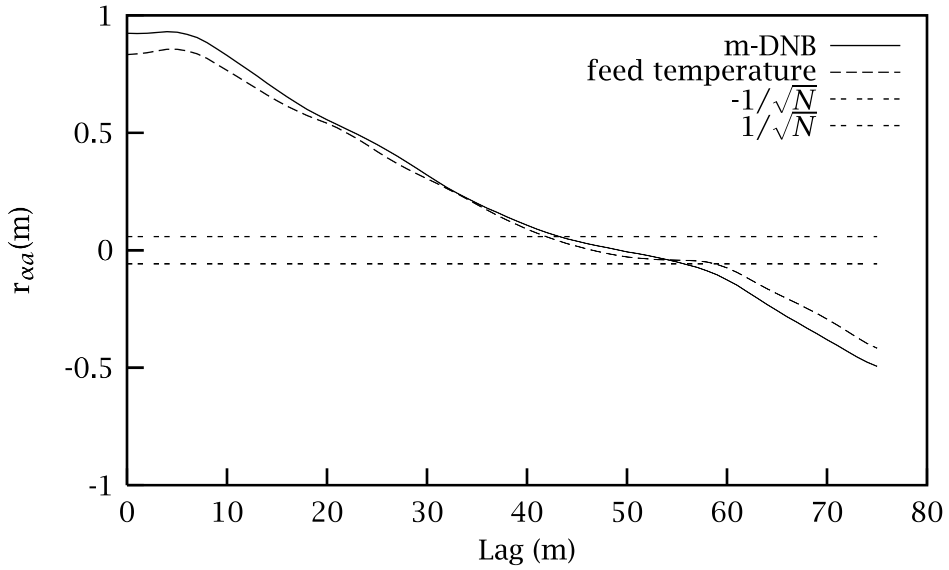

Figure 7.27: Cross correlation of tracking error from TLMPC with measured disturbances for copolymer composition (polymer data)

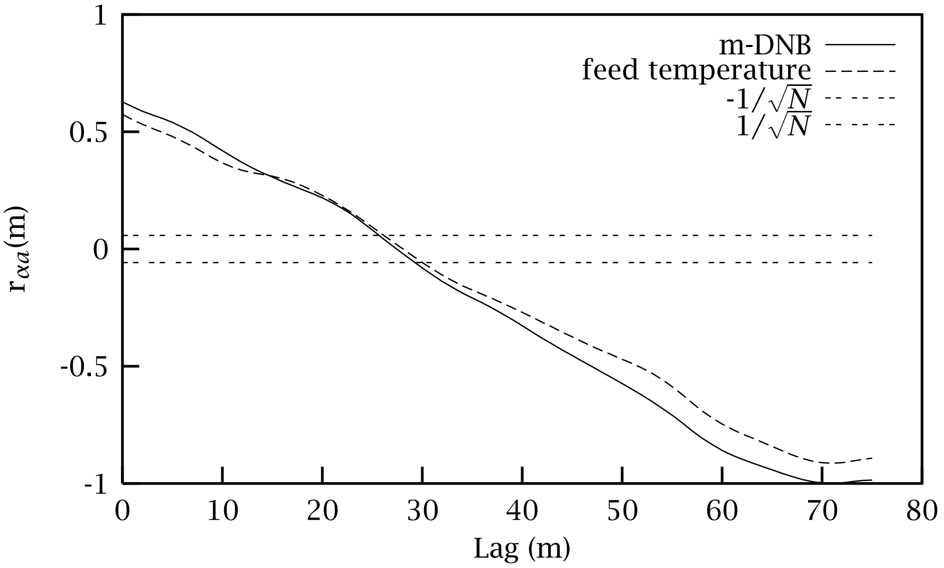

Figure 7.28: Cross correlation of tracking error from TLMPC with measured disturbances for copolymer viscosity (polymer data)

- Model representation for regulator
- Controller tuning

The disturbance model for the controller assumes that the measured disturbance remains constant in the future. In these simulations, the measured disturbances were ramping down instead of staying constant (Figures 6.4 and 6.5). A more representative disturbance model will enable the controller to counteract the effect of the measured disturbances more effectively. The full non-linear model representation is not used in the regulator thereby introducing errors with respect to measured disturbances in controller calculations. The controller could also be tuned to cancel out the effect of measured disturbances by manipulating the controlled inputs more aggressively.

7.3 Comments

The performance monitoring analysis shows the expected performance in the presence of modeling inadequacies and disturbances. The TLMPC results in superior performance compared to having a fixed linear model for feedback control (Table 7.1). The feedback controller performance is also compared to the theoretical performance of the minimum variance controller for the process. The identification of modeling inadequacies for a simple linear example using correlation checks is first analyzed. A comparison of modeling inadequacies in the linear and non-linear models that impose limitations on the performance of the feedback controller are indicated by using correlation analysis as a screening tool for typical process data. The diagnostic checks indicate that the non-linear process model gives a more accurate representation of the regulated outputs compared to the linear process model thereby resulting in better feedback controller performance. There are modeling limitations with respect to the unmeasured output disturbance in contrast to the measured disturbances for the non-linear process model. As indicated in the linear examples, the results from the correlation analysis can only serve as a diagnostic tool to further examine and pinpoint the actual modeling errors. The tracking error for the target linearization model predictive controller shows modeling deficiencies with respect to the measured disturbances even though the prediction error does not show modeling inadequacies with respect to the measured disturbances because of the limitations in the feedback regulator formulation.

Chapter 8

Conclusions

The goal of this work is to develop and analyze feedback control schemes for the control of prototypical industrial polymerization processes. The feedback controller is based on a fundamental model of the polymerization process that provides a quantitative representation of the physical phenomena. The physical model is validated for an industrial process using data sets from an actual plant. The model representation is then used to develop control strategies for typical plant operations. The performance of the feedback controller is assessed against the theoretical benchmark of a minimum variance controller and modeling inadequacies are identified using correlation checks. The contributions of this dissertation to the field of polymerization control can be classified in the following broad areas.

8.1 Process Modeling and Validation

This dissertation shows the details of typical polymerization processes and then develops a physical non-linear dynamic model for them. The significant modeling contribution made by this work is that the detailed process model is validated for historical plant data from an industrial polymerization process using maximum likelihood estimation for the kinetic parameters. The model validation problem has not been studied in much detail due to the fact that most researchers do not use industrial datasets. The approach taken in this work is to use the available industrial data for model representation without imposing any additional requirements on process measurements. The modeling objective is to produce the best available model representation with the available information for the stated process requirements. The physical non-linear model framework is chosen to capture the information that is present in the process measurements for the industrial datasets. The alternative approach of local linear models [9] is not used to avoid extensive bookkeeping arising from numerous grades of the polymer product that are rapidly evolving due to the changing needs of the customer and the desire of the manufacturers to find new uses for the polymers. This market scenario imposes new grade requirements for the product thereby making it harder to maintain a set of linear models that enables one to attain the required process objectives. The approach of empirical models also suffers from the same drawbacks.

The details of the non-linear model are tailored according to the available process information. The process measurements for the coolant flow and temperature are unreliable for the industrial process thereby resulting in lack of information to close an energy balance. The reactor temperature measurement, which is sufficiently accurate, is chosen as an input to the process model and not used for model validation because of the lack of an energy balance. The first three leading moments for polymer molecular weight distribution are evaluated for the process model because these moments are required to evaluate the weight-average molecular weight that is related to the measured polymer viscosity. There is no need to evaluate higher moments of polymer molecular weight distribution or the entire molecular weight distribution because the process measurements do not allow their validation. The appropriate assumptions of a well-mixed tank and the quasi-steady-state approximation for live polymer chains are made after a careful analysis of their validity to ensure that the model representation is adequate.

The physical model is validated by using extensive historical data after performing a careful analysis to determine the estimability of the model parameters based on the information content in the available process measurements. In the industrial process, only two kinetic parameters are estimable from the datasets. The datasets are then appropriately used to validate the fundamental model for the actual industrial polymerization process using maximum likelihood estimation. The analysis of parameter estimability is a contribution that illustrates that the parameter estimation problem is well-determined for real industrial datasets taken from the full-scale industrial polymerization process.

8.2 Feedback Control and Monitoring

The non-linear process model is used to develop a target linearization model predictive controller for the prototypical industrial polymerization process. The feedback control problem that is analyzed and studied in this dissertation is more representative of an actual polymerization process compared to the existing literature. The disturbance sets and plant-model mismatch are based on our experience with the datasets from a full-scale industrial process. Most previous literature does not assume significant disturbances or plant-model mismatch while carrying out feedback controller studies. There has been considerable work on development and implementation of feedback controllers for laboratory scale processes. These experiments do not show disturbances that are typical of a full-scale polymerization process. Most polymerization control work also ignores the fact that the key product quality measures often have long sampling times with associated delays. The infrequent product quality measures are used along with other on-line measurements in this work by constructing the equivalent raised system for the multi-rate sampling control problem [49].

The typical scenarios of reactor start-up, product grade change and regulation for polymerization control are examined in this work. Most of the polymerization control studies have only examined regulation. A target linearization model predictive controller (TLMPC) is formulated for achieving process objectives in a prototypical polymerization process after demonstrating cases where a fixed linear model predictive controller (LMPC) would fail to meet process objectives. Unlike the LMPC, the TLMPC is able to achieve the varying process goals during plant start-up, product grade change and regulation around a setpoint. An alternative approach is to use gain scheduled process control [86, 43]. This approach schedules linear controllers to achieve process objectives and is limited in its performance when the transients are rapid or the disturbances are significant. The non-linear model based approach proposed here gives better results without extra effort in terms of bookkeeping or data requirements, but requires an on-line solution of the non-linear program for target calculation.

The performance of the feedback controllers is evaluated against the theoretical benchmark of a minimum variance control law that is based on the process model. The explicit use of the process model to evaluate the minimum variance controller can be compared to the model-free approach that has been advocated in the literature [62, 40]. In general, the model-free approach fails for the multivariable case when the outputs have interacting loops and variable delays [126]. The solution is non-unique unless an assumption is made about the structure of the delay for the outputs. The fundamental model based approach proposed in this thesis overcomes these deficiencies compared to the statistical approach for the minimum variance controller. After evaluating the performance of the feedback controllers, the modeling inadequacies in linear and non-linear models that may impose limitations on controller performance are identified by doing correlation checks. Correlation patterns suggest greater modeling deficiencies in the linear model compared to the non-linear model for predicting regulated outputs, thereby corroborating the feedback controller results. Modeling deficiencies are present with respect to the unmeasured output disturbance in comparison to the measured disturbances for the non-linear process model. The correlation analysis also suggests that improvement in the performance of the target linearization model predictive controller may be achieved by using a dynamic disturbance model for feed inhibitor and feed temperature in the controller formulation.

Appendix A

Perfectly mixed tank assumption

The assumption of perfectly mixed tank is an approximation that is commonly used in the engineering analysis of tank-type devices. If there is large axial dispersion due to mixing then the vessel can be assumed to be perfectly mixed continuous stirred tank reactor (CSTR). If there is negligible axial dispersion then the vessel can be approximated as a plug flow reactor (PFR). The effect of axial dispersion can be evaluated by considering the plug flow of fluid in a vessel with some degree of mixing that is independent of position within the vessel [95]. This model is called the dispersed plug flow model or dispersion model. Let us consider a steady-flow reactor of length L and cross-sectional area S with fluid flowing with a constant velocity u and material mixing axially with a dispersion coefficient D as shown in Figure A.1. Let the reaction be of order n

$$A \rightarrow \text{products}, \qquad -r_A = kC_A^n \tag{A.1}$$

The material balance for component A is

$$\begin{aligned}&(\text{out-in})_{\text{bulk flow}} + (\text{out-in})_{\text{axial dispersion}} + \\ &\text{disappearance by reaction} + \text{accumulation} = 0\end{aligned}$$

The mole balance is

$$C_{A,l+\Delta l}uS - C_{A,l}uS - DS\frac{dC_A}{dl}\bigg|_{l+\Delta l} + DS\frac{dC_A}{dl}\bigg|_{l} + (-r_A)S\Delta l = 0 \tag{A.2}$$

Assuming constant properties and taking limits as $\Delta l \rightarrow 0$

$$u\frac{dC_A}{dl} - D\frac{d^2C_A}{dl^2} + kC_A^n = 0 \tag{A.3}$$

Substituting $z = l/L$ and $\tau = L/u$ the equation in dimensionless form is

$$\frac{D}{uL}\frac{d^2C_A}{dz^2} - \frac{dC_A}{dz} - k\tau C_A^n = 0 \tag{A.4}$$

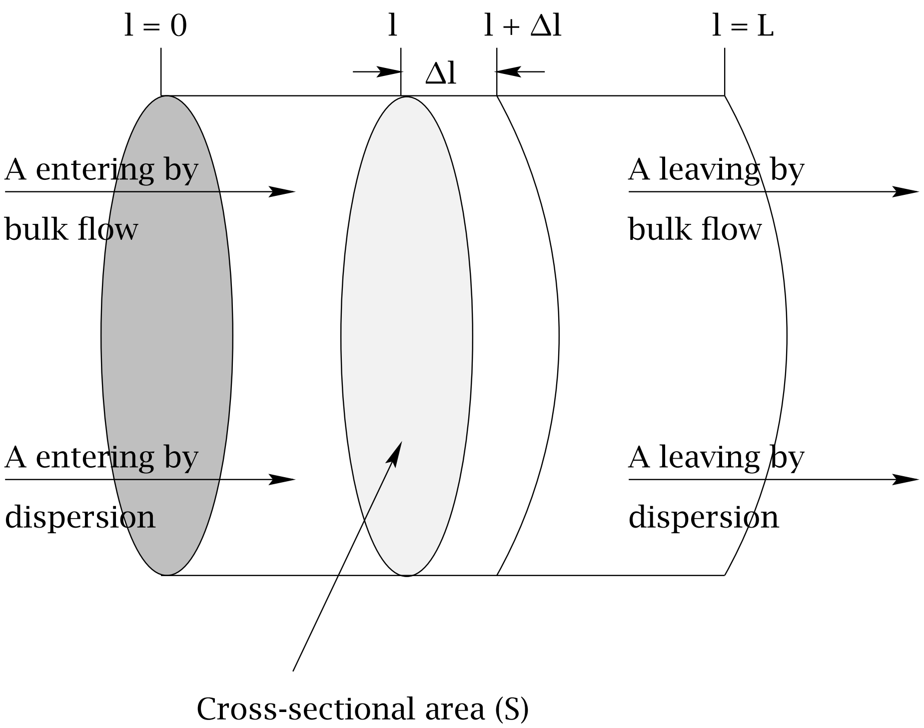

Figure A.1: Closed vessel with reaction and dispersion

The dimensionless group ($\frac{D}{uL}$), which is the reciprocal of Peclet number, is called the vessel dispersion number and measures the extent of axial dispersion. The vessel dispersion number can indicate whether flow in a reactor should be approximated as a PFR or CSTR [95] for the process model.

$$\frac{D}{uL} \to 0 \quad \text{negligible dispersion, plug flow} \tag{A.5}$$

$$\frac{D}{uL} \to \infty \quad \text{large dispersion, mixed flow} \tag{A.6}$$

Hence, the reactor can be approximated as a CSTR when there is large extent of axial dispersion. The agitators in an industrial reactor are designed to increase the dispersion coefficient (D) and also alter the flow patterns to decrease fluid velocity (u). This results in very high axial dispersion that allows the approximation of reacting vessel as a CSTR.

Appendix B

Mixing rule for reactor density

The assumption of a mixing rule that is linear in concentration is used for a reacting system with varying density [142]. Let us consider the following reaction

$$A + B \rightleftarrows nD \tag{B.1}$$

The mass balances for a CSTR are

$$\frac{d(\rho V)}{dt} = \rho_f q_f - \rho q \quad \text{(Overall)} \tag{B.2}$$

$$\frac{d(C_A V)}{dt} = C_{Af} q_f - C_A q - Vr \quad \text{(A)} \tag{B.3}$$

$$\frac{d(C_B V)}{dt} = C_{Bf} q_f - C_B q - Vr \quad \text{(B)} \tag{B.4}$$

$$\frac{d(C_D V)}{dt} = C_{Df} q_f - C_D q + nVr \quad \text{(D)} \tag{B.5}$$

The density of the reacting system (ρ) based on a linear mixing rule can be written as

$$\rho = \rho_o + \phi_A C_A + \phi_B C_B + \phi_D C_D \tag{B.6}$$

where ρ_o is the density of the solvent. Substituting equation B.6 into equation B.2 gives

$$\begin{aligned} & \rho_o \frac{dV}{dt} + \phi_A \frac{dC_A V}{dt} + \phi_B \frac{dC_B V}{dt} + \phi_D \frac{dC_D V}{dt} \\ = \; & \rho_o [q_f - q] + \phi_A [C_{Af} q_f - C_A q] + \phi_B [C_{Bf} q_f - C_B q] + \phi_D [C_{Df} q_f - C_D q] \end{aligned}$$

Equations B.3, B.4 and B.5 give

$$\begin{aligned} & \phi_A \frac{dC_A V}{dt} + \phi_B \frac{dC_B V}{dt} + \phi_D \frac{dC_D V}{dt} \\ = \; & \phi_A [C_{Af} q_f - C_A q] + \phi_B [C_{Bf} q_f - C_B q] + \phi_D [C_{Df} q_f - C_D q] + Vr[n\phi_D - \phi_A - \phi_B] \end{aligned}$$

The rate of change of volume can be written as

$$\frac{dV}{dt} = q_f - q + \frac{Vr}{\rho_o}[\phi_A + \phi_B - n\phi_D] \tag{B.7}$$

The rate of change of density with composition is nearly proportional to the molecular weight of the dissolved species in the reactor. Hence

$$\phi_A = \phi M_{wA}, \quad \phi_B = \phi M_{wB}, \quad \phi_D = \phi M_{wD} \tag{B.8}$$

The rate of change of volume can thus be expressed as

$$\frac{dV}{dt} = q_f - q + \frac{Vr\phi}{\rho_o}[M_{wA} + M_{wB} - nM_{wD}] \tag{B.9}$$

From reaction stoichiometry

$$M_{wA} + M_{wB} = nM_{wD} \tag{B.10}$$

Hence

$$\frac{dV}{dt} = q_f - q \tag{B.11}$$

Thus, we have obtained the important result that the volume rate of change equals the net volumetric flow rate when the density-concentration relation is linear. This important result is based on two assumptions:

- Density is linear in concentration (Equation B.6)
- Rate of change of density with concentration is proportional to molecular weight

Appendix C

Energy balance for a perfectly mixed tank

The law of conservation of energy is applied to a perfectly mixed tank (Figure C.1) with reactions [39].

$$\text{Reactants} \rightarrow \text{Products} \tag{C.1}$$

The total energy is the sum of the internal energy (U), the kinetic energy (KE) and the potential energy (PE). $\underline{U}$, $\underline{KE}$ and $\underline{PE}$ denote the respective energies per unit mass. The energy balance for the reactor is

$$\begin{aligned}
[U + KE + PE]_{t+\Delta t} \quad = \quad & [U + KE + PE]_t + [\text{Energy in during } \Delta t]_{\text{bulk flow}} \\
& -[\text{Energy out during } \Delta t]_{\text{bulk flow}} \\
& +[\text{Heat added to system during } \Delta t] \\
& -[\text{Work done by system during } \Delta t]
\end{aligned}$$

The energy that comes in due to bulk flow is

$$\rho_f q_f (\underline{U}_f + \underline{KE}_f + \underline{PE}_f)\Delta t \tag{C.2}$$

Similarly, the energy that goes out due to bulk flow

$$\rho_r q (\underline{U}_e + \underline{KE}_e + \underline{PE}_e)\Delta t \tag{C.3}$$

Taking limits as $\Delta t \rightarrow 0$, the energy balance can be written as

$$\begin{aligned}
\frac{d}{dt}(U + KE + PE) \quad = \quad & \rho_f q_f (\underline{U}_f + \underline{KE}_f + \underline{PE}_f) - \rho_r q (\underline{U}_e + \underline{KE}_e + \underline{PE}_e) \\
& +Q - W
\end{aligned}$$

Work is done on the system to push material in, whereas work is done by the system to push material out. The work that is except the flow work is called shaft work (W_s). The

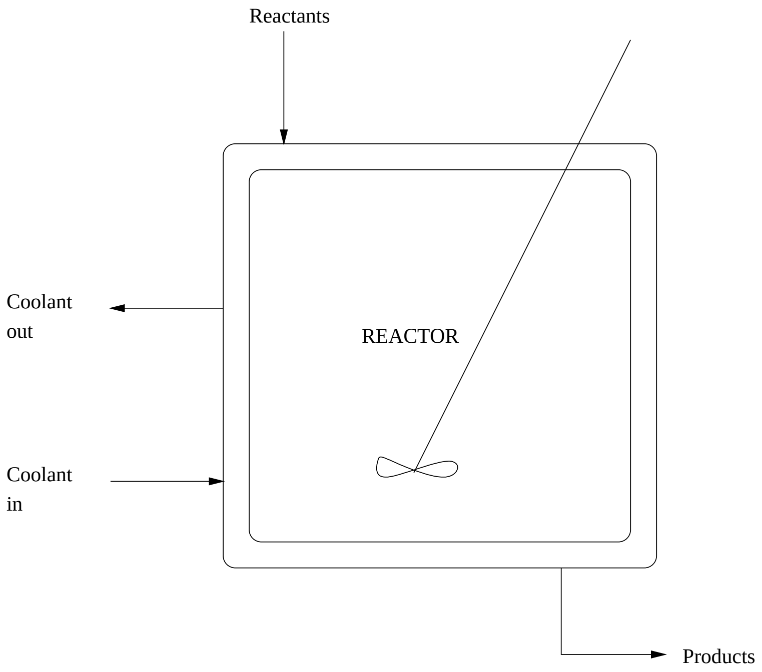

Figure C.1: Continuous stirred tank reactor with reactions

total work can be written as

$$W = P_e q - P_f q_f + W_s \tag{C.4}$$

where P_f and P_e are pressures just prior to entrance and exit. Assuming that the kinetic and potential energy terms are unimportant gives

$$\frac{dU}{dt} = \rho_f q_f(\underline{U}_f + \frac{P_f}{\rho_f}) - \rho_r q(\underline{U}_e + \frac{P_e}{\rho_e}) + Q - W_s \tag{C.5}$$

The definition of enthalpy gives

$$\frac{dU}{dt} = \rho_f q_f \underline{H}_f - \rho_r q \underline{H}_e + Q - W_s \tag{C.6}$$

The subscript e on H_e can be dropped because the enthalpy per unit mass is same everywhere in the tank.

$$\frac{dH}{dt} - \frac{d}{dt} P_r V_r = \rho_f q_f \underline{H}_f - \rho_r q \underline{H_r} + Q - W_s \tag{C.7}$$

The term $d(PV_r)/dt$ is negligible for liquid systems. Assuming constant heat capacities (C_p) gives

$$\frac{dH}{dt} = \rho_f q_f C_{pf}(T_f - T_r) + \rho_f q_f \underline{H}_f(T_r) - \rho_r q \underline{H}(T_r) + Q - W_s \tag{C.8}$$

H is a function of T_r, P_r and the number of moles of all species n_i. The pressure dependence is negligible for liquid systems and the partial molar enthalpy ($\tilde{H}_i$) is used to give the following

$$\frac{dH}{dt} = \rho_r V_r C_{pr} \frac{dT_r}{dt} + \sum_i \tilde{H}_i \frac{dn_i}{dt} \tag{C.9}$$

The summation can be expressed as

$$\sum_i \tilde{H}_i \frac{dn_i}{dt} = q_f \sum_i c_{if} \tilde{H}_i - q \sum_i c_i \tilde{H}_i + V_r r \Delta\tilde{H}_r \tag{C.10}$$

where $\Delta\tilde{H}_r$ is the enthalpy change of reaction and r is the rate of reaction per unit volume. Using $q \sum_i c_i \tilde{H}_i = \rho_r Q \underline{H}$ and $\rho_f \underline{H_f} = \sum_i c_{if} \tilde{H}_i$ yields

$$\rho_r V_r C_{pr} \frac{dT_r}{dt} = \rho_f q_f C_{pf} (T_f - T_r) + (-\Delta\tilde{H}_r) V_r r + Q - W_s \tag{C.11}$$

Dropping the shaft work term (W_s) and using an overall heat transfer coefficient (U_r) for the heat transfer between coolant (T_j) and reactor contents (T_r) gives the following energy balance for the continuous stirred tank reactor

$$\rho_r V_r C_{pr} \frac{dT_r}{dt} = \rho_f q_f C_{pf} (T_f - T_r) + (-\Delta\tilde{H}_r) V_r r - U_r S_r (T_r - T_j) \tag{C.12}$$

where S_r is the heat transfer area.

Bibliography

[1] Tae Oan Ahn, Sung Chol Hong, Jung Ho Kim, and Dong-Ho Lee. Control of molecular weight distribution in propylene polymerization with ziegler-natta/metallocene catalyst mixtures. *Journal of Applied Polymer Science*, 67:2213–2222, 1998.

[2] L.M. Alassia, D.A. Couso, and G.R. Meira. Molecular weight distribution control in a semibatch living-anionic polymerization. II. experimental study. *Journal of Applied Polymer Science*, 36:481–494, 1988.

[3] E.M. Ali, A.E. Abasaeed, and S.M. Al-Zahrani. Optimization and control of industrial gas-phase ethylene polymerization reactors. *Industrial and Engineering Chemistry Research*, 37(8):3414–3423, 1998.

[4] Jesús Alvarez, Rodolfo Suárez, and Arturo Sańchez. Nonlinear decoupling control of free-radical polymerization continuous stirred tank reactors. *Chemical Engineering Science*, 45(11):3341–3357, 1990.

[5] Jesús Alvarez, Rodolfo Suárez, and Arturo Sańchez. Semiglobal nonlinear control based on complete input-output linearization and its application to the start-up of a continuous polymerization reactor. *Chemical Engineering Science*, 49(21):3617–3630, 1994.

[6] H. L. Anderson, A. Kemmler, and R. Strey. The basic processes of polymerization and its real kinetic analysis. *Journal of Thermal Analysis*, 47(4):1041–1062, 1996.

[7] Karl J. Åström. *Introduction to Stochastic Control Theory*. Academic Press, San Diego, California, 1970.

[8] A. Banerjee and Y. Arkun. Model predictive control of plant transitions using a new identification technique for interpolating nonlinear models. *Journal of Process Control*, 5–6:441–457, 1998.

[9] A. Banerjee, Y. Arkun, B. Ogunnaike, and R. Pearson. Estimation of nonlinear systems using linear multiple models. *AIChE Journal*, 43(5):1204–1226, 1997.

[10] Yonathan Bard. *Nonlinear Parameter Estimation*. Academic Press, New York, 1974.

[11] L. F. Beste and H. K. Hall Jr. Equations for continuous control of molecular weight distribution in homogeneous free-radical polymerizations. *Journal of Macromolecular Chemistry*, 1:121–136, 1966.

[12] L. T. Biegler. Solution of dynamic optimization problems by successive quadratic programming and orthogonal collocation. *Computers & Chemical Engineering*, 8(3/4):243–248, 1984.

[13] L. T. Biegler, J. J. Damiano, and G. E. Blau. Nonlinear parameter estimation: a case study comparison. *AIChE Journal*, 32(1):29–45, 1986.

[14] J.A. Biesenberger and D.H. Sebastian. *Principles of Polymerization Engineering*. John Wiley, New York, 1983.

[15] Fred W. Billmeyer. *Textbook of Polymer Science*. John Wiley & Sons, Inc., New York, N.Y., 2nd edition, 1971.

[16] Rahul Bindlish, James B. Rawlings, and Robert E. Young. Parameter estimation in a dynamic model of a copolymerization process. In *Proceedings of the American Control Conference*, pages 2424–2428, Albuquerque, NM, June 1997.

[17] George E. P. Box, Gwilym M. Jenkins, and Gregory C. Reinsel. *Time Series Analysis: Forecasting and Control*. Prentice Hall, Englewood Cliffs, New Jersey, third edition, 1994.

[18] J. Brandrup and E.H. Immergut, editors. *Polymer Handbook*. John Wiley & Sons, New York, 2nd edition, 1975.

[19] P. Canu and W.H. Ray. Discrete weighted residual methods applied to polymerization reactors. *Computers & Chemical Engineering*, 15(8):549–564, 1991.

[20] C.C. Chang, J.W. Miller, Jr., and G.R. Schorr. Fundamental modeling in anionic polymerization processes. *Journal of Applied Polymer Science*, 39:2395–2417, 1990.

[21] Jyh-Shyong Chang and Po-Hsun Liao. Molecular weight control of a batch polymerization reactor: Experimental study. *Industrial and Engineering Chemistry Research*, 38(1):144–153, 1999.

[22] E.G. Chatzi and C. Kiparissides. Steady-state drop-size distributions in high holdup fraction dispersion systems. *AIChE Journal*, 41(7):1640–1652, 1995.

[23] Show-an Chen and Wen-Fong Jeng. Minimum end time policies for batchwise radical chain polymerization. *Chemical Engineering Science*, 33:735–743, 1978.

[24] Daniel C.H. Chien and Alexander Penlidis. Effect of impurities on continuous solution methyl methacrylate polymerization reactors – II. Closed-loop real-time control. *Chemical Engineering Science*, 49(11):1855–1868, 1994.

[25] K.Y. Choi and D.N. Butala. An experimental study of multiobjective dynamic optimization of a semibatch copolymerization process. *Polymer Engineering & Science*, 31(5):353–364, 1991.

[26] R. W. Chylla and D. Randall Haase. Temperature control of batch reactors. *Computers & Chemical Engineering*, 17:257–264, 1213, 1993.

[27] Tracy Clarke-Pringle and John F. MacGregor. Nonlinear adaptive temperature control of multi-product, semi-batch polymerization reactors. *Computers & Chemical Engineering*, 21(12):1395–1409, 1997.

[28] J. P. Congalidis, J. R. Richards, and W. H. Ray. Feedforward and feedback control of a solution copolymerization reactor. *AIChE Journal*, 35(6):891–907, 1989.

[29] John P. Congalidis and John R. Richards. Process control of polymerization reactors : An industrial perspective. *Polymer Reaction Engineering*, 6(2):71–111, 1998.

[30] Mario Rui N. Costa and Jacques Villermaux. Mathematical and experimental foundations of linear polycondensation modeling. 2. Computational aspects of the evaluation of chain-length distributions and average degrees of polymerization for linear reversible polycondensations. *Industrial and Engineering Chemistry Research*, 28(6):702–710, 1989.

[31] Mario Rui N. Costa and Jacques Villermaux. Mathematical and experimental foundations of linear polycondensation modeling. 3. Experimental study of catalyzed polyesterification of adipic acid and triethylene glycol: Equilibrium and kinetics. *Industrial and Engineering Chemistry Research*, 28(6):711–719, 1989.

[32] M.R.N. Costa and J. Villermaux. Mathematical and experimental foundations of linear polycondensation modeling. 1. Modeling and simulation of linear, irreversible polycondensation. *Industrial and Engineering Chemistry Research*, 27(3):421–429, 1988.

[33] Timothy J. Crowley and Kyu-Yong Choi. On-line monitoring and control of a batch polymerization reactor. *Journal of Process Control*, 6(2/3):119–127, 1996.

[34] Timothy J. Crowley and Kyu Yong Choi. Discrete optimal control of molecular weight distribution in a batch free radical polymerization process. *Industrial and Engineering Chemistry Research*, 36(9):3676–3684, 1997.

[35] Timothy J. Crowley and Kyu Yong Choi. Control of molecular weight distribution and tensile strength in a free radical styrene polymerization process. *Journal of Applied Polymer Science*, 70:1017–1026, 1998.

[36] Timothy J. Crowley and Kyu Yong Choi. Experimental studies on optimal molecular weight distribution control in a batch-free radical polymerization process. *Chemical Engineering Science*, 53(15):2769–2790, 1998.

[37] Isabel Sáenz de Buruaga, Antonio Echevarría, Philip D. Armitage, José C. de la Cal, José R. Leiza, and José M. Asua. On-line control of a semibatch emulsion polymerization reactor based on calorimetry. *AIChE Journal*, 43(4):1069–1081, 1997.

[38] A.B. de Carvalho, P.E. Gloor, and A.E. Hamielec. A kinetic mathematical model for heterogeneous Ziegler-Natta copolymerization. *Polymer*, 30:280–296, 1989.

[39] Morton M. Denn. *Process Modeling.* Longman, White Plains, NY, 1986.

[40] Lane Desborough and Thomas Harris. Performance assessment measures for univariate feedback control. *The Canadian Journal of Chemical Engineering*, 70:1186–1197, 1992.

[41] John Dimitratos, Guillermo Elicabe, and Christos Georgakis. Control of emulsion polymerization reactors. *AIChE Journal*, 40(12):1993–2021, December 1994.

[42] Rainer Dittmar, Zbigniew Ogonowski, and Klaus Damert. Predictive control of a nonlinear open-loop unstable polymerization reactor. *Chemical Engineering Science*, 46(10):2679–2689, 1991.

[43] Francis J. Doyle III, Harpreet S. Kwatra, and James S. Schwaber. Dynamic gain scheduled process control. *Chemical Engineering Science*, 53(15):2675–2690, 1998.

[44] Antonio Echevarría, José R. Leiza, José C. de la Cal, and José M. Asua. Molecular-weight distribution control in emulsion polymerization. *AIChE Journal*, 44(7):1667–1679, 1998.

[45] Mark F. Ellis, Tad W. Taylor, and Klavs F. Jensen. On-line molecular weight distribution estimation and control in batch polymerization. *AIChE Journal*, 40(3):445–462, 1994.

[46] Marcelo Embirucu, Enrique L. Lima, and Jose Carlos Pinto. A survey of advanced control of polymerization reactors. *Polymer Engineering & Science*, 36(4):433–447, 1996.

[47] Jorge N. Farber and Robert L. Laurence. The minimum time problem in batch radical polymerization: A comparison of two policies. *Chemical Engineering Communications*, 46:347–364, 1986.

[48] H. Fathi, A.E. Hamielec, and E.J. Davison. Modelling the anionic solution polymerization of butadiene – the effects of chain termination and long chain branching on molecular weight distribution development. *Polymer Reaction Engineering*, 4(4):243–277, 1996.

[49] Arie Feuer and Graham C. Goodwin. *Sampling in digital signal processing and control*. Birkhauser, Boston, 1996.

[50] P.J. Flory. *Principles of Polymer Chemistry*. Cornell University Press, Ithaca, New York, 1953.

[51] S. Floyd, K. Y. Choi, T. W. Taylor, and W. H. Ray. Polymerization of olefins through heterogeneous catalysis. III. Polymer particle modelling with an analysis of intraparticle heat and mass transfer effects. *Journal of Applied Polymer Science*, 32:2935–2960, 1986.

[52] S. Floyd, Tomi Heiskanen, T.W. Taylor, G.E. Mann, and W.H. Ray. Polymerization of olefins through heterogeneous catalysis. VI. Effect of particle heat and mass transfer on polymerization behavior and polymer properties. *Journal of Applied Polymer Science*, 33:1021–1065, 1987.

[53] G.L. Frontini, G.E. Elicabe, and G.R. Meira. Optimal periodic control of a continuous "living" anionic polymerization II. new theoretical results. *Journal of Applied Polymer Science*, 33:2165–2177, 1987.

[54] Robert W. Gallant. Physical properties of hydrocarbons, part 29 - acetates. *Hydrocarbon Processing*, 47(10):115–121, 1968.

[55] Sanjeev Garg, Santosh K. Gupta, and D.N. Saraf. On-line optimization of free radical bulk polymerization reactors in the presence of equipment failure. *Journal of Applied Polymer Science*, 71:2101–2120, 1999.

[56] Gangadhar Gattu and Evanghelos Zafiriou. State estimation model based algorithm for on-line optimization and control of batch processes. In *Proceedings of the American Control Conference*, pages 480–484, Baltimore, Maryland, June 1994.

[57] Elmer G. Gilbert and Kok Tin Tan. Linear systems with state and control constraints: The theory and application of maximal output admissible sets. *IEEE Transactions on Automatic Control*, 36(9):1008–1020, September 1991.

[58] Philip E. Gill, Walter Murray, and Margaret H. Wright. *Practical Optimization*. Academic Press, London, 1981.

[59] F. Gobin, L.C. Zullo, and J.P. Calvet. Model predictive control of an open-loop unstable train of polymerization reactors. *Computers & Chemical Engineering*, 18(Suppl.):S525–S528, 1994.

[60] J.W. Hamer, T.A. Akramov, and W.H. Ray. The dynamic behavior of continuous polymerization reactors – II. *Chemical Engineering Science*, 36(12):1897–1914, 1981.

[61] T. J. Harris, F. Boudreau, and J. F. MacGregor. Performance assessment of multivariate feedback controllers. *Automatica*, 32(11):1505–1518, 1996.

[62] Thomas J. Harris. Assessment of control loop performance. *The Canadian Journal of Chemical Engineering*, 67:856–861, 1989.

[63] James Hicks, Amar Mohan, and W. Harmon Ray. The optimal control of polymerization reactors. *The Canadian Journal of Chemical Engineering*, 47:590–597, December 1969.

[64] P. M. Hidalgo and C. B. Brosilow. Nonlinear model predictive control of styrene polymerization at unstable operating points. *Computers & Chemical Engineering*, 14(4/5):481–494, 1990.

[65] William E. Houston and F. Joseph Schork. Adaptive predictive control of a semibatch polymerization reactor. *Polymer Process Engineering*, 5(2):119–144, 1987.

[66] B. Huang, S. L. Shah, and E. K. Kwok. Good, bad or optimal? performance assessment of multivariable processes. *Automatica*, 33(6):1175–1183, 1997.

[67] Biao Huang, Sirish L. Shah, K. Ezra Kwok, and Jim Zurcher. Performance assessment of multivariate control loops on a paper-machine headbox. *The Canadian Journal of Chemical Engineering*, 75:134–142, 1997.

[68] R.A. Hutchinson, C.M. Chen, and W.H. Ray. Polymerization of olefins through heterogeneous catalysis. X. Modeling of particle growth and morphology. *Journal of Applied Polymer Science*, 44:1389–1414, 1992.

[69] R.A. Hutchinson and W.H. Ray. Polymerization of olefins through heterogeneous catalysis. VIII. Monomer sorption effects. *Journal of Applied Polymer Science*, 41:51–81, 1990.

[70] R.A. Hutchinson and W.H. Ray. Polymerization of olefins through heterogeneous catalysis–the effect of condensation cooling on particle ignition. *Journal of Applied Polymer Science*, 43:1387–1390, 1991.

[71] R.A. Hutchinson and W.H. Ray. Polymerization of olefins through heterogeneous catalysis. IX. Experimental study of propylene polymerization over a high activity $MgCl_2$-supported Ti catalyst. *Journal of Applied Polymer Science*, 43:1271–1285, 1991.

[72] L. L. Jacobsen and W. H. Ray. Unified modeling for polycondensation kinetics. *Journal of Macromolecular Science. Reviews in Macromolecular Chemistry and Physics*, C32:407–519, 1992.

[73] Lance L. Jacobsen and W. Harmon Ray. Analysis and design of melt and solution polycondensation processes. *AIChE Journal*, 38(6):911–925, 1992.

[74] Shi-shang Jang and Pin-ho Lin. Discontinuous minimum end-time temperature/initiator policies for batch emulsion polymerization of vinyl acetate. *Chemical Engineering Science*, 46(12):3153–3163, 1991.

[75] Shi-shang Jang and Wei-liang Yang. Dynamic optimization of batch emulsion polymerization of vinyl acetate – an orthogonal polynomial initiator policy. *Chemical Engineering Science*, 44(3):515–528, 1989.

[76] Andrew H. Jazwinski. *Stochastic Processes and Filtering Theory*. Academic Press, New York, 1970.

[77] George Kalfas and W. Harmon Ray. Modeling and experimental studies of aqueous suspension polymerization processes. 1. modeling and simulations. *Industrial and Engineering Chemistry Research*, 32(9):1822–1830, 1993.

[78] George Kalfas, Huigen Yuan, and W. Harmon Ray. Modeling and experimental studies of aqueous suspension polymerization processes. 2. experiments in batch reactors. *Industrial and Engineering Chemistry Research*, 32(9):1831–1838, 1993.

[79] Leonardo C. Kammer, Robert R. Bitmead, and Peter L. Bartlett. Optimal controller properties from closed-loop experiments. *Automatica*, 34(1):83–91, 1998.

[80] Joseph P. Kennedy and Ernest Maréchal. *Carbocationic Polymerization*. Krieger Publishing Company, Malabar, Florida, 1991.

[81] Kee Jeong Kim and Kyu Yong Choi. On-line estimation and control of a continuous stirred tank polymerization reactor. *Journal of Process Control*, 1:96–109, 1991.

[82] Kee Jeong Kim, Kyu Yong Choi, and James C. Alexander. Dynamics of a cascade of two continuous stirred tank polymerization reactors with a binary initiator mixture. *Polymer Engineering & Science*, 31(5):333–352, 1991.

[83] C. Kiparissides. Polymerization reactor modeling: A review of recent developments and future directions. *Chemical Engineering Science*, 51(10):1637–1659, 1996.

[84] C. Kiparissides, E. Sidiropoulou, S. Voutetakis, and C. Frousakis. Control of molecular weight in a batch polymerization reactor using long-range predictive control methods. *Chemical Engineering Communications*, 92:1–22, 1990.

[85] C. Kiparissides, G. Verros, and A. Pertsinidis. On-line optimization of a high-pressure low-density polyethylene tubular reactor. *Chemical Engineering Science*, 49(24B):5011–5024, 1994.

[86] K.-U. Klatt and S. Engell. Gain-scheduling trajectory control of a continuous stirred tank reactor. *Computers & Chemical Engineering*, 22(4–5):491–502, 1998.

[87] Derrick J. Kozub and Carlos E. Garcia. Monitoring and diagnosis of automated controllers in the chemical process industries. AIChE Annual Meeting, St. Louis, November 1993.

[88] Derrick J. Kozub and John F. MacGregor. Feedback control of polymer quality in semi-batch copolymerization reactors. *Chemical Engineering Science*, 47(4):929–942, 1992.

[89] Milan Kubíček, Hanns Hofmann, Vladimír Hlaváček, and Jiří Sinkule. Multiplicity and stability in a sequence of two nonadiabatic nonisothermal CSTR. *Chemical Engineering Science*, 35(4):987–996, 1980.

[90] Michael J. Kurtz and Michael A. Henson. Input-output linearizing control of constrained nonlinear processes. *Journal of Process Control*, 7(1):3–17, 1997.

[91] N. M. Lakshmanan and Y. Arkun. Estimation and model predictive control of non-linear batch processes using linear parameter varying models. *International Journal of Control*, 72(7–8):659–675, 1999.

[92] Leon Lapidus and Rein Luus. *Optimal Control of Engineering Processes*. Blaisdell Publishing Co., Waltham, MA, 1967.

[93] Charles L. Lawson and Richard J. Hanson. *Solving Least Squares Problems*. SIAM, Philadelphia, PA, 1995.

[94] Moo Ho Lee, Chonghun Han, and Kun Soo Chang. Hierarchical time-optimal control of a continuous co-polymerization reactor during start-up or grade change operation using genetic algorithms. *Computers & Chemical Engineering*, 21(Suppl.):S1037–S1042, 1997.

[95] Octave Levenspiel. *Chemical Reaction Engineering*. John Wiley and Sons, New York, 2nd edition, 1972.

[96] Daniel R. Lewin. Modeling and control of an industrial pvc suspension polymerization reactor. *Computers & Chemical Engineering*, 20(Suppl.):S865–S870, 1996.

[97] Daniel R. Lewin and David Bogle. Controllability analysis of an industrial polymerization reactor. *Computers & Chemical Engineering*, 20(Suppl.):S871–S876, 1996.

[98] Jeffery S. Logsdon and Lorenz T. Biegler. Accurate solution of differential-algebraic optimization problems. *Industrial and Engineering Chemistry Research*, 28(11):1628–1639, 1989.

[99] G.G. Lowry. *Markov Chains and Monte Carlo Calculations in Polymer Science*. Marcel Dekker, New York, 1970.

[100] J. F. MacGregor, A. Penlidis, and A. E. Hamielec. Control of polymerization reactors: A review. *Polymer Process Engineering*, 2(2 & 3):179–206, 1984.

[101] John F. MacGregor, Christiane Jaeckle, Costas Kiparissides, and M. Koutoudi. Process monitoring and diagnosis by multiblock PLS methods. *AIChE Journal*, 40(5):826–838, 1994.

[102] R.A.F. Machado and A. Bolzan. Control of batch suspension polymerization reactor. *The Chemical Engineering Journal*, 70:1–8, 1998.

[103] Frederick K. Mallon and W. Harmon Ray. Modeling of solid-state polycondensation. I. particle models. *Journal of Applied Polymer Science*, 69:1233–1250, 1998.

[104] Frederick K. Mallon and W. Harmon Ray. Modeling of solid-state polycondensation. II. reactor design issues. *Journal of Applied Polymer Science*, 69:1775–1788, 1998.

[105] Bryon R. Maner and Francis J. Doyle III. Polymerization reactor control using autoregressive-plus volterra-based mpc. *AIChE Journal*, 43(7):1763–1784, 1997.

[106] Bryon R. Maner, Francis J. Doyle III, Babatunde A. Ogunnaike, and Ronald K. Pearson. Nonlinear model predictive control of a simulated multivariable polymerization reactor using second-order volterra models. *Automatica*, 32(9):1285–1301, 1996.

[107] Herman F. Mark, Norbert M. Bikales, Charles G. Overberger, Georg Menges, and Jacqueline I. Kroschwitz, editors. *Encyclopedia of Polymer Science and Engineering*, volume 1. John Wiley & Sons, New York, 1985.

[108] K.B. McAuley and J.F. MacGregor. Nonlinear product property control in industrial gas-phase polyethylene reactors. *AIChE Journal*, 39(5):855–866, 1993.

[109] Abderrazak M. Meziou, Pradeep B. Deshpande, Charles Cozewith, Norman I. Silverman, and William G. Morrison. Dynamic matrix control of an ethylene-propene-diene polymerization reactor. *Industrial and Engineering Chemistry Research*, 35(1):164–168, 1996.

[110] K.W. Min and W.H. Ray. The computer simulation of batch emulsion polymerization reactors through a detailed mathematical model. *Journal of Applied Polymer Science*, 22:89–112, 1978.

[111] Kenneth R. Muske and James B. Rawlings. Model predictive control with linear models. *AIChE Journal*, 39(2):262–287, 1993.

[112] H. Ni, K. Debelak, and D. Hunkeler. Temperature control of highly exothermic batch polymerization reactors. *Journal of Applied Polymer Science*, 63(6):761–772, 1997.

[113] Paul Nomikos and John F. MacGregor. Monitoring batch processes using multiway principal component analysis. *AIChE Journal*, 40(8):1361–1375, 1994.

[114] Morimasa Ogawa, Masahiro Ohshima, Koji Morinaga, and Fuminao Watanabe. Quality inferential control of an industrial high density polyethylene process. *Journal of Process Control*, 9:51–59, 1999.

[115] Babatunde A. Ogunnaike. On-line modeling and predictive control of an industrial terpolymerization reactor. *International Journal of Control*, 59(3):711–729, 1994.

[116] D.A. Paquet, Jr. and W.H. Ray. Tubular reactors for emulsion polymerization: I. Experimental investigation. *AIChE Journal*, 40(1):73–87, 1994.

[117] D.A. Paquet, Jr. and W.H. Ray. Tubular reactors for emulsion polymerization: II. Model comparisons with experiments. *AIChE Journal*, 40(1):88–96, 1994.

[118] A. Penlidis, J.F. MacGregor, and A.E. Hamielec. Dynamic modeling of emulsion polymerization reactors. *AIChE Journal*, 31(6):881–889, 1985.

[119] Alexander Penlidis, John F. MacGregor, and Alvin E. Hamielec. Continuous emulsion polymerization: Design and control of cstr trains. *Chemical Engineering Science*, 44(2):273–281, 1989.

[120] Robert H. Perry, Don W. Green, and James O. Maloney, editors. *Perry's Chemical Engineer's Handbook*. McGraw-Hill Book Company, New York, 6th edition, 1984.

[121] T. Peterson, E. Hernández, Y. Arkun, and F.J. Schork. A nonlinear DMC algorithm and its application to a semibatch polymerization reactor. *Chemical Engineering Science*, 47(4):737–753, 1992.

[122] J.C. Pinto and W.H. Ray. The dynamic behavior of continuous solution polymerization reactors – VIII. A full bifurcation analysis of a lab-scale copolymerization reactor. *Chemical Engineering Science*, 50(6):1041–1056, 1995.

[123] Saty R. Ponnuswamy, Sirish L. Shah, and Costas A. Kiparissides. Computer optimal control of batch polymerization reactors. *Industrial and Engineering Chemistry Research*, 26:2229–2236, 1987.

[124] L. S. Pontryagin, V. G. Boltyanskiy, R. V. Gamkrelidze, and Ye. F. Mishchenko. *Matematicheskaya Teoriya Optimalńykh Protsessov (Mathematical Theory of Optimal Processes)*. State Publishing House of Mathematical Physics Literature, Moscow, Russia, 1961.

[125] H. Qammar, K.R. Sheshadhri, R. Gomatam, and A. Venkatesan. Control of a chaotic polymerization reaction using linear and nonlinear controllers. *The Chemical Engineering Journal*, 64:141–148, 1996.

[126] S. Joe Qin. Controller performance monitoring – a review and assessment. *Computers & Chemical Engineering*, 23:173–186, 1998.

[127] Christopher V. Rao and James B. Rawlings. Steady states and constraints in model predictive control. *AIChE Journal*, 45(6):1266–1278, 1999.

[128] J. B. Rawlings and W. H. Ray. The modelling of batch and continuous emulsion polymerization reactors. Part I: Model formulation and sensitivity to parameters. *Polymer Engineering & Science*, 28:237–256, 1988.

[129] J. B. Rawlings and W. H. Ray. The modelling of batch and continuous emulsion polymerization reactors. Part II: Comparison with experimental data from continuous stirred tank reactors. *Polymer Engineering & Science*, 28:257–273, 1988.

[130] James B. Rawlings and Kenneth R. Muske. Stability of constrained receding horizon control. *IEEE Transactions on Automatic Control*, 38(10):1512–1516, October 1993.

[131] W. H. Ray. Molecular weight distributions in copolymer systems. I. Living copolymers. *Macromolecules*, 4(2):162–165, 1971.

[132] W. H. Ray. On the mathematical modeling of polymerization reactors. *Journal of Macromolecular Science. Reviews in Macromolecular Chemistry*, pages 1–56, 1972.

[133] W. H. Ray, T. L. Douglas, and E. W. Godsalve. Molecular weight distributions in copolymer systems. II. Free radical copolymerization. *Macromolecules*, 4(2):166–174, 1971.

[134] W. H. Ray and R. L. Laurence. Polymerization reaction engineering. In Leon Lapidus and Neal R. Amundson, editors, *Chemical Reactor Theory: A Review*, pages 532–582. Prentice Hall, 1977.

[135] W. Harmon Ray. Polymerization reactor control. *IEEE Control Systems Magazine*, pages 3–8, August 1986.

[136] W. Harmon Ray. Modelling of addition polymerization processes - free radical, ionic, group transfer, and Ziegler-Natta kinetics. *The Canadian Journal of Chemical Engineering*, 69:626–629, 1991.

[137] Darren Redfern. *The Maple Handbook.* Springer, New York, N.Y., 1996.

[138] Hyung-Jun Rho, Yun-Jun Huh, and Hyun-Ku Rhee. Application of adaptive model-predictive control to a batch mma polymerization reactor. *Chemical Engineering Science*, 53(21):3729–3739, 1998.

[139] J. R. Richards and J. P. Congalidis. Feedforward and feedback control of a copolymerization reactor. In *Proceedings of the 1987 American Control Conference*, pages 286–306, 1987.

[140] John R. Richards, John P. Congalidis, and Robert G. Gilbert. Mathematical modeling of emulsion copolymerization reactors. *Journal of Applied Polymer Science*, 37:2727–2756, 1989.

[141] Ferdinand Rodriguez. *Principles of Polymer Systems.* Taylor & Francis, Washington, D.C., 4th edition, 1996.

[142] T. W. F. Russell and M. M. Denn. *Introduction to Chemical Engineering Analysis.* John Wiley & Sons, New York, 1972.

[143] Louis P. Russo and B. Wayne Bequette. Operability of chemical reactors: multiplicity behavior of a jacketed styrene polymerization reactor. *Chemical Engineering Science*, 53(1):27–45, 1998.

[144] Enrique Saldívar, Petros Dafniotis, and W. Harmon Ray. Mathematical modeling of emulsion copolymerization reactors. I. model formulation and applications to ractors operating with micellar nucleation. *Journal of Macromolecular Science. Reviews in Macromolecular Chemistry and Physics*, C38:207–325, 1998.

[145] Claudio Scali, Roberto Ciari, Tiziana Bello, and Giuseppe Maschio. Optimal temperature for the control of the product quality in batch polymerization: Simulation and experimental results. *Journal of Applied Polymer Science*, 55:945–959, 1995.

[146] A.D. Schmidt, A.B. Clinch, and W.H. Ray. The dynamic behaviour of continuous polymerization reactors – III. *Chemical Engineering Science*, 39(3):419–432, 1984.

[147] Phillip D. Schnelle and David L. Rollins. Industrial model predictive control technology as applied to continuous polymerization processes. *ISA Transactions*, 36(4):281–292, 1998.

[148] F. Joseph Schork, Pradeep B. Deshpande, and Kenneth F. Leffew. *Control of Polymerization Reactors.* Marcel Dekker, New York, 1993.

[149] Pierre O.M. Scokaert and James B. Rawlings. Constrained linear quadratic regulation. *IEEE Transactions on Automatic Control*, 43(8):1163–1169, August 1998.

[150] Argmiro R. Secchi, Enrique Luis Lima, and José Carlos Pinto. Constrained optimal batch polymerization reactor control. *Polymer Engineering & Science*, 30(19):1209–1219, 1990.

[151] D. Semino, M. Morretta, and C. Scali. Parameter estimation in extended kalman filters for quality control in polymerization reactors. *Computers & Chemical Engineering*, 20(Suppl.):S913–S918, 1996.

[152] Daniele Semino and W. Harmon Ray. Control of systems described by popualtion balance equations–II. emulsion polymerization with constrained control action. *Chemical Engineering Science*, 50(11):1825–1839, 1995.

[153] Ashuraj Sirohi and Kyu Yong Choi. On-line parameter estimation in a continuous polymerization process. *Industrial and Engineering Chemistry Research*, 35(4):1332–1343, 1996.

[154] Masoud Soroush and Costas Kravaris. Nonlinear control of a batch polymerization reactor: an experimental study. *AIChE Journal*, 38(9):1429–1448, 1992.

[155] Masoud Soroush and Costas Kravaris. Multivariable nonlinear control of a continuous polymerization reactor: an experimental study. *AIChE Journal*, 39(12):1920–1937, 1993.

[156] Masoud Soroush and Costas Kravaris. Nonlinear control of a polymerization CSTR with singular characteristic matrix. *AIChE Journal*, 40(6):980–990, 1994.

[157] W. E. Stewart, M. Caracotsios, and J. P. Sørensen. Parameter estimation from multiresponse data. *AIChE Journal*, 38(5):641–650, 1992.

[158] W. E. Stewart, M. Caracotsios, and J. P. Sørensen. *Computer-Aided Modelling of Reactive Systems*. 1999. In preparation.

[159] Makoto Takeda. Optimal grade transition strategies for multistage olefin polymerization reactors with bimodal products. Master's thesis, University of Wisconsin–Madison, 1997.

[160] Srinivas Tatiraju, Masoud Soroush, and Babatunde A. Ogunnaike. Multi-rate nonlinear state estimation in a polymerization reactor. In *Proceedings of the American Control Conference*, pages 3165–3169, Philadelphia, PA, June 1998.

[161] F. Teymour and W.H. Ray. The dynamic behavior of continuous polymerization reactors – V. Experimental investigation of limit-cycle behavior for vinyl acetate polymerization. *Chemical Engineering Science*, 47(15/16):4121–4132, 1992.

[162] F. Teymour and W.H. Ray. The dynamic behavior of continuous polymerization reactors – VI. Complex dynamics in full-scale reactors. *Chemical Engineering Science*, 47(15/16):4133–4140, 1992.

[163] Isabelle M. Thomas and Costas Kiparissides. Computation of the near-optimal temperature and initiator policies for a batch polymerization reactor. *The Canadian Journal of Chemical Engineering*, 62:284–291, 1984.

[164] Andy Yen-Di Tsen, Shi Shang Jang, David Shan Hill Wong, and Babu Joseph. Predictive control of quality in batch polymerization using hybrid ann models. *AIChE Journal*, 42(2):455–465, 1996.

[165] Athanasios Tsoukas, Matthew Tirrell, and George Stephanopoulos. Multiobjective dynamic optimization of semibatch copolymerization reactors. *Chemical Engineering Science*, 37(12):1785–1795, 1982.

[166] Vassilios K. Tzouanas and Sirish L. Shah. Adaptive pole-assignment control of a batch polymerization reactor. *Chemical Engineering Science*, 44(5):1183–1193, 1989.

[167] A. Uppal, W. H. Ray, and A. B. Poore. On the dynamic behavior of continuous stirred tank reactors. *Chemical Engineering Science*, 29:967–985, 1974.

[168] Agustín Urretabizkaia, José R. Leiza, and José M. Asua. On-line terpolymer composition control in semicontinuous emulsion polymerization. *AIChE Journal*, 40(11):1850–1864, 1994.

[169] J.R. Vega, G.L. Frontini, and G.R. Meira. Optimal periodic control of a continuous "living" anionic polymerization III. presence of impurities in the monomer feed. *Journal of Applied Polymer Science*, 42:3181–3193, 1991.

[170] Z.L. Wang, J.P. Corriou, and F. Pla. Nonlinear adaptive control of batch polymerization. *Computers & Chemical Engineering*, 18(Suppl.):S397–S401, 1994.

[171] Z.L. Wang, F. Pla, and J.P. Corriou. Nonlinear adaptive control of batch styrene polymerization. *Chemical Engineering Science*, 50(13):2081–2091, 1995.

[172] Tuyu Xie, Kim B. McAuley, James C. Hsu, and David W. Bacon. Gas phase ethylene polymerization: Production processes, polymer properties, and reactor modeling. *Industrial and Engineering Chemistry Research*, 33(3):449–479, 1994.

[173] Yasuaki Yabuki and John F. MacGregor. Product quality control in semibatch reactors using midcourse correction policies. *Industrial and Engineering Chemistry Research*, 36(4):1268–1275, 1997.

[174] Y. Yoshimoto, H. Yanagawa, T. Suzuki, T. Araki, and Y. Inaba. Optimal control of radical thermal polymerization. *International Chemical Engineering*, 11(1):147–151, January 1971.

[175] Robert E. Young, 1996. Personal communication.

[176] H. G. Yuan, G. Kalfas, and W. H. Ray. Suspension polymerization. *Journal of Macromolecular Science. Reviews in Macromolecular Chemistry and Physics*, C31:215–299, 1991.

[177] Jorge Jardim Zacca and W. Harmon Ray. Modelling of the liquid phase polymerization of olefins in loop reactors. *Chemical Engineering Science*, 48(22):3743–3765, 1993.

[178] Simon X. Zhang and W. Harmon Ray. Modeling and experimental studies of aqueous suspension polymerization processes. 3. mass-transfer and monomer solubility effects. *Industrial and Engineering Chemistry Research*, 36(4):1310–1321, 1997.

[179] S. Zhu, Y. Tian, A.E. Hamielec, and D.R. Eaton. Termination of trapped radicals at elevated temperatures during copolymerization of MMA/EGDMA. *Polymer*, 31:1726–1734, 1990.

Vita

Rahul Bindlish, son of Naresh Chander Bindlish and Chanderkanta Bindlish, was born on October 20, 1968 in Rohtak, India. He grew up in various parts of India till the age of twenty. He finished high school from Delhi Public School, New Delhi in May 1985. He received his Bachelor of Technology in Chemical Engineering from Indian Institute of Technology, Kanpur in May 1989. He moved to Texas A & M University, College Station and finished his master's degree in August 1991. He then worked in the area of Process Systems for three years at Stone & Webster Engineering, and Linnhoff March before returning to graduate school for a doctorate degree in the Process Systems research area. He joined University of Texas in September 1994 before moving with Professor Rawlings to the Chemical Engineering department at the University of Wisconsin, Madison.

Permanent Address: 506 Eagle Heights, Apt H
Madison, WI 53705

This dissertation was prepared with LaTeX 2_ε[1] by the author.

[1] This particular University of Wisconsin complient style was carved from The University of Texas at Austin styles as written by Dinesh Das (LaTeX 2_ε), Khe–Sing The (LaTeX), and John Eaton (LaTeX). Knives and chisels wielded by John Campbell and Rock Matthews.